

DESIGN AND ANALYSIS OF OTA BASED 5TH ORDER CHEBYSHEV FILTER

A Thesis

Submitted towards the partial fulfillment of requirements for the award of the degree of

Master of Technology (VLSI Design & CAD)

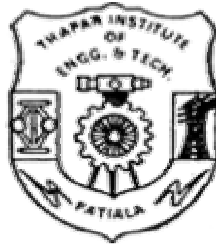
Submitted by

Jyoti Jain
Roll No. 6040409

Under the Guidance of

Mrs. Alpana Agarwal
Assistant Professor

Mr. R. Khanna
Assistant Professor



Department Of Electronics and Communication Engineering
THAPAR INSTITUTE OF ENGINEERING & TECHNOLOGY,
(Deemed University),
PATIALA- 147004, PUNJAB, INDIA

June, 2006

Certificate

I hereby certify that the work which is being presented in the thesis entitled, **“Design And Analysis of OTA Based 5TH Order Chebyshev Filter”** in partial fulfillment of the requirements for the award of degree of M.Tech. (VLSI Design And CAD) at Electronics and Communication Department of Thapar Institute of Engineering and Technology (Deemed University), Patiala, is an authentic record of my own work carried out under the supervision of Mrs. Alpana Agarwal, Assistant Professor, ECED (guide) and Mr. Rajesh Khanna, Assistant Professor, ECED (co-guide).

The matter presented in this thesis has not been submitted in any other University/Institute for the award of any degree.

Date: -----

Jyoti Jain
Roll. No. 6040409

It is certified that the above statement made by the student is correct to the best of my knowledge and belief.

Alpana Agarwal
Guide

Rajesh Khanna
Co-guide

Counter signed by:

Head
Electronics & Communication
Engineering Department,
TIET, Patiala

Dean of Academic Affairs
TIET, Patiala

Acknowledgement

To discover, analyze and to present something new is to venture on an untrodden path towards an unexplored destination is an arduous adventure unless one gets a true torchbearer to show the way. I would have never succeeded in completing my task without the cooperation, encouragement and help provided to me by various people. The enlightening guidance, I found in my revered guide Mrs. Alpana Agarwal, Asstt. Professor, Electronics & Communication Engineering Deptt., Thapar Institute of Engineering & Technology (Deemed University), Patiala, without whose patronization it was never possible to give final shape to this thesis. I wish to express my deep gratitude towards her for providing individual guidance and support.

I express my heartfelt gratitude towards my co-guide Mr. Rajesh Khanna, Assistant Professor, Electronics and Communication Department, TIET (Deemed University) for his valuable guidance, encouragement, constant involvement, inspiration and the enthusiasm with which he solved my difficulties.

I shall be failing in my duties if I do not express my deep sense of gratitude towards Dr. R. S. Kaler, Professor & Head of the Department, Electronics & Communication Engineering Department and Dr. A.K. Chatterjee, P.G. Coordinator, Electronics and Communication Engineering Department.

I am also thankful to Mr. Sanjay Batish and Mrs. Sushma Jain for extending their help in the VLSI Laboratory.

I would also like to thank all the staff members and my co-students who were always there at the need of the hour and provided with all the help and facilities, which I required for the completion of my thesis. I am also thankful to the authors whose works I have consulted and quoted in this work.

My greatest thanks are to all who wished me success especially my parents. Above all I render my gratitude to the Almighty who bestowed self-confidence, ability and strength in me to complete this work for not letting me down at the time of crisis and showing me the silver lining in the dark clouds.

Jyoti Jain

ABSTRACT

Today, with the development in the field of telecommunication and video processing applications, the components, that are the main building blocks of communication equipments, have caught the eyes of many research scholars. These developments in wireless communication have motivated many design challenges. Design of filter, which is one of the basic circuits used in these systems, is the most critical and important issue as this block contributes to the overall power consumption of receivers.

All the filters can be designed in different ways depending upon the applications for which they are being designed. Filters can be classified on the basis of response characteristics, components used, signals used, or mathematical approximations. One of the mathematical approaches is Chebyshev filter, which is the very much popular and widely used filter. Further, the filter implementation can be either active or passive. But typically for very low frequency applications (< 10 MHz), active filters are suitable, in which the prototype element values are too large to be implemented using discrete components. Video filters for industrial and broadcast applications require around 5 MHz cutoff frequencies. Thus, in order to solve the very purpose Chebyshev filter is designed. In active implementation of filter, an active device has to be chosen for a desirable response of the filter. A range of devices like Operational Amplifier, Difference Differential Amplifier (DDA), and Operational Transconductor Amplifier (OTA) etc. can be used to design an active filter. After extensive study, of all the choices Operational Transconductor Amplifier is chosen to design a Chebyshev filter. Amongst all the topologies of OTA, on the basis of literature survey, Folded Cascode OTA is chosen as it allows shorting of input and output terminals with negligible swing limitations. The design procedure for a single stage Folded Cascode OTA is developed using design equations. The circuit designed is then simulated on Tanner EDA tool. The simulated results are validating the theoretical values.

The passive network of the 5th order Chebyshev filter is chosen and all the passive components, like resistors, inductors are implemented using the active device (OTA), to get the active network of 5th order Chebyshev filter. The result of the designed filter schematic is then compared with the layout drawn on Tanner EDA tool. The passband frequency response of 5.77 MHz and gain of 0 dB is achieved after simulation which,

well justifies that the filter may be used for video applications like HDTV (High Definition Television) in broadband communication.

Change in transconductance and hence the 3dB-frequency of filter due to change in bias voltage of the OTA, is analyzed. The results of the analysis are in accordance with the literature. Finally an equation is proposed that relates the two parameters, transconductance g_m and 3dB-frequency.

Table Of Contents

Certificate.....	i
Acknowledgements.....	ii
Abstract.....	iii

List of Figures.....	ix
List of Tables.....	xii

Chapter 1 INTRODUCTION.....	1-4
1.1 Objective of the Thesis Work.....	1
1.2 Abbreviations and Color Schemes used.....	2
1.3 Contribution and Organization of Thesis.....	3
1.4 Operating System and EDA Tools used.....	4

Chapter 2 DIFFERENT METHODS FOR DESIGNING ANALOG CMOS FILTERS
.....5-15

2.1 Introduction.....	5
2.2 Chebyshev Filter Design for Reduced Sensitivity.....	5
2.2.1 Sensitivity Analysis.....	6
2.3 Designing Low Pass Chebyshev Filter with Sharp Cutoff.....	7
2.4 Design of Chebyshev Filter with Flat Group-Delay Characteristics.....	7
2.5 Different Devices used for Active Implementation of Filters.....	8
2.5.1 Filter Design using OTA.....	9
2.5.1.1 CMOS Implementation of Transconductor.....	10
2.5.2 DDA Based Fully Differential Sallen-Key Filter.....	12
2.5.3 Differential Current Control Follower (DCCF) Method.....	14
2.5.4 Comparison.....	15

Chapter 3 FILTER THEORY AND CHEBYSHEV FILTER.....16-46

3.1 Introduction.....	16
3.2 Frequency Response.....	17
3.2.1 Gain vs. Frequency Plots.....	19
3.3 Important Properties of Filters	20
3.4 Classifications of Filters.....	23
3.4.1 Digital Filters and Analog Filter.....	24
3.4.2 Continuous Time and Switched Capacitor Filters Different.....	24
3.4.3 Lowpass, Highpass, Bandpass, Allpass, Bandstop Filters.....	26

3.4.4 Butterworth, Bessel, Chebyshev, Elliptic Filters.....	27
3.5 Chebyshev Filters.....	38
3.5.1 Chebyshev Type I Filters.....	39
3.5.2 Chebyshev Type II Filters.....	42
3.5.3 Chebyshev Polynomials.....	44
3.5.4 Order of Chebyshev Filter	45
Chapter 4 INTRODUCTION TO TANNER EDA TOOL.....	47-57
4.1 Introduction.....	47
4.2 S-EDIT (Schematic Edit).....	47
4.3 T-EDIT (Simulation Edit).....	48
4.3.1 DC Operating Point Analysis.....	49
4.3.2 DC Transfer Analysis.....	50
4.3.3 Transient Analysis.....	51
4.3.4 AC Analysis.....	51
4.3.5 Noise Analysis.....	52
4.4 W-EDIT (Waveform Edit).....	53
4.5 L-EDIT (Layout Edit).....	53
4.5.1 L-Edit: An Integrated Circuit Layout Tool.....	54
Chapter 5 FOLDED CASCODE OTA: DESIGN, SIMULATION AND SYNTHESIS58-81
5.1 Introduction.....	58
5.2 Operational Amplifier.....	58
5.3 Commonly used Topologies for Operational Amplifiers.....	59
5.3.1 Two Stage Op-amp.....	60
5.3.2 Folded Cascode Amplifier.....	61
5.3.3 Telescopic Cascode Amplifier.....	62
5.4 OTA (Operational Transconductance Amplifier).....	64
5.5 Folded Cascode CMOS OTA.....	66

5.5.1 Why I choose Folded Cascode Configuration?.....	69
5.5.2 Design Procedure of A Folded Cascode CMOS OTA.....	71
5.5.3 Design of Folded Cascode Op-amp with Specifications.....	73
5.5.4 Simulation Results of Folded Cascode OTA.....	76
5.5.5 Analysis of the Simulation Results.....	78
5.5.6 Physical Design of Folded Cascode OTA	79

Chapter 6 DESIGN AND ANALYSIS OF 5TH ORDER CHEBYSHEV FILTER

.....**82-102**

6.1 Introduction.....	82
6.2 Active vs. Passive Filters	82
6.3 Passive Network of 5 th Order Chebyshev Filter	84
6.4 Equivalent Active Network of 5 th Order Chebyshev Filter	85
6.5 Analysis of Experimental Calculation of Transconductance of OTA.....	92
6.6 Analysis of Variation of 3dB-Frequency with g_m and V_b	96
6.6.1 Analysis of Various Graphs.....	97
6.7 Proposed Equation	100
6.8 Physical Design of 5 th Order Chebyshev Filter.....	100

Chapter 7 CONCLUSION AND FUTURE SCOPE.....103-104

REFERENCES.....105-108

APPENDIX.....109

List of Figures

Figure No.	Title of Figure	Page No.
2.1	4 th order Butterworth LPF using OTA integrators	10
2.2	The CMOS implementation of the transconductor	11
2.3	Block diagram of DDA	13
2.4	DDA based fully differential Sallen-Key filter	13
2.5	DCCF CMOS realization	15
3.1	Simple block diagram of filter	16
3.2	Frequency spectrum of filter	17
3.3	The response of a low pass filter to various input frequencies	18
3.4	Gain vs. frequency plot	19
3.5	Different examples of amplitude response	22
3.6	Different response categories of filter	27
3.7	Butterworth filter response	29
3.8	Chebyshev I filter response	31
3.9	Chebyshev II filter response	31
3.10	Magnitude response of Bessel filter as a function of filter order	33
3.11	Elliptic filter response	34
3.12	Different views of voltage-frequency curve	36
3.13	Group delay	37
3.14	Phase response	37
3.15	Pole-zero diagram	38
3.16	Various responses of Chebyshev type I filter	41
3.17	Various responses of Chebyshev type II filter	44
5.1	Two stage op-amp broken into V-I and I-V stages	60
5.2	Folded cascode op-amp broken into stages	61

Figure No.	Title of Figure	Page No.
5.3	(a) Single ended (b) Double ended Telescopic OTA	63
5.4	Symbol of OTA	64
5.5	Symbol and small signal equivalent of OTA	65
5.6(a)	Simplified version of N-channel input, folded cascode OTA	67
5.6(b)	Practical version of 5.6(a)	67
5.7	Small signal model of Fig. 5.6(b)	68
5.8	Telescopic OTA with input and output shorted	70
5.9	Folded cascode op-amp topology	71
5.10	Schematic of folded cascode OTA	76
5.11	Frequency vs. gain response of schematic	77
5.12	Frequency vs. phase response	78
5.13	Layout of folded cascode OTA	80
5.14	Frequency vs. gain response of layout	81
6.1	Passive network of 5 th order Chebyshev filter	84
6.2	Implementation of grounded resistor using OTA	85
6.3	Frequency response of OTA implemented grounded resistor	86
6.4	Implementation of floating resistor using OTA	87
6.5	Frequency response of OTA implemented floating resistor	87
6.6	Implementation of inductor using OTA	88
6.7	Frequency response of OTA implemented inductor	88
6.8	5 th order Chebyshev filter using folded cascode OTAs	89
6.9	Frequency response of 5 th order Chebyshev filter	90

6.10 Enlarged view to show ripples 91

Figure No.	Title of Figure	Page No.
6.11	Frequency response of passive network of 5 th order Chebyshev filter	93
6.12	Folded cascode op-amp for calculation of g_m	94
6.13	VTC curve of folded cascode	95
6.14	V_b vs. g_m graph	98
6.15	V_b vs. 3dB-frequency of active network	98
6.16	g_m vs. 3dB-frequency of active network	99
6.17	g_m vs. 3dB-frequency of both networks	99
6.18	Simulation results of layout of 5 th order Chebyshev filter	102

List of Tables

Table No.	Title of Table	Page No.
1.1	Color scheme used for layout design	3
3.1	Comparison of various parameters of filters	35
5.1	Calculated aspect ratios for the folded cascode OTA	75
6.1	Different parameters of 5 th order Chebyshev filter with change in bias voltage	96
6.2	Values of resistances and inductances required for particular 3dB-frequency	97

Chapter 1

INTRODUCTION

1.1 Objective of the Thesis Work

In recent years, the broadband communication systems, such as video applications, wireless telephony and computer networking has been a strong driving force for the IC technology. Filters constitute a small part of a complete communication system. So, they need to be low in power, small in size and they must not limit the performance of the overall system.

Filter implementation can be either active or passive. In general, for very high frequencies (> 10 GHz), the distributed passive filter is typically used and for the medium frequency range (between 100 MHz and 1 GHz), lumped passive filter is suitable. But at higher frequency the power consumption and noise contribution of active circuitry would be too large for practical purposes and IC implementation too challenging.

For very low frequency applications (< 10 MHz) like video applications, active filters are suitable, in which the prototype element values are too large to be implemented using discrete components. This thesis is a step forward to this rapidly growing communication systems field.

The objective of the work was to design an active 5th order Chebyshev filter for low frequency applications. After study of different active devices (those can be used in designing active filter), folded cascode OTA was designed with well defined design steps. The second objective was to analyze that how transconductance (g_m) and 3dB-frequency varies with bias voltage of OTA and also how 3dB-frequency varies with transconductance.







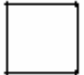




1.2 Abbreviations and Color Schemes used

The abbreviations used in this report are listed below followed by the color scheme used while drawing layout.

AC	Alternating Current
BPF	Band Pass Filter
CAD	Computer Aided Design
CMOS	Complementary Metal Oxide Semiconductor
dB	Decibel
DC	Direct Current
DDA	Difference Differential Amplifier
Dec	Decade
EDA	Electronic Design Automation
HPF	High Pass Filter
Hz	Hertz
IC	Integrated Circuit
LPF	Low Pass Filter
MHz	Mega Hertz
NMOS	N-Channel metal-Oxide Semiconductor
Op-Amp	Operational Amplifier
OTA	Operational Transconductor Amplifier
PMOS	P-Channel metal-Oxide Semiconductor
SPICE	Simulation Program With Integrated Circuit Emphasis
UGB	Unity Gain Bandwidth
W	Width of transistor
L	Length of transistor

Table 1.1 Color scheme used for layout design

	Poly		N Well
--	------	---	--------

			
	Active		N Select
	Metal1		P Select
	Metal2		Via
	Poly Contact		Overglass
	Active Contact		Pad Comment

1.3 Contribution and Organization of Thesis

Main contributions of this thesis are:

- Study of different methods to design an analog CMOS filter.
- Design, simulation and synthesis of folded cascode OTA.
- Active implementation of a 5th order Chebyshev filter.
- Analysis of 5th order Chebyshev filter in terms of bias voltage, transconductance, and 3dB-frequency.
- Proposal of an equation showing relation between 3dB-frequency and transconductance.

The thesis report is organized into seven chapters. The chapter wise detail is given below:

Chapter 1: In this chapter, the objective of the thesis work is presented along with the abbreviations used in the report and the color scheme followed during the layout.

Chapter 2: This chapter is based on the literature survey done for this thesis.

Chapter 3: In this chapter, basic theory of filters and its types are discussed.

Chapter 4: In this chapter, brief introduction to the Tanner EDA tool is presented.

Chapter 5: This chapter discusses the design steps for the design of folded cascode OTA with results of the schematic and layout simulations.

Chapter 6: This chapter discusses the active implementation of 5th order Chebyshev filter, generalization of calculating the transconductance of OTA experimentally and analysis of implemented filter in terms of bias voltage, g_m and 3dB-frequency.

Chapter 7: This chapter presents the conclusion of the work done and future scope.

1.4 Operating System and EDA Tools used

The operating system and tools used in thesis are as follows:

Operating System	: Windows XP
Tools	: Tanner EDA Tool
	S-Edit
	T-Spice Pro
	W-Edit
	L-Edit Pro

Chapter 2

DIFFERENT METHODS FOR DESIGNING ANALOG CMOS FILTERS

2.1 Introduction

Recently, developments in wireless communication and biomedical equipments have motivated many design challenges specifically in low voltage and low power integrated circuits. As a critical block of portable wireless devices, baseband filters operating with kilohertz to a few megahertz cutoff frequencies significantly contribute the overall power consumption of receivers. One basic circuit used in these equipments is filters. Filters can be classified on the basis of mathematical approximations, frequency response, elements used in circuit (active and passive) etc.

On the basis of mathematical approximations, the filters are of four types- Butterworth, Bessel, Chebyshev and Elliptic filter. Chebyshev filter is one the popular approach of designing analog filters for the applications where ripples are allowed like voice synthesizer, in video applications etc. From the literature survey it has been found that efforts are being done to improve the characteristics of Chebyshev filters. Some examples, proving the statement, are given below:

2.2 Chebyshev Filter Design for Reduced Fabrication Sensitivity

A technique for redistributing the reflection lobes of a Chebyshev filter has been proposed to improve immunity against manufacturing inaccuracies while maintaining better selectivity compared to chained function responses [2].

Mainly distinguished by their equiripple behavior, Chebyshev filters provide a compromise between insertion loss and selectivity. The in-band reflection loss of the Chebyshev filtering function is characterized by a number of lobes whose maximum value is set to a constant limit. The different reflection zeros of the Chebyshev filter has varying sensitivities as far as their positions in the frequency do-main is concerned.

Inaccuracies in coupling coefficients result in shifting these nulls from their designated locations, and hence possibly violate required specifications.

A possible solution to this problem has been suggested through Chained Filter functions [24]. Here, a filtering function formulated by the product of ‘seed functions’ is used to control the positions of reflection zeros. While this pays off in terms of containing the effects of tolerance and manufacturing inaccuracies, selectivity is compromised. To control the tradeoff between these two conflicting characteristics, the current letter presents a methodology by which reflection zeros of a normal Chebyshev filter can be relocated on the frequency axis in such a way so as to contain reflection lobes within a dome-shaped envelope. Reflection lobes closer to the band edge will have lower peak values compared to those close to the center frequency. This is particularly useful as lobes closer to the band edge are more vulnerable to manufacturing defects.

Furthermore, the insertion loss suffers more from resistive losses at the band edges and would benefit from a smaller ripple. Thus the amount of adjustment that happens to reflection lobes is controlled through an arbitrary constant. As this redistribution of reflection zeros impinges on the maximum reflection loss, an increase in the maximum ripple will be necessary to account for the reshaping of the response. A relation between the steepness of the curvature and the required new ripple value is derived. A comparison is finally provided to compare the performance of the three different filtering functions.

2.2.1 Sensitivity Analysis

To test sensitivity to fabrication errors, a tolerance with a maximum value of 0.001 was assumed for the coupling coefficients of the previous example along with random decreases in the input and output external quality factors down to 90% of the original value. The tolerance described was simulated by adding randomly generated numbers to the elements of the normalized coupling matrix [27].

2.3 Designing Low pass Chebyshev Filter with Sharp Cutoff

Budak and Aronhime [3] and Dutta Roy [29] have suggested modifications of the original Butterworth function by introducing either single or multiple pairs of imaginary axis zeros. These functions provide maximally flat magnitude response in the passband and have a cutoff characteristic much sharper than that of the Butterworth function of the same order. The most attractive feature of these functions is that they offer the filter designer.

A great degree of freedom in choosing the location and number of zeros, depending upon the complexity of the filter he desires. Chebyshev filters have been known to provide a much sharper cutoff response than the corresponding Butterworth filters at the expense of ripples in the passband. In this paper, we study the effects of introducing single or multiple pairs of $j\omega$ axis zeros in the original Chebyshev filter transfer functions, and show that the cutoff rate can be increased much beyond that attainable by either Chebyshev or modified Butterworth filter functions of [3] and [29]. The modified Chebyshev functions introduced also have a stopband attenuation characteristic much better than those of [3] and [29].

An effect of introducing single or multiple pairs of coincident $j\omega$ axis zeros in all-pole Chebyshev filter transfer functions are investigated [23]. For the same order N , Chebyshev filters with finite $j\omega$ axis zeros provide much sharper cutoff than all-pole Chebyshev filters. It is also shown that for the same n , the same number of pairs of zeros m , and the same locations of zeros, the cutoff slope and stopband characteristic of the finite zero Chebyshev filters are much better than those of the finite zero Butterworth filters.

2.4 Design of Chebyshev Filter with Flat Group-Delay Characteristics

The design of filters with Chebyshev performance in their passbands has been exhaustively studied by an author [22]. For filters used in transmission systems, the group-delay characteristic in the passband plays a more and more important role. Especially for filters in compatible use in both telephone and data transmissions, Chebyshev attenuation characteristics in the passband are required for speech transmissions, and at the same time the flat group-delay performance in the main part of the passband is also required for pulse transmissions.

Usually, in order to satisfy such requirements, a combination of a conventional minimum phase-shift filter and an all-pass group-delay equalizer connected in cascade is used. The

number of elements of such an equalizer is usually comparable to or even greater than that of the filter, and therefore the whole network becomes large in size and is uneconomical.

The use of a Chebyshev filter with complex attenuation poles, suggested in [12], is very effective for this purpose. Introduction of complex attenuation poles into a Chebyshev filter not only improves the group-delay characteristic of the filter, in the passband, but also contributes considerably to the attenuation in the stopbands. A similar idea was presented by Colin, but he did not treat the Chebyshev filter.

A method for designing Chebyshev filters having flat group-delay characteristics in the main part of the passband is presented in [25]. From the general approximation theory, a method for obtaining the transfer function of Chebyshev filters with complex transmission zeros is derived, which are so determined that the group-delay characteristics may be flat in the main part of the passband. A new theory of cascade synthesis, which is an extension of Belevitch's cycle, and an extended bisection theorem are introduced. By the applications of these results, Chebyshev filters with flat group delay can be realized [25].

2.5 Different Devices used for Active Implementation of Filters

Filter implementation can be active or passive, based on the components used.

Since passive filters use no active elements, they cannot provide signal gain.

Input impedances can be lower than desirable, and output impedances can be higher the optimum for some applications, so buffer amplifiers may be needed.

Inductors are necessary for the synthesis of most useful passive filter characteristics, and these can be prohibitively expensive if high accuracy (1% or 2%, for example), small physical size, or large value is required. Standard values of inductors are not very closely spaced, and it is difficult to find an off-the-shelf unit within 10% of any arbitrary value, so adjustable inductors are often used.

Tuning these to the required values is time-consuming and expensive when producing large quantities of filters. Furthermore, complex passive filters (higher

than 2nd-order) can be difficult and time-consuming to design. Due to all these limitations active implementation of filters is required.

Further, active filters can be implemented using different active devices like OTA (Operational Transconductance Amplifiers), DDA (Direct Differential Amplifiers), DCCF (Differential Current Control Follower), which are discussed in following sections.

2.5.1 Filter Design using OTA

Filter design using OTA (Operational Transconductance Amplifier) is the most common method. Butterworth, Chebyshev, Bessel and Elliptic filters can be designed easily and efficiently using OTAs. An OTA is a voltage controlled current source (VCCS), more specifically the term “operational” comes from the fact that it takes the difference of two voltages as the input for the current conversion. In addition to the voltage control characteristics, the OTA based circuits show promise for high frequency applications where conventional opamp based circuits become bandwidth limited.

High-speed filters are increasingly based on an Operational Transconductance Amplifiers (OTAs) Capacitor (g_m -C) approach, because of their simple circuitry and improved frequency response. However, the nonidealities of the transconductor limit overall filter performance. Several linearization techniques [26,35] (one of the techniques utilizes triode-biased transconductors exploiting an active-cascode scheme which is similar to conventional cascode circuits except that the current of the triode transistor is sensed through another path rather than the cascode transistor, allowing for regulation of the drain voltage by negative feedback.) have been developed to enhance the linearity of the transconductor, but precise cancellation of nonlinearities is limited by matching accuracy.

The performance of OTA-C filters depends on: (i) the OTA circuit, which is the main noise and distortion contributor in the filter, and (ii) the OTA-C filter structure. The later is a fourth-order Butterworth, realized by cascading two biquadratic sections. Each biquad is implemented with 4 OTAs and 2 capacitors. The fully differential

transconductor- capacitor filter is shown in fig. 2.1. All transconductors are identical. The designed stop- band attenuation is 60 dB at 80 MHz for a 10 MHz cutoff frequency [7].

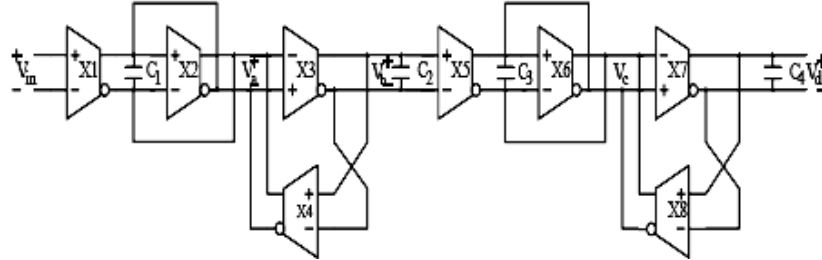


Figure 2.1. 4th-order Butterworth LPF using OTA integrators: $C_1 = 6.40 \text{ pF}$, $C_2 = 3.84 \text{ pF}$, $C_3 = 2.40 \text{ pF}$ and $C_4 = 9.60 \text{ pF}$

2.5.1.1 CMOS Implementation of Transconductor

The differential transconductance circuit is shown in fig. 2.2. It comprises a source-coupled pair with poly-silicon degeneration resistors and a cross-coupled high-impedance load. The linearity is enhanced by the degenerated resistors at the cost of a smaller effective transconductance, g_m , and a smaller tunable g_m range. Transistors M4, M5, M6 and M7 are matched. M8 and M9 operate in the triode region, acting as degeneration resistors. M4 and M7 act like a pair of positive resistors R_+ , while M5 and M6 function as negative resistors R_- . The output impedance of the transconductor depends on the parallel combination of R_+ and R_- , the values of which are controlled by voltages v_{cp} and v_{cn} respectively. As a result, the output impedance, and therefore, the Q of the integrator, can be maximized with proper combinations of v_{cp} and v_{cn} . With this transconductor, a tunable integrator for very-high-frequency integrated filters can be realized by adjusting the voltage v_{ba} , which controls the tail current, and thus G_m . Good high-speed properties stem from the absence of internal high impedance nodes, which pushes non-dominant poles to the gigahertz ranges [7].

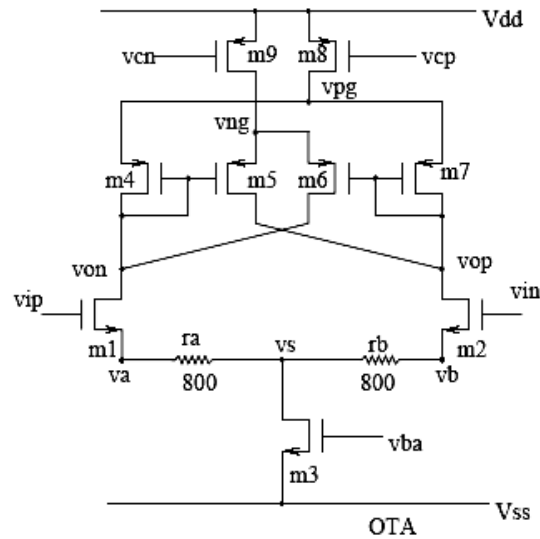


Figure 2.2. The CMOS implementation of the transconductor

Low-frequency filters are important building blocks for biomedical systems where bioelectric signals (of range $1 \mu\text{V}$ – 100 mV , frequencies below 100 Hz) are employed and these circuits should not introduce any form of distortion that can destroy the information contained.

One such design for implementing low frequency filters, a 2.4 Hz low-pass filter achieving a 60 dB dynamic range is presented. Capacitors ranging from 18 pF to 200 pF are implemented by using 5 pF capacitors and impedance scalars. This approach allows a considerable saving of silicon area. As a result of the large capacitors emulated in the implementation a huge reduction in the filter noise is obtained. For electrocardiograph (ECG) applications where the magnitude of the signal is around 1 mV – 25 mV , and considering a preamplifier gain of 10 dB , the magnitude of the signal to be processed by the low-pass filter (LPF) is around 10 mV – 250 mV . To sense the T wave signal, a cutoff frequency as low as 2.4 Hz is required. The requirements for such a filter leads to a design of 6^{th} order Bessel filter with dynamic range of 60 dB , minimum power consumption of $50 \mu\text{W}$ and $\text{THD} < -50 \text{ dB}$. For easier analysis and better understanding, the OTA based integrator is first considered [32].

Increasing demand for high-speed data services in recent years has led to the evolution of Digital Subscriber Line (DSL) technology. It is necessary for DSL networks to design

spectral shaping filters, that shape the transmit signal such that it complies with the time and frequency templates allowed in the network. For this application, Butterworth filter is designed using OTAs so as to decrease the power consumption [8].

2.5.2 DDA Based Fully-Differential Sallen-Key filter

In recent years, the portable communication market has been a strong driving force for the IC technology. With the emergence of the third-generation (3G) mobile systems, high-bit-rate multimedia services are turning into reality. One concern with wideband CDMA receiver is the power consumption. With up to 20 MHz bandwidth, the power of baseband filter will be huge if proper power optimization techniques are not taken. The portable applications and the desire to extend the battery lifetime had made the low power design a must. Another concern is to reduce noise figure.

After it was presented by Edward Sackinger and Walter Guggenbuhl in 1987 [10], the CMOS Differential Difference Amplifier (DDA) has gained wide applications in analog signal processing. As shown in fig. 2.3, the DDA is actually an extension to the concept of the opamp. The main difference is that DDA has four inputs (V_{pp} , V_{pn} , V_{nn} and V_{np}) and the output of DDA can be written as:

$$V_o = V_{op} - V_{on} = A_o [(V_{pp} - V_{pn} - (V_{np} - V_{nn})] \dots\dots\dots(2.1)$$

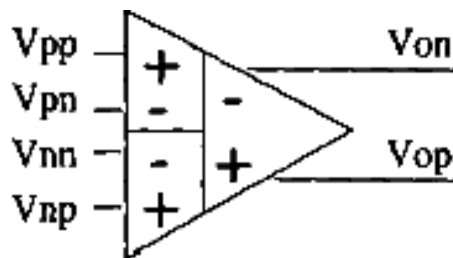


Figure 2.3. Block diagram of DDA

When a negative feedback is introduced, i.e., to V_{pn} and/or V_{np} , which appear in (2.1) with a negative sign, the following expression is obtained:

$$V_{pp} - V_{pn} = V_{np} - V_{nn} \text{ with } A_o \rightarrow \infty \dots\dots\dots(2.2)$$

In practice, A_o is always finite, so there is a difference between the two differential voltages. Therefore, the open-loop gain should be as large as possible in order to achieve high-performance operation.

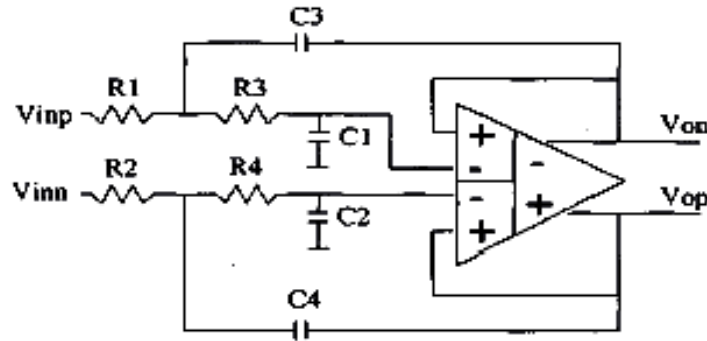


Figure 2.4. DDA based fully differential Sallen-Key filter

The DDA can be used to implement fully differential Sallen- Key filter as shown in fig. 2.4 (where $R_1 = R_2$, $R_3 = R_4$, $C_1 = C_2$, $C_3 = C_4$). Assume A_o is large enough, then from (2.2) we have $V_{pn} - V_{nn} = V_{pp} - V_{np} = V_{on} - V_{op}$, and after some mathematics manipulation, the transfer function of the filter can be derived as:

$$H(s) = (V_{on} - V_{op}) / (V_{inp} - V_{inn}) = \omega_o^2 / (s^2 + s\omega_o/Q + \omega_o^2) \dots\dots\dots(2.3)$$

Where $\omega_o = \sqrt{1/R_2 R_3 C_1 C_3}$ is the undamped natural frequency, $Q = \sqrt{(R_2 R_3 C_1 C_3 / (R_1 + R_3) C_1)}$ is the quality factor, which defines the sharpness at which the peak of the magnitude response occurs. When $R_1 = R_3$, this unity-gain filter has the advantage of low sensitivity to component value when compared to other Sallen-Key filter structures.

2.5.3 Differential Current Control Follower (DCCF) Method

Second-Generation (2G) systems dominated by Global System for Mobile Communications (GSM) in Europe, North American Digital Cellular IS-54 and IS-95 in the U.S., and Personal Digital Cellular (PDC) in Japan are mainly limited to voice and low data-rate services. The highly competitive market demands low cost, low power, and small form factor devices. Eventually, this will result in the development of a single-chip transceiver capable of adapting to various communications standards in a low-cost CMOS technology. Thus, development of a programmable analog baseband filter shared

by different wireless standards is feasible. This results in a simplified, low-power and cost-effective system design solution. A possible solution is to do all channel filtering digitally. The technique is used to implement a baseband channel-select filter for multistandard fully integrated wireless receivers. The filter accommodates the following wireless standards: PDC, IS-54, GSM, IS-95, and WCDMA with bandwidths of 2, 13, 15, 100, and 630 MHz, respectively.

A CMOS realization of the DCCF is shown in fig. 2.5. The two biasing transistors M9 and M10 force an equal current through transistors M1 and M2. Since the gate voltage of transistors M1 and M2 are equal, the source voltage of transistor M1 equals the source voltage of M2 which results in a virtual ground at the X-terminal, assuming that the CDN exhibits a small resistance. The X-terminal current is provided by the action of the class-AB negative feedback loop formed by transistors M3, M4, M5, and M7. The feedback loop operates in a class-AB mode to minimize the standby power dissipation. Digital trimming is performed by the current division network (CDN) [1].

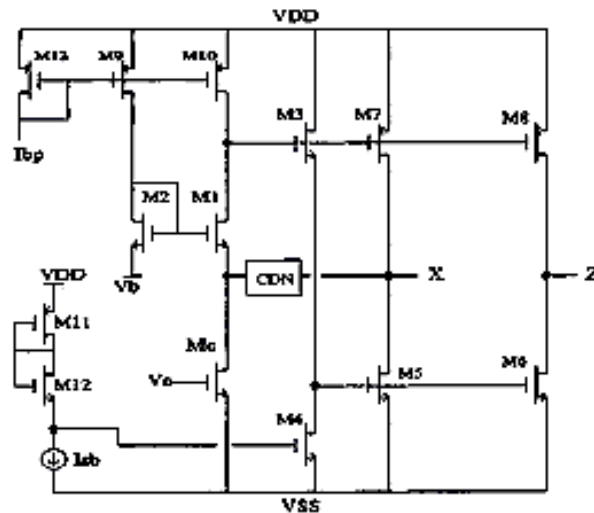


Figure 2.5 DCCF CMOS realization

2.5.4 Comparison

A filter design using DDA, OTA and DCCF have been discussed in previous sections.

Conventional OTAs do not achieve high dynamic range. Also, OTA-C filters are expected to lose more dynamic range as well as tuning range when power-supply voltage levels are further reduced. If two OTA-C filters are designed, one for low power while

the other was designed for low noise, the low-power filter exhibits a low dynamic range while the low-noise filter exhibits improved dynamic range but consumes excessive power.

If a 2nd order fully differential Sallen-Key filter is designed using OTAs then it uses two OTAs and an RC network. Whereas, one DDA along with RC network completes the same design of 2nd order Sallen-Key filter. This structure results in 50% power saving with the reduction in number of components and area as well.

In contrast, DCCF results in a simplified, low-power and cost-effective system design solution. The technique exhibits the wide frequency range of the transconductance amplifier filters while offering improved linearity. It also provides precise frequency characteristics and wide tuning range. But in a multistandard receiver, a separate RF front end is required for each standard because of noise–linearity–power tradeoffs.

Chapter 3

FILTER THEORY AND CHEBYSHEV FILTER

3.1 Introduction

A filter is defined as an electric network, which passes or allows unattenuated transmission of electric signal with in certain frequency range and stops or disallows transmission of electric signal outside this range. Filters are signal conditioners. Each function by accepting an input signal, blocking prespecified frequency components, and passing the original signal minus those components to the output. For example, a typical phone line acts as a filter that limits frequencies to a range considerably smaller than the range of frequencies human beings can hear. That's why listening to CD-quality music over the phone is not as pleasing to the ear as listening to it directly.



Figure 3.1 Simple block diagram of filter

Filters are the indispensable parts, used virtually in every modern electronic system. A filter is an electronic device used to select a particular pass band range. Signals with in that range are allowed to pass while the signals outside that range are disallowed. According to circuit theory a more general definition is, a filter is an electrical network that alters the amplitude and/or phase characteristics of a signal with respect to frequency. Ideally, a filter will not add new frequencies to the input signal, nor will it change the component frequencies of that signal, but it will change the relative amplitudes of the various frequency components and/or their phase relationships. Filters are often used in electronic systems to emphasize signals in certain frequency ranges and reject signals in other frequency ranges. Most A/D converters (ADCs) are preceded by a filter, which removes frequency components that are beyond the ADC's range. Such a

filter has a gain, which is dependent on signal frequency. Since their frequency-domain effects on signals define filters, it makes sense that the most useful analytical and graphical descriptions of filters also fall into the frequency domain. Thus, curves of gain vs. frequency and phase vs. frequency are commonly used to illustrate filter characteristics, and the most widely used mathematical tools are based in the frequency domain. The frequency-domain behavior of a filter is described mathematically in terms of its transfer function or network function. This is the ratio of the Laplace transforms of its output and input signals. The voltage transfer function $H(s)$ of a filter can therefore be written as:

$$H(s) = V_{out}(s)/V_{in}(s) \dots \dots \dots (3.1)$$

Where $V_{in}(s)$ and $V_{out}(s)$ are the input and output signal voltages and s is the complex frequency variable [20].

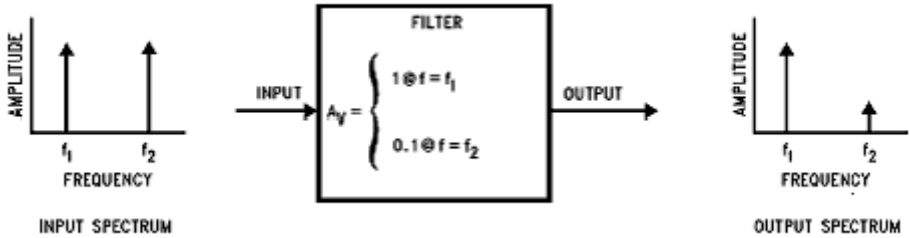


Figure 3.2 Frequency spectrum of filter

3.2 Frequency response

Simple filters are usually defined by their responses to the individual frequency components that constitute the input signal. There are three different types of responses. A filter's response to different frequencies is characterized as **pass band, transition band, or stop band**.

The *pass band response* is the filter's effect on frequency components that are passed through (mostly) unchanged. Frequencies within a filter's *stop band* are, by contrast, highly attenuated. The *transition band* represents frequencies in the middle, which may receive some attenuation but are not removed completely from the output signal.

In fig. 3.3, which shows the frequency response of a low pass filter, ω_p is the pass band ending frequency, ω_s is the stop band beginning frequency, and A_s is the amount of attenuation in the stop band. Frequencies between ω_p and ω_s fall within the transition band and are attenuated to some lesser degree.

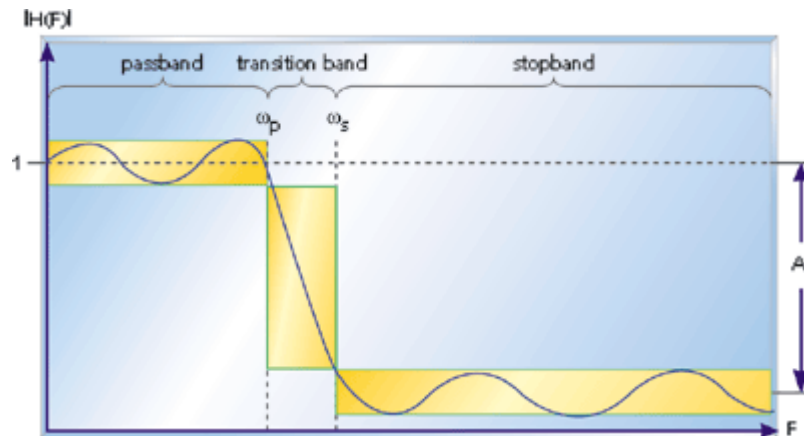


Figure 3.3 Response of a low pass filter to various input frequencies

Given these individual filter parameters, one can generate the required signal processing equations and coefficients for implementation on a DSP. There are some additional terms, which are needed to be introduced.

Ripple is usually specified as a peak-to-peak level in decibels. It describes how little or how much the filter's amplitude varies within a band. Smaller amounts of ripple represent more consistent response and are generally preferable.

Transition bandwidth describes how quickly a filter transitions from a pass band to a stopband, or vice versa. The more rapid this transition, the higher the transition bandwidth; and the more difficult the filter is to achieve. Though an almost instantaneous transition to full attenuation is typically desired, real-world filters don't often have such ideal frequency response curves.

There is, however, a tradeoff between ripple and transition bandwidths, so that decreasing either will only serve to increase the other.

3.2.1 Gain vs. frequency Plots

The gain vs. frequency plot is also called bode plot. *Bode plots* describe relation between magnitude of the filter's response (gain in dB) and its frequency (in hertz) on a logarithmic scale. An example of this type of plot is shown in fig. 3.4.

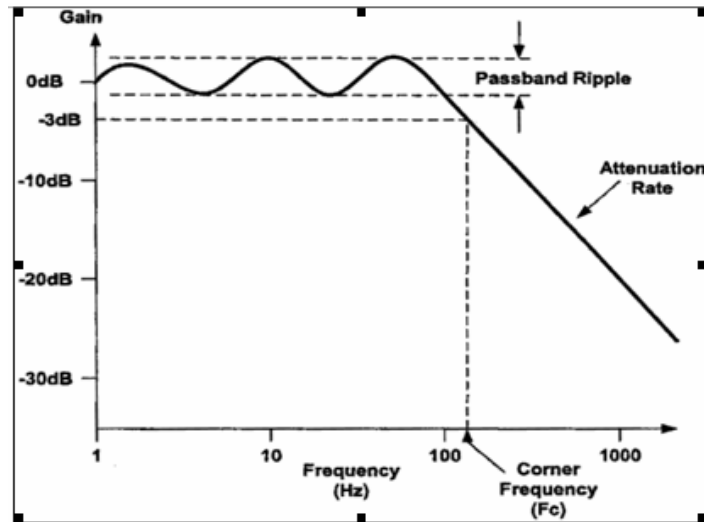


Figure 3.4 Gain vs. frequency plot

Bode plot provides an easy way to describe the filter's response over several decades of frequency and several orders of magnitude [4]. The decibels of gain of a filter relate to the ratio between input and output voltages:

$$dB = 20 \log \left[\frac{V_{out}}{V_{in}} \right] \dots \dots \dots (3.2)$$

Few terms to understand the bode pot are:

Corner Frequency is the frequency at which gain is 3dB down the zero frequency. That's why it is also called 3dB-frequency. As a real filter rolls off gradually, we usually specify the corner frequency as the frequency at which the response is $1/\sqrt{2}$ (0.707) of that in the pass band.

Attenuation Rate is commonly expressed in terms of decibels per decade, where a decade is a factor of 10 in frequency. Attenuation rate is the rate at which transition between the

pass band and the stop band occurs. It is a continuous function, and the rate at which this transition occurs is a common metric used to select a filter. A high attenuation rate is usually a desirable feature. It helps a filter distinguish between signals of similar frequency. The attenuation rate is also related to the order of a filter. For a low-pass or a high-pass filter, the attenuation rate will be -20 times the filter's order, in dB/decade. For example, a first-order filter will have an attenuation rate of -20 dB/decade, while a fourth-order filter will have an -80 dB/decade attenuation rate.

Pass-Band Ripple is the variation of the magnitude of the response inside the pass band. For many types of filters, the response does not decrease monotonically as frequency moves from the center of the pass band out toward the stop band. Pass-band ripple causes the frequency components of a signal to be amplified to different degrees. This has the effect of distorting the waveform of a signal passing through the filter. Again, this metric is also specified in decibels. In addition to affecting the amplitude of a signal, a filter can also cause changes in the phase of signal components.

3.3 Important Properties of Filters

1. **Filter Order:** The order of a filter is important for several reasons. It is directly related to the number of components in the filter, and therefore to its cost, its physical size, and the complexity of the design task. Therefore, higher-order filters are more expensive, take up more space, and are more difficult to design. The primary advantage of a higher order filter is that it will have a steeper roll-off slope than a similar lower-order filter.
2. **Ultimate Roll-off Rate:** Usually expressed as the amount of attenuation in dB for a given ratio of frequencies. The most common units are " dB/octave " and " dB/decade ". While the ultimate roll-off rate will be 20 dB/decade for every filter pole in the case of a low-pass or high-pass filter and 40 dB/decade for every pair of poles for a bandpass filter, some filters will have steeper attenuation slopes near the cutoff frequency than others of the same order.

3. **Attenuation Rate near Cutoff Frequency:** If a filter is intended to reject a signal very close in frequency to a signal that must be passed, a sharp cutoff characteristic is desirable between those two frequencies. Note that this steep slope may not continue to frequency extremes.
4. **Transient Response:** Curves of amplitude response show how a filter reacts to steady-state sinusoidal input signals. Since a real filter will have far more complex signals applied to its input terminals, it is often of interest to know how it will behave under transient conditions. An input signal consisting of a step function provides a good indication of this.
5. **Monotonicity:** A filter has a monotonic amplitude response if its gain slope never changes signs. In other words, if the gain always increases with increasing frequency or always decreases with increasing frequency. Obviously, this can happen only in the case of a low-pass or high-pass filter. A bandpass or notch filter can be monotonic on either side of the center frequency, however.
6. **Passband Ripple:** If a filter is not monotonic within its passband, the transfer function within the passband will exhibit one or more "bumps". These bumps are known as "ripple". Some systems don't necessarily require monotonicity, but do require that the passband ripple be limited to some maximum value (usually 1 dB or less). Although bandpass and notch filters do not have monotonic transfer functions, they can be free of ripple within their passbands.
7. **Stopband Ripple:** Some filter responses also have ripples in the stopband. One is normally unconcerned about the amount of ripple in the stopband, as long as the signal to be rejected is sufficiently attenuated. Given that the "ideal" filters amplitude response curves are not physically realizable, an acceptable approximation to the ideal response must be chosen. The word "acceptable" may have different meanings in different situations. The acceptability of a filter design will depend on many interrelated factors, including the amplitude response characteristics, transient

response, and the physical size of the circuit and the cost of implementing the design. The "ideal" lowpass amplitude response is shown again in fig. 3.5(a). If one is willing to accept some deviations from this ideal in order to build a practical filter, he might end up with a curve like the one in fig. 3.5(b) which allows ripple in the passband, a finite attenuation rate, and stopband gain greater than zero.

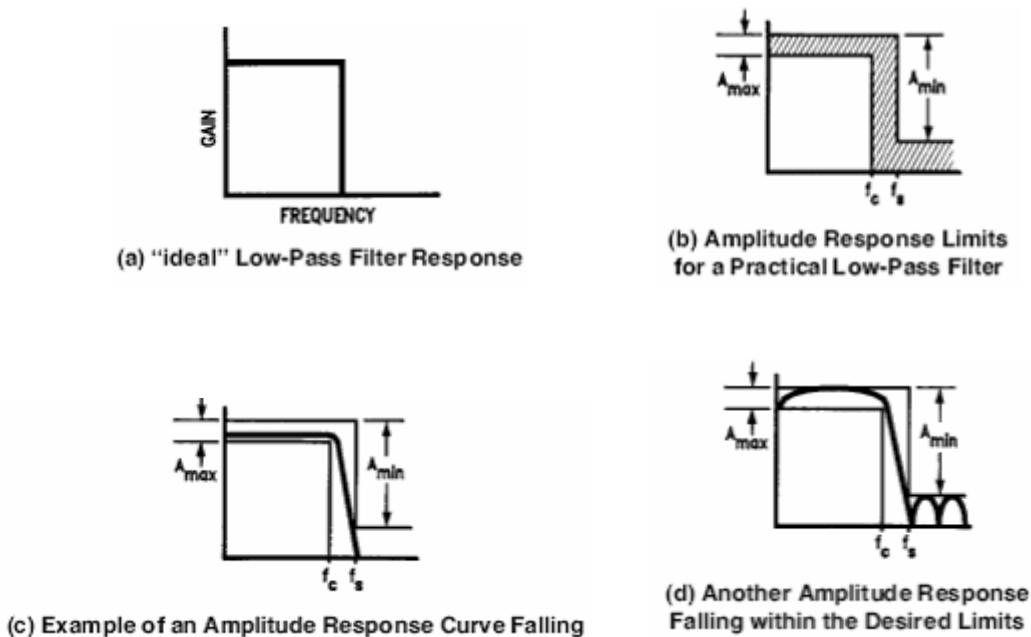


Figure 3.5 Different examples of amplitude response

A_{max} is the maximum allowable change in gain within the passband. This quantity is also often called the maximum passband ripple, but the word "ripple" implies non-monotonic behavior, while A_{max} can obviously apply to monotonic response curves as well.

A_{min} is the minimum allowable attenuation (referred to the maximum passband gain) within the stopband.

f_c is the cutoff frequency or passband limit and

f_s is the frequency at which the stopband begins.

If one can define filter requirements in terms of these parameters, he will be able to design an acceptable filter using standard "cookbook" design methods. It should be apparent that an unlimited number of different amplitude response curves could fit within the boundaries determined by these parameters, as shown in fig. 3.5(c) and (d)

3.4 Classification of Filters

- **Filters based on signals used**
 - **Digital filters and**
 - **Analog filters**
- **Filters based on components used**
 - **Continuous time filters**
 - ❖ **Passive filters**
 - ❖ **Active filters**
 - **Switched capacitor filters**
- **Filters based on frequency response**
 - **Low pass filters**
 - **High pass filters**
 - **Band pass filters**
 - **All pass filters**
 - **Band stop filters**
- **Filters based on mathematical functions**
 - **Butterworth filters**
 - **Chebyshev filters**
 - **Bessel filters**
 - **Elliptic filters**

3.4.1 Digital Filters and Analog Filter

A **digital filter** takes a digital input, gives a digital output, and consists of digital components. In a typical digital filtering application, software running on a digital signal processor (DSP) reads input samples from an A/D converter, performs the mathematical manipulations dictated by theory for the required filter type, and outputs the result via a D/A converter.

An **analog filter**, by contrast, operates directly on the analog inputs and is built entirely with analog components, such as resistors, capacitors, and inductors. The performance of

analog filters is directly related to the quality of the components used and the circuit design. Operational amplifiers are commonly used to increase the performance of these filters.

3.4.2 Continuous Time and Switched Capacitor Filters

The **continuous-time filters** are processed on a discrete-time, rather than continuous, basis. They usually need some external components to adjust for corner frequency, making them limited in their flexibility.

Passive filters are made up of passive components like resistors, capacitors, and inductors, so they are referred to as passive filters. A passive filter uses no amplifying elements (transistors, operational amplifiers, etc.).

3.4.2.1 Advantages

- Provide simplest implementation of a given transfer function.
- Require no power supplies.
- Can work well at very high frequencies.
- Used in applications involving large current or voltage levels.
- Generate little noise when compared with active filters.

3.4.2.2 Disadvantages

- Cannot provide signal gain.
- Input impedances can be lower than desirable, and output impedances can be higher for some applications, so buffer amplifiers may be needed.
- Require inductors for the synthesis of most useful passive filter characteristics and can be prohibitively expensive if high accuracy (1% or 2%) is required.
- Tuning these to the required values is time-consuming and expensive.
- Complex passive filters (higher than 2nd-order) can be difficult and time-consuming to design.

Active filters use amplifying elements, especially op amps, with resistors and capacitors in their feedback loops, to synthesize the desired filter characteristics. Active filters can have high input impedance, low output impedance, and virtually any arbitrary gain. They are easier to design than passive filters. They do not require any inductor. Still, the problems of accuracy and value spacing also affect capacitors. At high frequencies their performance is limited by the gain-bandwidth product of the amplifying elements. Active filters generate noise due to the amplifying circuitry, but this can be minimized by the use of low-noise amplifiers and by designing the circuit carefully.

Switched-capacitor filters are clocked, sampled-data systems; the input signal is sampled at a high rate and is processed on a discrete-time, rather than continuous, basis. *Switched capacitors* can, due to their architecture, be very flexible. If used properly, they can be an excellent alternative to both discrete and integrated continuous-time filters. The operation of switched-capacitor filters is based on the ability of on-chip capacitors and MOS switches to simulate resistors. The primary weakness of switched-capacitor filters is that they have more noise than active filter at their outputs.

3.4.3 Lowpass, Highpass, Bandpass, Allpass, Bandstop Filters

A **low pass filter** allows only low frequency signals (below some specified cutoff) through to its output and attenuates all signal components higher than the frequency cut-off. A low pass filter is handy, in that regard, for limiting the uppermost range of frequencies in an audio signal. It is the type of filter that a phone line resembles. Low-Pass filters. This filter type is useful in improving signal to noise ratio by also reducing system intrinsic noise.

A **high pass filter** does just the opposite, attenuate all low frequency components below the cut-off frequency and remove the dc component (0 Hz) from the signal. This is useful in removing the dc offset that may be causing an overload condition to occur. An example of high pass application is cutting out the audible 60 Hz AC power "hum", which can be picked up as noise accompanying almost any signal in the U.S.

Band pass filter allows certain band of frequency to pass. Band-Pass filters can be designed for broadband or narrow-band applications and are essentially the combination of a High-Pass and Low-Pass filter pair. The designer of a cell phone or any other sort of wireless transmitter would typically place an analog band pass filter in its output RF stage, to ensure that only output signals within its narrow, government-authorized range of the frequency spectrum are transmitted.

All pass or a phase-shift filter has no effect on the amplitude of the signal at different frequencies. Instead, its function is to change the phase of the signal without affecting its amplitude. This type of filter is particularly useful in dealing with group-delay problems or shaping the phase response of a transfer function.

Band stop filters sometimes called a Notch Filters pass both low and high frequencies and block a predefined range of frequencies in the middle; just reverse of band pass filters. This filter offers high attenuation over a narrow range of frequencies.

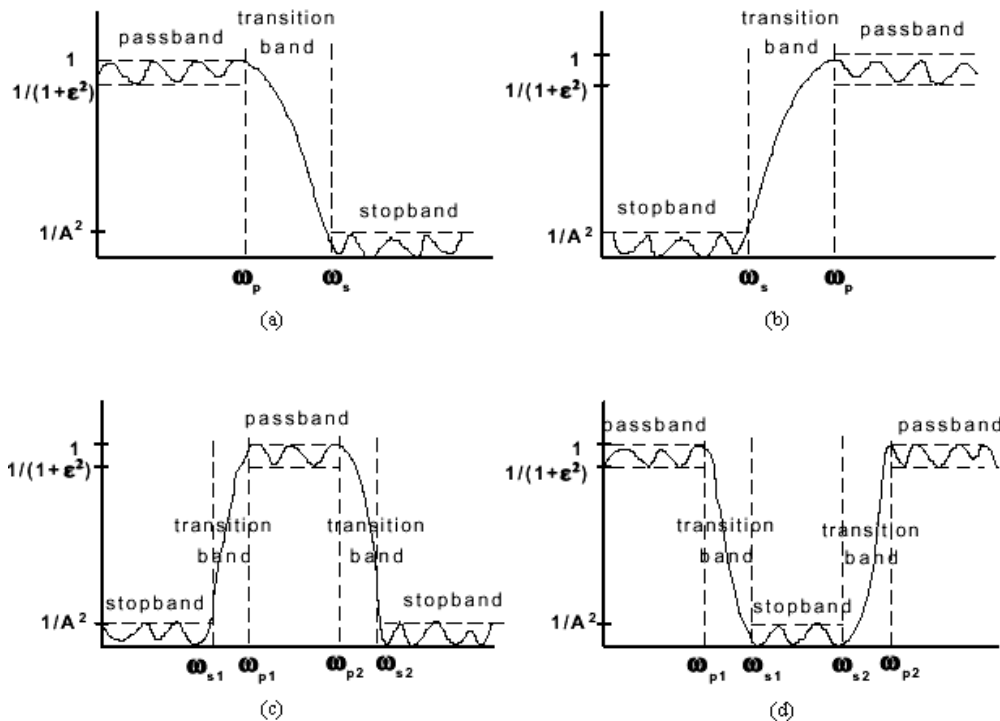


Figure3.6 Different response categories of filters

3.4.4 Butterworth, Bessel, Chebyshev, Elliptic Filters

The "classic" filter functions were developed by mathematicians (most bear their inventors' names), and each was designed to optimize some filter property. Filters with acceptable amplitude response curves may differ in terms of such characteristics as transient response, pass band and stopband flatness, and complexity. A great deal of work has already been done in this area, and a number of standard filter characteristics have already been defined. These usually provide sufficient flexibility to solve the majority of filtering problems. Widely used filters are discussed below [30].

3.4.4.1 Butterworth filters

Butterworth filters are causal in nature and of various orders, the lowest order being the best (Shortest) in the time domain, and the higher orders being better in the frequency domain. Butterworth filters are suitable for applications in which any ripples are intolerable. These filters have a monotonic amplitude frequency response, which is maximally flat at zero frequency response, and the amplitude frequency response decreases logarithmically with increasing frequency. Their monotonic response shape is due to maximization of the number of derivatives whose value is zero around the filter center frequency. For a filter of order n , the maximum number of zero derivatives is $2n-1$. For this reason, the Butterworth filter is also called a "maximally-flat amplitude" filter. The roll off is smooth and monotonic, with a low-pass or high-pass roll off rate of 20 dB/decade (6 dB/octave) for every pole. The Butterworth filter has minimal phase shift over the filter's band pass when compared to other conventional filters. The general equation for Butterworth filter's amplitude response is

$$H(\omega) = \frac{1}{1 + \left(\frac{\omega}{\omega_0}\right)^{2n}} \dots\dots\dots(3.3)$$

Where n is the order of the filter, and can be any positive whole number (1, 2, 3 . . .), and ω_0 is the 3 dB frequency.

If ϵ is passband ripple, A is stopband attenuation, ω_0 is passband edge frequency and ω_s is stopband edge frequency, required filter order can be found by the formula [34]:

$$n = \frac{\ln(\epsilon / \sqrt{A^2 - 1})}{\ln(\omega_p / \omega_s)} \dots\dots\dots(3.4)$$

These filters provide the best Taylor Series approximation to the ideal low pass filter response at analog frequencies $\Omega = 0$ and $\Omega = \infty$; for any order n , the magnitude squared response has $2n-1$ zero derivatives at these locations (maximally flat at $\Omega = 0$ and $\Omega = \infty$). Response is monotonic, decreasing smoothly from $\Omega = 0$ to $\Omega = \infty$.

$$|H(j\Omega)| = \sqrt{1/2} \text{ at } \Omega = 1 \dots\dots\dots(3.5)$$

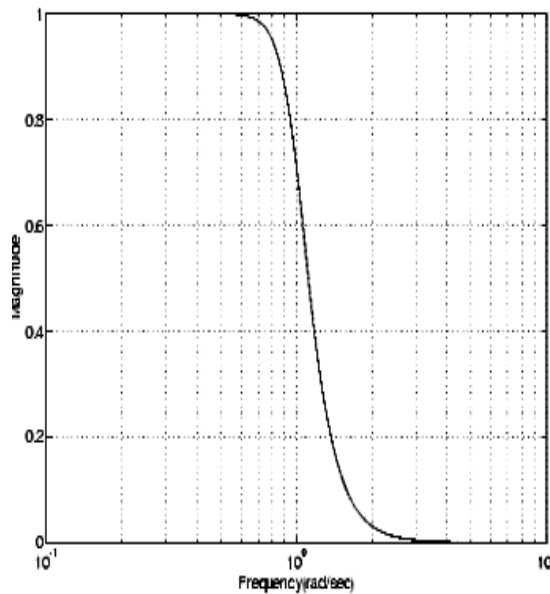


Figure 3.7 Butterworth filter response

3.4.4.2 Chebyshev filters

The term Chebyshev refers to a type of filter response, not a type of filter. It is sometimes referred to as an equal-ripple approximation, and sometimes spelled "Tschebysheff" or some variation thereof. The response of Chebyshev filters is based on the minimization of the maximum error in the entire passband, resulting in passband ripples with equal amplitude. The greater the ripple amplitude allowed, the steeper the transition roll-off. Chebyshev filters are also known as "equiripple" or "minimax" filters because of their characteristics. Although Butterworth filters possess a monotonic response, they constrain other filter shape properties such as transition steepness and out-of-band rejection. If the passband's non-monotonicity is tolerable, a filter design based on Chebyshev polynomials can achieve a prescribed attenuation level with lower filter order. The Chebyshev lowpass magnitude response can be described by

$$\left|H(\omega)\right|^2 = \frac{1}{1 + \varepsilon^2 T_n^2(\omega/\omega_p)} \dots\dots\dots(3.6)$$

The function $T_n(x)$ is a Chebyshev polynomial given by

$$T_n(x) = \begin{cases} \cos(n \cos^{-1} x); |x| \leq 1 \\ \cosh(n \cosh^{-1} x); |x| > 1 \end{cases} \dots\dots\dots(3.7)$$

The $T_n(x)$ magnitude oscillates between ± 1 for $|x| \leq 1$ and grows as n^x for $|x| > 1$

If ε is passband ripple, A is stopband attenuation, ω_0 is passband edge frequency and ω_s is stopband edge frequency, required filter order can be determined by the formula

$$n = \frac{\cosh^{-1}\left(\sqrt{A^2 - \frac{1}{\varepsilon^2}}\right)}{\cosh^{-1}\left(\frac{\omega_s}{\omega_p}\right)} \dots\dots\dots(3.8)$$

Comparing (3.4) and (3.8), it can be shown that a Chebyshev filter achieves a $(6n-6)$ dB lower out-of-band attenuation than a Butterworth filter for a filter order n [34].

Chebyshev filters are of two types: chebyshev type I and chebyshev type II

The **Chebyshev Type I filters** are all pole filters which are equiripple in the pass band and are monotonic in the stop band. These minimize the absolute difference between the ideal and actual frequency response over the entire pass band by incorporating an equal ripple of R_p dB in the pass band. Stop band response is maximally flat. The transition from pass band to stop band is more rapid than for the Butterworth filter, but at the expense of monotonicity in the pass band and poorer transient response. It features superior attenuation in the stop band, at the expense of ripple in the pass band. Generally the designer will choose a ripple depth of between 0.1 dB and 3 dB. Chebyshev filter response, therefore, is not limited to a single value of response. The amount of pass band ripple is one of the parameters used in specifying a Chebyshev filter.

$$|H(j\omega)| = 10^{-R_p/20} \text{ at } \Omega = 1 \dots\dots\dots(3.9)$$

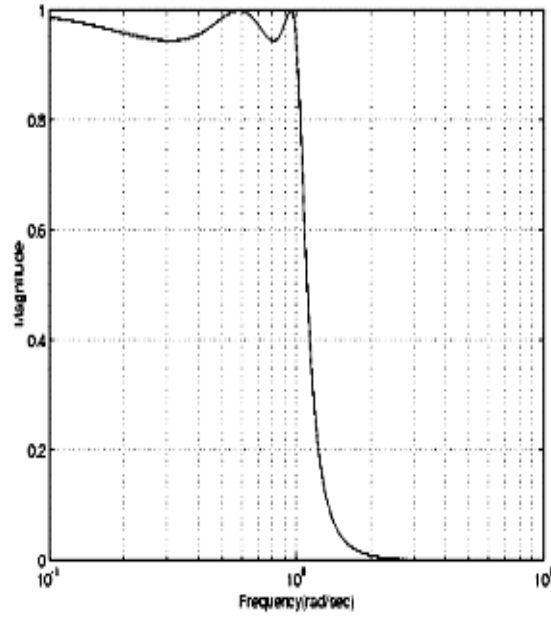


Figure 3.8 Chebyshev I filter response

The **Chebyshev Type II filter** contains both poles and zeros exhibiting a monotonic behavior in the passband and equiripple of R_s dB in the stopband and thus minimizes the absolute difference between the ideal and actual frequency response over the entire.

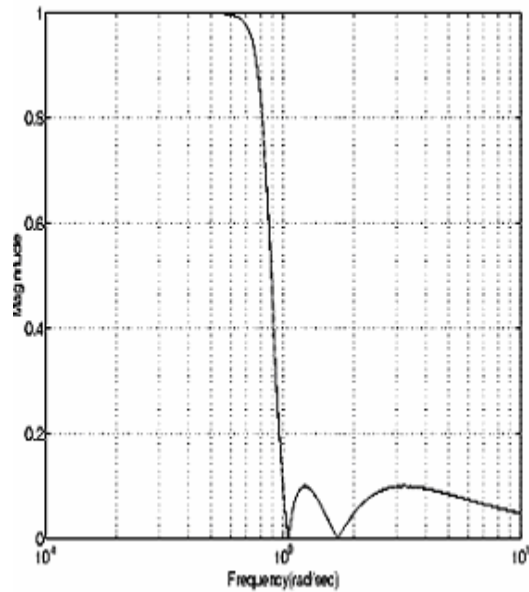


Figure 3.9 Chebyshev II filter response

Its passband response is maximally flat. The stopband does not approach zero as quickly as the type I filter (and does not approach zero at all for even-valued filter order n). The absence of ripple in the passband, however, is often an important advantage.

$$|H(j\Omega)| = 10^{-R_s/20} \text{ at } \Omega = 1 \dots \dots \dots (3.10)$$

3.4.4.3 Bessel filters

Certain applications, e.g., pulse transmission, prefer a filter response with constant group delay to filter bandwidth in order to prevent transient dispersion. Analog **Bessel filters** (low pass) have a linear phase and maximally flat delay characteristics at the expense of slowest roll-off, at zero frequency and retain nearly constant group delay across the entire passband, however, the magnitude response is much less selective than in the other filter types. Filtered signals therefore maintain their wave shapes in the passband frequency range. The lowpass magnitude response is given by [34]

$$|H(\omega)|^2 = \frac{1}{\left(\frac{\omega}{\omega_c}\right)^{n+1} \sqrt{\frac{\pi}{2} \left(\frac{\omega_c}{\omega}\right) \left[J_{-n-1/2}^2\left(\frac{\omega}{\omega_c}\right) + J_{n+1/2}^2\left(\frac{\omega}{\omega_c}\right) \right]}} \dots \dots \dots (3.11)$$

at $\Omega = 1$, it is given by

$$|H(j\omega)| < \sqrt{1/2} \dots \dots \dots (3.12)$$

Where $J_n(x)$ is the n^{th} -order Bessel function. As filter order n increases, the region of flat delay is extended into the stopband. However, the steepness of the roll-off in the transition region does not improve significantly. This restricts the use of Bessel filters to applications where the transient properties are the major consideration. Bessel filters generally require a higher filter order than other for satisfactory stopband attenuation. The higher the filter order, the more linear the Bessel's phase response.

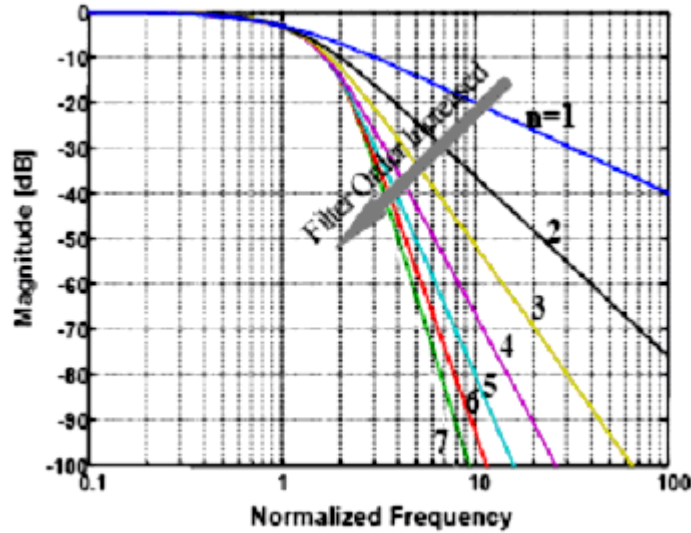


Figure 3.10 Magnitude response of Bessel filter as a function of filter order

All filters exhibit phase shift that varies with frequency. However, if the phase shift is not directly proportional to frequency, components of the input signal at one frequency will appear at the output, shifted in phase (or time) with respect to other frequencies. The overall effect is to distort non-sinusoidal wave shapes. Bessel or Thompson filters help in avoiding this phenomenon and exhibits approximately linear phase shift with frequency.

3.4.4.4 Elliptic filters

If ripples are allowed in both the passband and the stopband, steeper transition rolloff can be achieved. An Elliptic filter is an example of a filter that can achieve steeper transition rolloff by introducing complex zero pair to provide notching at the stopband frequency, at the expense of a stopband response that bounces back up beyond the notch frequency. The Elliptic filter’s lowpass magnitude response is given by [34]

$$|H(\omega)|^2 = \frac{1}{1 + \varepsilon^2 Z_n^2(\omega/\omega_c)} \dots\dots\dots(3.13)$$

Where $Z_n(x)$ is an Elliptic function of order n.

$$Z_n(x) = \int_0^x \frac{dy}{\sqrt{(1-y^2)(1-n^2y^2)}} \dots\dots\dots(3.14)$$

Similar to Chebyshev polynomials, Elliptic functions oscillate within a narrow bound for arguments less than unity and grow in magnitude for arguments outside the unity range. In addition, instead of growing monotonically as Chebyshev polynomials do, Elliptic functions oscillate between infinity and some finite value for arguments outside the unity range. Thus, the Elliptic filter response exhibits ripples in the stopband. These filters generally meet filter requirements with the lowest order of any supported filter type. Given a filter order n , passband ripple R_p in decibels, and stopband ripples R_s in decibels, elliptic filters minimize transition width.

$$|H(j\Omega)| = 10^{-R_p/20} \text{ at } \Omega = 1 \dots \dots \dots (3.15)$$

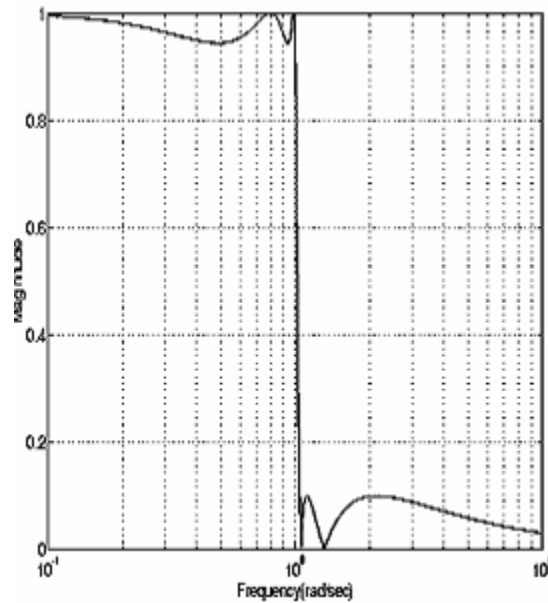


Figure 3.11 Elliptic filter response

The elliptic function gives a sharp cutoff by adding notches in the stopband. These cause the transfer function to drop to zero at one or more frequencies in the stopband. Ripple is also introduced in the passband. An elliptic filter function can be specified by three parameters (again excluding gain and cutoff frequency): passband ripple, stopband attenuation, and filter order n . Because of the greater complexity of the elliptic filter, determination of coefficients is normally done with the aid of a computer. The cutoff slope of an elliptic filter is steeper than that of a Butterworth, Chebyshev, or Bessel at the expense of the presence of ripples in both passband and stopband.

3.4.4.5 Comparison of Various Filters

Comparison of the responses of Butterworth, Chebyshev, Bessel, and Elliptic filters for the same frequency specifications, with regard to flatness, transition-band characteristics, and phase response

Table 3.1 Comparison of various parameters of filters

	Bessel filter	Butterworth filter	Chebyshev filter	Elliptic filter
Flatness:	monotonic passband and stopband response	monotonic passband and stopband characteristics	ripples in passband and monotonic stopband (Chebyshev I) or vice-versa (Chebyshev II)	magnitude response has ripples in both passband and stopband
Phase:	phase response linear over the entire passband	phase response linear over three quarters of passband	phase response linear over half of passband	phase response linear over one quarter of passband
Transition:	transition band wider than Butterworth	transition band is wide	transition band wider than elliptic but narrower than Butterworth	transition band is narrowest
Model:	all-pole transfer function	all-pole transfer function transfer	function has both poles and zeroes	transfer function has both poles and zeroes

Comparison of various magnitude responses

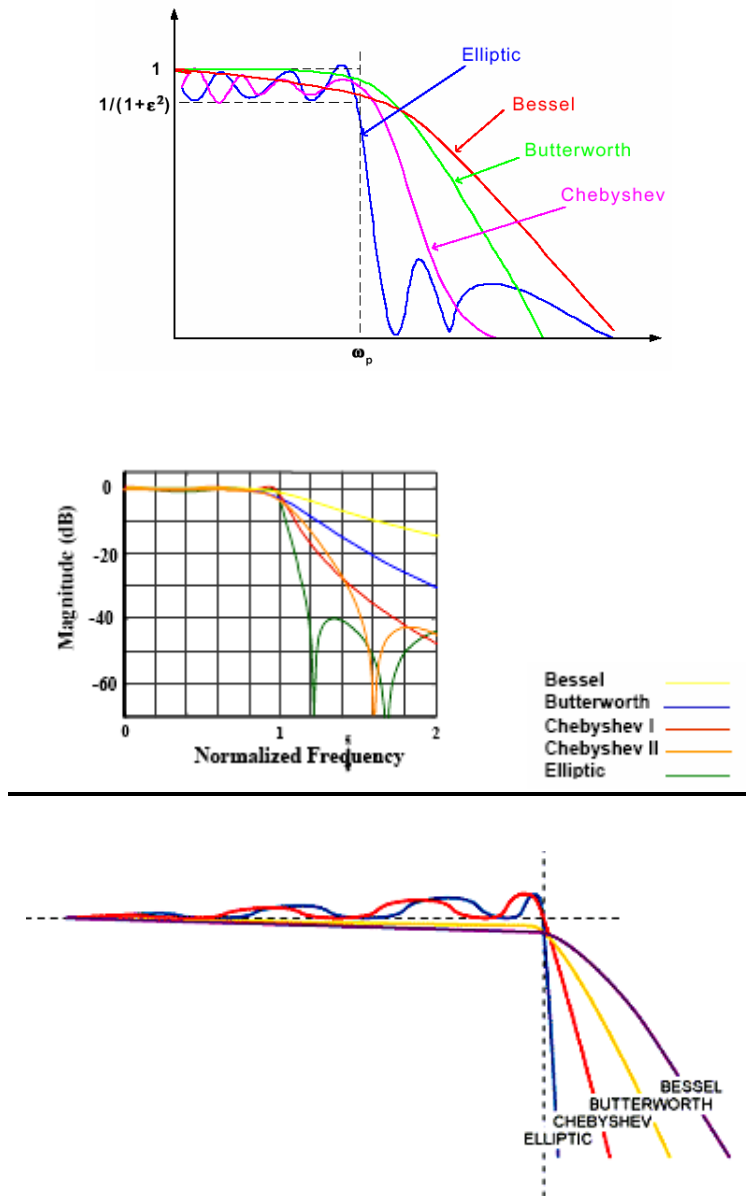


Figure 3.12 Different views of voltage-frequency curve

It can be seen (fig. 3.12) that there is ripple in the passband of a Chebyshev filter. The number and position of ripples is determined by the order of the filter. Filters with even orders generate ripple that appears above the 0 dB intercept and with odd orders generate ripple below the 0 dB intercept.

Comparison of various group delays

Group delay is defined as the derivative of the phase response with respect to frequency. Group Delay is the phase slope on a linear phase vs. frequency plot. The group delay of the three filters is shown below (fig. 3.13). The Chebyshev response has the longest group delay [16].

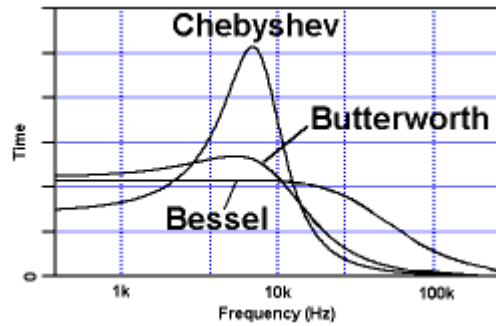


Figure 3.13 Group delay

Comparison of various phase responses

The phase response of the three filter types is shown below (fig. 3.14). The Chebyshev response has the fastest rate of phase change.

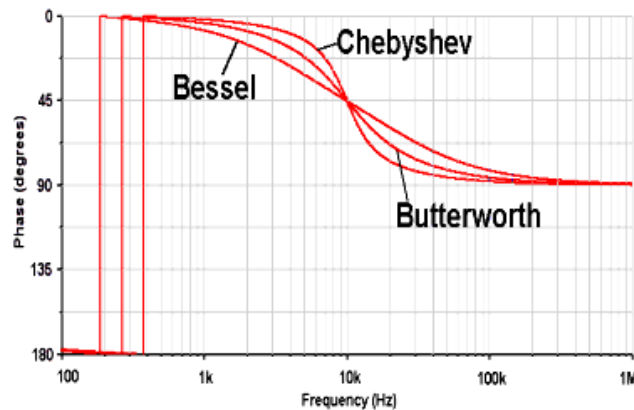


Figure 3.14 Phase response

Comparison of various singularities

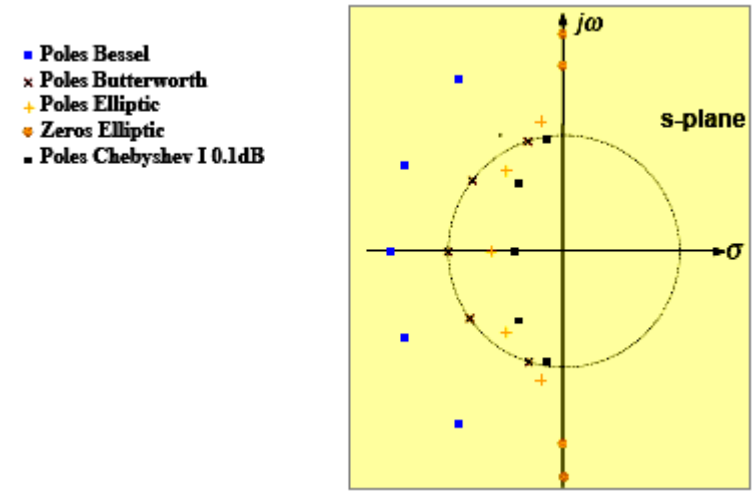


Figure 3.15 Pole-zero diagram

3.5 Chebyshev Filters

The Chebyshev response is a mathematical strategy for achieving a faster *roll-off* by allowing *ripple* in the frequency response. Analog and digital filters that use this approach are called *Chebyshev filters*. Chebyshev filters, are analog or digital filters having a steeper roll-off and more passband ripple than Butterworth filters. Chebyshev filters have the property that they minimise the error between the idealised filter characteristic and the actual over the range of the filter, but with ripples in the passband. As the ripple increases (bad), the roll-off becomes sharper (good). The Chebyshev response is an optimal trade-off between these two parameters. These filters are named from their use of the *Chebyshev polynomials*, developed by the Russian mathematician Pafnuti Chebyshev (1821-1894). This name has been translated from Russian and appears in the literature with different spellings, such as: Chebychev, Tschebyscheff, Tchebysheff and Tchebichef.

It is worth noting that the cutoff frequency of a Chebyshev filter is not assumed to be the -3 dB frequency as in the case of a Butterworth filter. Instead, the Chebyshev's cutoff frequency is normally the frequency at which the ripple specification is exceeded. The addition of passband ripple as a parameter makes the specification process for a

Chebyshev filter a bit more complicated than for a Butterworth filter, but also increases flexibility [20].

Further Chebyshev filter of order n will have n-1 peaks or dips in its passband response. Also the nominal gain of the filter is equal to the filter's maximum passband gain. An odd order Chebyshev will have a dc gain (in the low-pass case) equal to the nominal gain, with "dips" in the amplitude response curve equal to the ripple value. An even-order Chebyshev low-pass will have its dc gain equal to the nominal filter gain minus the ripple value; the nominal gain for an even-order Chebyshev occurs at the peaks of the passband ripple. Therefore, if one is designing a fifth-order Chebyshev low-pass filter with 0.5 dB ripple and you want it to have unity gain at dc; he has to design for a nominal gain of 0.5 dB [20].

3.5.1 Chebyshev Type I Filters

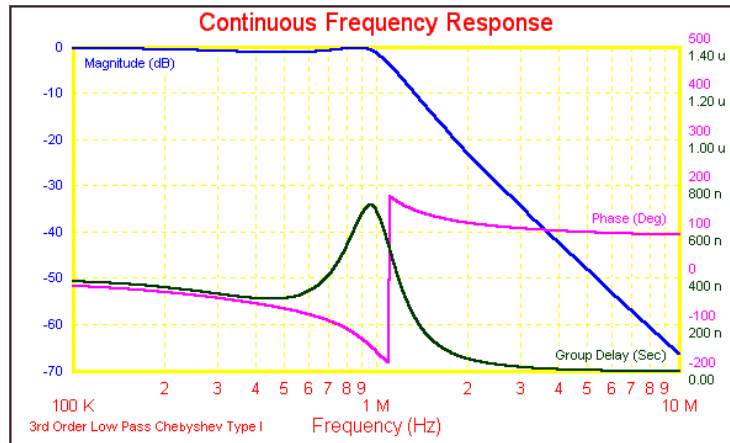
The Chebyshev Type I Filter is the filter type that results in the sharpest pass band cut off and contains the largest group delay. The most notable feature of this filter is the ripple in the pass band magnitude. The zeros of this class of filters lie on the imaginary axis in s-plane. That's why it is called as an all-pole filter. The magnitude squared of this frequency response characteristic this type is given as

$$|H(\Omega)|^2 = \frac{1}{1 + \varepsilon^2 T_n^2(\Omega/\Omega_p)} \dots\dots\dots(3.16)$$

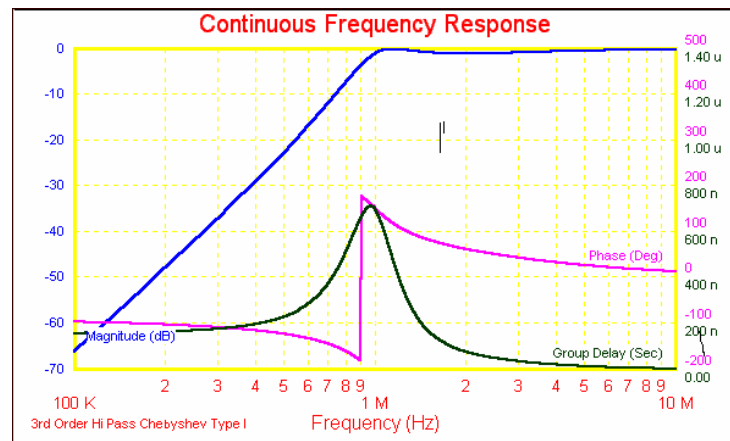
Where ε is the parameter of filter related to ripple in passband and $T_n(x)$ is nth-order Chebyshev polynomial [19].

A standard Chebyshev Type I Filter's pass band attenuation is defined to be the same value as the pass band ripple amplitude. However, Filter Solutions allows the user the option of selecting any pass band attenuation in dB's that will define the filters cut off frequency. Filter Solutions also offers the user the option of placing user-defined zeros in the stop band.

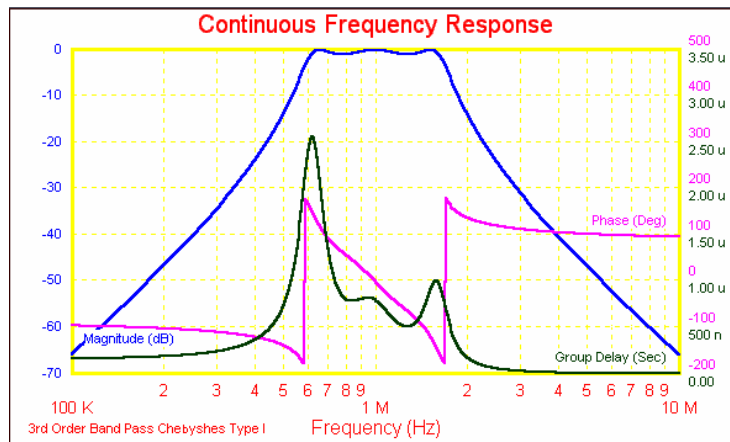
Below (fig. 3.16) are examples of Chebyshev Type I low pass, high pass, band pass and band stop filters and the low pass step response [13].



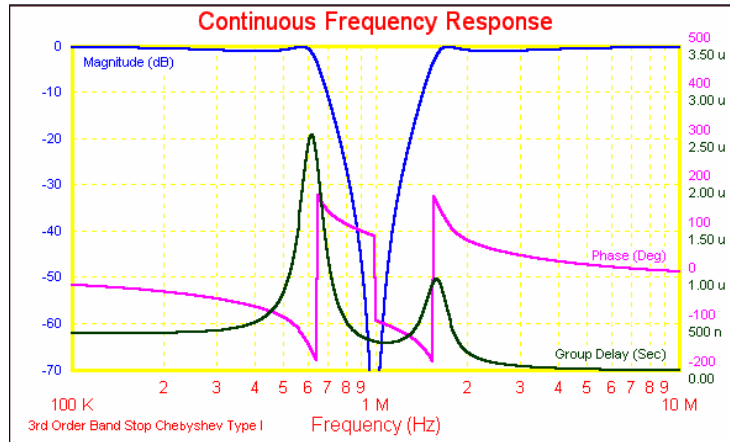
Chebyshev Type I Low Pass filter, 1MHz Pass Band Frequency



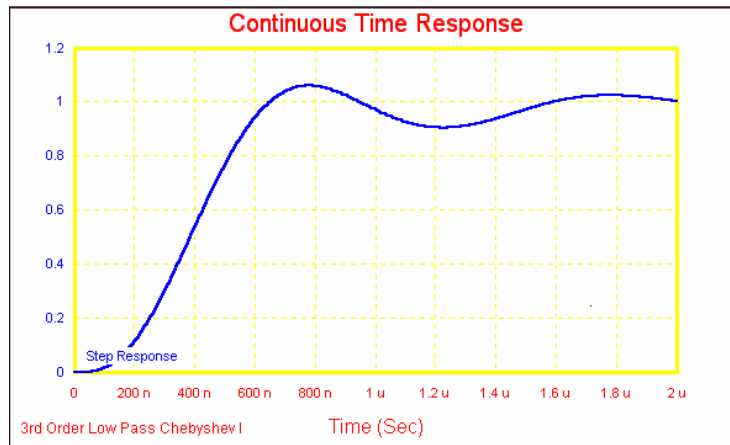
Chebyshev Type I High Pass filter, 1MHz Pass Band Frequency



Chebyshev Type I Band Pass filter, 1MHz Center Frequency, 1MHz Pass Band Width



Chebyshev Type I Band Stop filter, 1MHz Center Frequency, 1MHz Pass Band Width



Chebyshev Type I Low Pass Step Response

Figure 3.16 Various responses of Chebyshev type I filter

3.5.2 Chebyshev Type II Filters

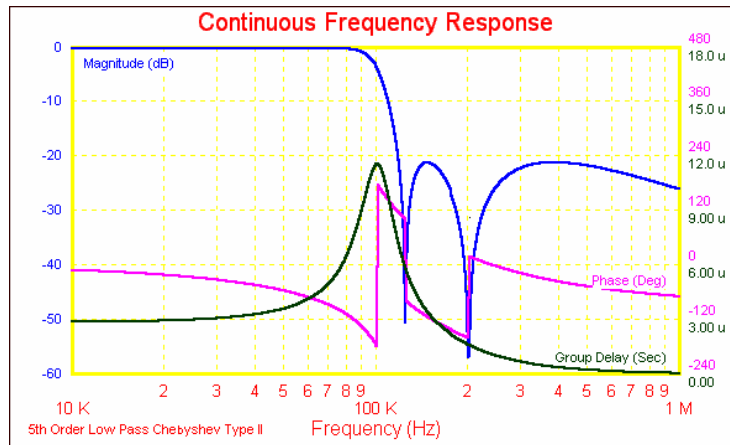
The Chebyshev Type II Filter, also known as the Inverse Chebyshev Filter, contains a Butterworth style, or maximally flat, pass band, a moderate group delay, and an equiripple stop band. This type contains zeros as well as poles. The zeros lie on imaginary axis. The magnitude squared of its frequency response is given as

$$|H(\Omega)|^2 = \frac{1}{1 + \varepsilon^2 \left[T_n^2(\Omega/\Omega_p) / T_n^2(\Omega_s/\Omega) \right]} \dots\dots\dots(3.17)$$

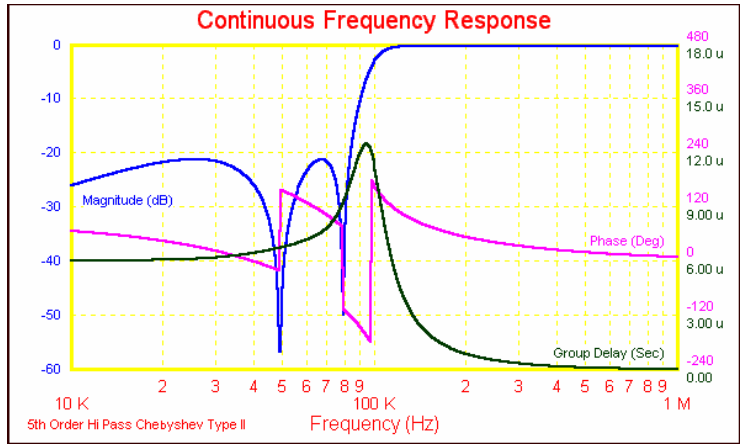
Where $T_n(x)$ is, again, n th-order Chebyshev polynomial and Ω_S is the stopband frequency [19].

Like the Butterworth Filter, the pass band attenuation of the Chebyshev Type II Filter is defined to be -3.01 dB. However, Filter Solutions allows the user the option of selecting any pass band attenuation in dB's that will define the filters cut off frequency.

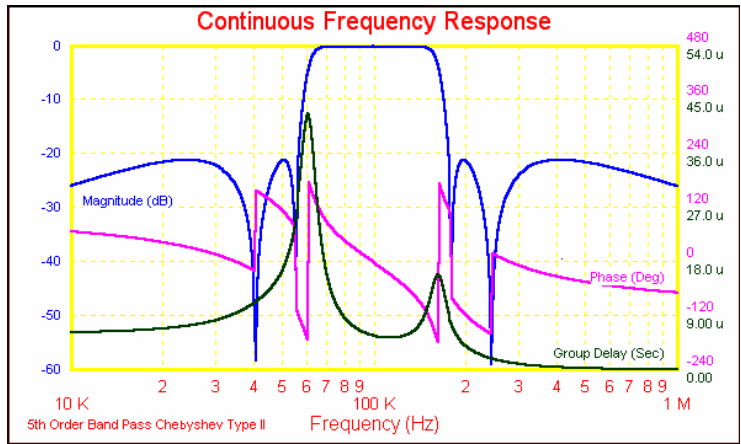
Below (fig. 3.17) are examples of 5th order Chebyshev Type II low pass, high pass, band pass and band stop filters and the low pass step response. The stop band ratio is 1.2 in all cases shown. Compare the stop band attenuation and the group delay to that of the Hourglass and Elliptic Filters [14].



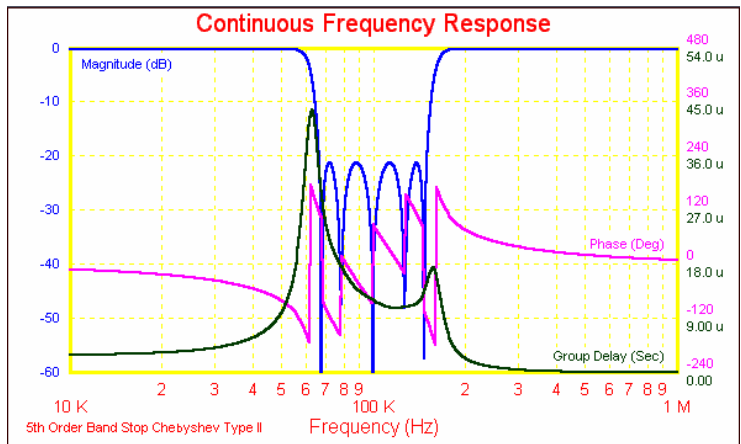
Chebyshev Type II Low Pass filter, 100KHz Pass Band Frequency



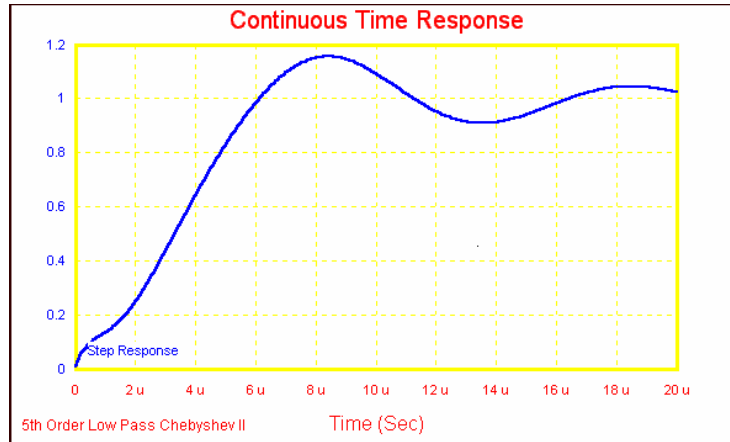
Chebyshev Type II High Pass filter, 100KHz Pass Band Frequency



Chebyshev Type II Band Pass filter, 100KHz Center Frequency, 100KHz Pass Band Width



Chebyshev Type II Band Stop filter, 100KHz Center Frequency, 100KHz Pass Band Width



Chebyshev Type II Low Pass Step Response

Figure 3.17 Various responses of Chebyshev type II filter

3.5.3 Chebyshev Polynomials

In mathematics the Chebyshev polynomials, named after Pafnuty Chebyshev, are a sequence of orthogonal polynomials which are related to de Moivre's formula and which are easily defined recursively, like Fibonacci or Lucas numbers. Chebyshev polynomials are denoted by $T_n(x)$ and here the letter T is used because of the alternative transliterations of the name *Chebyshev* as *Tchebyshef* or *Tschebyscheff* [15].

$$T_n(x) = \begin{cases} \cos(n \cos^{-1} x); & |x| \leq 1 \\ \cosh(n \cosh^{-1} x); & |x| > 1 \end{cases} \dots\dots\dots(3.18)$$

The chebyshev polynomial can be generated by the recursive equation [18]

$$T_{n+1}(x) = 2x T_n(x) - T_{n-1}(x), n = 1,2,\dots \dots\dots(3.19)$$

Where $T_0(x) = 1$ and $T_1(x) = x$. Using above equation

$$T_2(x) = 2x^2 - 1, T_3(x) = 4x^3 - 3x, \text{ and so on.}$$

Some properties of these polynomials are as follows:

1. $T_n(x) \leq 1$ for all $x \leq 1$.
2. $T_n(1) = 1$ for all N .
3. All the roots of polynomial $T_n(x)$ occur in the interval $-1 \leq x \leq 1$.

The Chebyshev polynomials can be defined by the trigonometric identity [14]

$$T_n(\cos(\theta)) = \cos(n\theta) \dots \dots \dots (3.20)$$

for $n = 0, 1, 2, 3, \dots$. That $\cos(nx)$ is an n th-degree polynomial in $\cos(x)$ can be seen by observing that $\cos(nx)$ is the real part of one side of de Moivre's formula, and the real part of the other side is a polynomial in $\cos(x)$ and $\sin(x)$, in which all powers of $\sin(x)$ are even and thus replaceable via the identity $\cos^2(x) + \sin^2(x) = 1$.

3.5.4 Order of Chebyshev filter

Chebyshev filters are characterized by the parameters n , ϵ , δ_2 and the ratio Ω_s/Ω_p .

n is the order of filter.

ϵ is the parameter related to ripple (δ_1), $\delta_1 = 10 \log_{10} (1+\epsilon^2)$.

Ω_s/Ω_p is the ratio of stopband and passband frequency.

δ_2 is the attenuation gain at stopband frequency.

For a given set of specifications on ϵ , δ_2 and Ω_s/Ω_p , the order of the filter can be

determined from the equation [19]

$$n = \frac{\log \left[\left(\sqrt{1 - \delta_2^2} + \sqrt{1 - \delta_2^2 (1 + \epsilon^2)} \right) / \epsilon \delta_2 \right]}{\log \left[\left(\Omega_s / \Omega_p \right) + \sqrt{\left(\Omega_s / \Omega_p \right)^2 - 1} \right]} \dots \dots \dots (3.21)$$

$$n = \frac{\cosh^{-1} \left(\frac{\delta}{\epsilon} \right)}{\cosh^{-1} \left(\frac{\Omega_s}{\Omega_p} \right)} \dots \dots \dots (3.22) \text{ Where, } \delta_2 = 1 / \sqrt{1 + \delta^2}$$

Chapter 4

INTRODUCTION TO TANNER TOOL

4.1 Introduction

Tanner Tool is a SPICE Computer Analysis Programmed for Analog Integrated circuits. Tanner Tool consists of the following Engine Machines:

1. S-EDIT (Schematic Edit)
2. T-EDIT (Simulation Edit)
3. W-EDIT (Waveforms Edit)
4. L-EDIT (Layout Edit)

Using these Engine tools, SPICE Programmes provides facility to the user to design and simulate new ideas in analog integrated circuits before going to the time consuming and costly process of chip fabrication.

4.2 S-EDIT (Schematic Edit)

S-Edit is hierarchy of files, modules and pages. It introduces symbol and schematic modes. S-Edit provides the facility of:

1. Beginning a design
2. Viewing, drawing and editing of objects
3. Design connectivity
4. Properties, net lists and simulations
5. Instance and browser schematic and symbol mode

In S-Edit, the available components from the library can be selected to make the schematic of the desired circuit. It explains the design process in detail in terms of file

module operation and module [6]. Effective schematic design requires a working knowledge of the S-Edit design files consist of modules. A module is a functional unit of design such as a transistor, a gate and an amplifier. Modules contain two components:

- a) Primitives – Geometrical objects created with drawing tools.
- b) Instances – References to other modules in file. The instanced module is the original.

Two viewing modes of the S-Edit are:

- a) Schematic mode – This mode helps in creating or viewing a schematic.
- b) Symbol mode – It represents symbol of a larger functional unit such as operational amplifier.

4.3 T-EDIT (Simulation Edit)

The heart of T-Spice operation is the output file (also known as the circuit description, the net list and the input deck). This is a plain text file that contains the device statement and simulation commands, drawn from the SPICE circuit description language with which T-Spice constructs a model of the circuit to be simulated. Input files can be created and modified with any text editor.

T-Spice is a tool used for simulation of the circuit. It provides the facility of

- a) Design Simulation
- b) Simulation commands
- c) Device Statements
- d) User-defined External Models
- e) Small Signal and noise models

T-spice uses Kirchoff's Current Law (KCL) to solve circuit problems. To T-Spice, a circuit is a set of devices attached to the nodes. The voltage at all nodes represents the circuit state. T-Spice solves for a set of node voltage that satisfied KCL (implying that sum of currents flowing into each node is zero).

In order to evaluate whether a set of node voltages is a solution, T-Spice computers and sums all the current flowing out of each device into nodes connected to it (its terminals). The relationship between the voltages at device terminals and the currents through the

terminal is determined by the device model for a resistor R is $I = \Delta V/R$. Where ΔV represents the voltage difference across the device.

4.3.1 DC Operating point analysis

DC operating point analysis finds a circuit's steady-state condition, obtained (in principle) after the input voltages have been applied for an infinite amount of time. The **.include** command causes T-Spice to read in the contents of the model file `m12_125.md` for the evaluation of transistors `m1n` and `m1p`. This file (which must be in the same directory as `invert1.sp`) consists of two **.model** commands, describing two MOSFET models called `nmos` and `pmos`:

```
.model nmos nmos
+ Level=2 Ld=0.0u Tox=225.00E-10
+ Nsub=1.066E+16 Vto=0.622490 Kp=6.326640E-05
+ Gamma=0.639243 Phi=0.31 Uo=1215.74
+ Uexp=4.612355E-2 Ucrit=174667 Delta=0.0
+ Vmax=177269 Xj=0.9u Lambda=0.0
+ Nfs=4.55168E+12 Neff=4.68830 Nss=3.00E+10
+ Tpg=1.000 Rsh=60 Cgso=2.89E-10
+ Cgdo=2.89E-10 Cj=3.27E-04 Mj=1.067
+ Cjsw=1.74E-10 Mjsw=0.195

.model pmos pmos
+ Level=2 Ld=0.03000u Tox=225.000E-10
+ Nsub=6.575441E+16 Vto=-0.63025 Kp=2.635440E-05
+ Gamma=0.618101 Phi=0.541111 Uo=361.941
+ Uexp=8.886957E-02 Ucrit=637449 Delta=0.0
+ Vmax=63253.3 Xj=0.112799u Lambda=0.0
+ Nfs=1.668437E+11 Neff=0.64354 Nss=3.00E+10
+ Tpg=-1.000 Rsh=150 Cgso=3.35E-10
+ Cgdo=3.35E-10 Cj=4.75E-04 Mj=0.341
+ Cjsw=2.23E-10 Mjsw=0.307
```

m12_125.md assigns values to various Level 2 MOSFET model parameters for both n - and p -type devices. When read by the input file, these parameters are used to evaluate Level 2 MOSFET model equations, and the results are used to construct internal tables of current and charge values. Values read or interpolated from these tables are used in the computations called for by the simulation. Two transistors, m1n and m1p, are defined in invert1.sp. These are MOSFETs, as indicated by the key letter m, which begins their names. Following each transistor name are the names of its terminals. The required order of terminal names is: drain–gate–source–bulk. Then the model name (nmos or pmos in this example), and physical characteristics such as length and width, is specified. The **.op** command performs a DC operating point calculation and writes the results to the file specified in the Simulate > Start Simulation dialog. The output file lists the DC operating point information for the circuit described by the input file.

4.3.2 DC Transfer analysis

DC transfer analysis is used to study the voltage or current at one set of points in a circuit as a function of the voltage or current at another set of points. This is done by *sweeping* the source variables over specified ranges, and recording the output. The **.dc** command, indicating transfer analysis, is followed by a list of sources to be swept, and the voltage ranges across which the sweeps are to take place.

For example, for inverter with dc input vin and output out, vin will be swept from 0 to 3 volts in 0.02 volt increments, and vdd will be swept from 2 to 4 volts in 0.5 volt increments. The transfer analysis will be performed as follows: vdd will be set at 2 volts and vin will be swept over its specified range; vdd will then be incremented to 2.5 volts and vin will be reswept over its range; and so on, until vdd reaches the upper limit of its range. The **.dc** command ignores the values assigned to the voltage sources vdd and vin in the voltage source statements, but they must still be declared in those statements. The results for nodes in and out are reported by the **.print** dc command to the specified destination.

4.3.3 Transient analysis

Transient analysis provides information on how circuit elements vary with time. The basic T-Spice command for transient analysis has three *modes*. In the *default* mode, the DC operating point is computed, and T-Spice uses this as the starting point for the transient simulation.

```
.tran 2n 600n  
.print tran in out
```

For the commands shown above, The **.tran** command specifies the characteristics of the transient analysis to be performed: it will last for 600 nanoseconds, with time steps no larger than 2 nanoseconds..

4.3.4 AC Analysis

AC analysis characterizes the circuit's behavior dependence on small-signal input frequency. It involves three steps: (1) calculating the DC operating point; (2) linearizing the circuit; and (3) solving the linearized circuit for each frequency.

```
Vin1 in1 GND 2  
Vdd Vdd GND 5.0  
vbias vbias GND 0.8  
vdiff in2 in1 -0.0007 AC 1 90  
.ac DEC 5 1 100MEG  
.print ac vdb(out)  
.print ac vp(out)  
.acmodel opamp1m.out {*}
```

For the commands shown above, three voltage sources (besides Vdd) are defined. vdiff sets the DC voltage difference between nodes in2 and in1 to -0.0007 volts; its AC magnitude is 1 volt and its AC phase is 90 degrees.

- Vin1 sets node in1 to 2 volts, relative to GND.
- vbias sets node vbias to 0.8 volts, relative to GND.

The **.ac** command performs an AC analysis. Following the **.ac** keyword is information concerning the frequencies to be swept during the analysis. In this case, the frequency is swept logarithmically, by decades (DEC); 5 data points are to be included per decade; the starting frequency is 1 Hz and the ending frequency is 100 MHz.

The two **.print** commands write the voltage magnitude (in decibels) and phase (in degrees), respectively, for the node out to the specified file. The **.acmodel** command writes the small-signal model parameters and operating point voltages and currents for all circuit devices (indicated by the wildcard symbol *) to the file opamp1m.out.

This example will generate two output files: opamp1.out, specified by the Simulate > Start Simulation command, and opamp1m.out, specified by the **.acmodel** command.

4.3.5 Noise Analysis

Real circuits, of course, are never immune from small, “random” fluctuations in voltage and current levels. In T-Spice, the influence of noise in a circuit can be simulated and reported in conjunction with AC analysis. The purpose of noise analysis is to compute the effect of the noise associated with various circuit devices on an output voltage or voltages as a function of frequency. Noise analysis is performed in *conjunction* with AC analysis; if the **.ac** command is missing, then the **.noise** command is ignored. With the **.ac** command present, the **.noise** command causes noise analysis to be performed at the same frequencies: starting at 1 Hz, ending at 100 MHz, 5 data points per decade. The **.noise** command takes two arguments: the *output* at which the effects of noise are to be computed, and the *input* at which the noise can be considered to be concentrated for the purposes of estimating the equivalent noise spectral density [33].

4.4 W- EDIT (Waveform Edit)

The ability to visualize the complex numerical data resulting from VLSI circuit simulation is critical to testing, understanding and improving these circuits. W-Edit is a waveform viewer that provides ease of use, power and speed in flexible environment designed for graphical data representation. The advantages of W-Edit include;

- a) Tight integration with T-Spice, Tanner EDA’s circuit level simulator. W-Edit can chart data generated by T-Spice directly, without modification of the output text data files. The data can also be charted dynamically as it is produced during the simulation.
- b) Chart can automatically configure for the type of data being presented.

- c) A data is treated by W-Edit as a unit called a trace. Multiple traces from different output files can be viewed simultaneously in single or several windows; traces can be copied and moved between charts and windows. Trace arithmetic can be performed on existed tracing to create new ones.
- d) Chart views can be panned back and forth and zoomed in and out, including specifying the exact X-Y co-ordinate range.
- e) Properties of axes, traces, rides, charts, text and colors can be customized.

Numerical data is input to W-Edit in the form of plain or binary text files. Header and comment information supplied by T-Spice is used for automatic chart configuration. Run time update of results is made possible by linking W-Edit to a running simulation in T-Spice. W-Edit saves data with chart, trace, axis and environment settings in files with the WDB (W-Edit Database) [33].

4.5 L-EDIT (Layout Edit)

It is a tool that represents the masks that are used to fabricate an integrated circuit. It describes the layout design in terms of files, cells and mask primitives. On the layout level the component parameters are totally different from schematic level. So, it provides the facility to the user to analyze the response of circuit before forwarding it to the time consuming and costly process of fabrication. There are rules for designing layout diagram of a schematic circuit using which user can compare the output response with the expected one [33].

4.5.1 L-Edit: An Integrated Circuit Layout Tool

In L-Edit layers are associated with masks used in fabrication process. Different layers can be conveniently represented by different colors and patterns. L-Edit describes a layout design in terms of files, cells, instances and mask primitives. One may load as many files as desired into memory. A file may be composed of any number of sets. These cells may be hierarchically related, as in a typical design, or they may be independent, as in a “library” file. Cells may contain any number or combination of mask primitives and instances of other cells.

Cells: The Basic Building Blocks

The basic building block of the integrated circuit design in L-edit is a cell.

Design layout occurs within cells. A cell can:

- ...Contain part or all of entire design.
- ...Be referenced in other cells as a sub-cell, or instance.
- ...Be made up entirely of instances of other cells.
- ...Contain original drawn objects, or primitives.
- ...Be made up entirely of primitives or a combination of primitives and instances of other cells.

Hierarchy

L-Edit supports fully hierarchical mask design. Cells may contain instances of other cells. An instance is a reference to a cell; should you edit the instanced cell, the change is reflected in all the instances of that cell. Instances simplify the process of updating a design, and also reduce data within the instanced cell— instead, only a reference to the instanced cell is stored, along with the information on the position of instance and on how the instance may be rotated or mirrored. There is no preset limit to the size or complexity of hierarchy. Cells may contain instances of other cells that in turn contain instances of other cells, to an arbitrary number of levels (subject only to hardware constraints).

L-Edit does not use a “separated” hierarchy: instances and primitives may coexist in the same cell at any level in the hierarchy. Design files are self-contained. The “pointer” to a cell contained in an instance always points to a cell within the same design file. When cells are copied from one file to another, L-Edit automatically copies across any cells that are instanced by the copied cell, to maintain the self-contained nature of the destination file.

Design Rules

Manufacturing constraints can be defined in L-Edit as design rules. Layout can be checked against these design rules.

Design Features

L-Edit is a full-custom mask editor. Manual layout can be accomplished more quickly because of L-Edit's intuitive user interface. In addition, one can construct special structures to utilize a technology without, worrying about problems caused by automatic transformations. Phototransistors, guard bars, vertical and horizontal bipolar transistors, static structures and Schottky diodes, for example, are as easy to design in CMOS-bulk technology as are conventional MOS transistors.

Floor plans

L-Edit is a manual floor-planning tool. One has the choice of displaying in—outline, identified only by name, or as fully fleshed-out mask geometry. When he displays his design in outline, he can manipulate the arrangement of the cells in the design quickly and easily to achieve the desired floor plan.

One can manipulate instances at any level in the hierarchy, with insides hidden or displayed, using the same graphical move/select operations or rotation/mirror commands that he use on primitive mask geometry.

Memory Limits

In L-Edit, one can make your design files as large as one like, given available RAM and disk space.

Hard Copy

L-Edit provides the capability to print hard copy of the design. A multistage option allows very large plots to be printed to a specific scale on multiple 8 ½ x 11-inch page. An L-Edit macro is available to support large-format, high-resolution, color plotting on inkjet plotters.

Variable Grid

L-Edit's grid options support lambda-based design as well as micron based and mil-based design.

Error Recovery

L-Edit's error-trapping mechanism catches system errors and in most cases provides a mean to recover without losing or damaging data.

L-Edit Module

...L-Edit™ : a layout editor

...L-Edit □ Extract™: a layout extractor

...L-Edit □ DRC™: a design rule checker

L-Edit is a full featured, high performance, interactive, graphical mask layout editor. L-Edit generates layouts quickly and easily, supports fully hierarchical design, and allows an unlimited number of layers, cells, and level of hierarchy. It includes all major drawing primitives and supports 90°, 45°, and all-angle drawing modes.

L-Edit □ Extract creates SPICE- compatible circuit netlists from L-Edit layouts. It can recognize active and passive devices, sub circuits and the most common device parameters, including resistance, capacitance, device length, width, and area, and device source and drain area.

L-Edit □ DRC features user- programmable rules and handles minimum width, exact width, minimum space, minimum surround, non-exist, overlap, and extension rules. It can handle full chip and region-only DRC. DRC offers Error Browser and Object browser functions for quickly and easily cycling through rule-checking errors [33].

Chapter 5

FOLDED CASCODE CMOS OTA (DESIGN, SIMULATION AND SYNTHESIS)

5.1 Introduction

This chapter discusses the general theory of Operational Amplifiers and the commonly used configuration for op-amps. Then it introduces the reader with the OTAs (Operational Transconductance Amplifiers). As discussion continues, a design procedure of the folded cascode CMOS OTA with some specifications is discussed. This section also includes the simulation results of designed OTA. In the end, a physical design (with simulation results) of OTA, designed is presented.

5.2 Operational-Amplifiers

The evolution of very large scale integration (VLSI) technology has developed to the point where millions of transistors can be integrated on a single die or “chip”. Integrated circuits once filled the role of subsystem components, partitioned at analog-digital boundaries; they now integrate complete system on a chip by combining both analog and digital functions. Complementary Metal-oxide semiconductor (CMOS) technology has been the mainstay in mixed-signal implementations because it provides density and power savings on digital side, and a good mix of components for analog design.

In a few years from now CMOS technology will overpower the whole electronic industry. Designing High Performance analog circuits is becoming increasingly challenging with the persistent trend toward reduced supply voltages. The main

bottleneck in an analog circuit is *Operational-Amplifier*. At large supply voltages, there is a trade-off among speed, power and gain amongst other performance parameters. Often these parameters present contradictory choices for operational-amplifier architecture [9,17].

Operational Amplifiers (usually referred to as op-amps) have become one of the most versatile building blocks in analog processing system and are an integral part of many analog and mixed-signal systems. Ideally they perform the function of a voltage controlled current source, with an infinite voltage gain. Op-amps with vastly different levels of complexity are used to realize functions ranging from DC bias generation to high-speed amplification or filtering. The design of op-amps continues to pose a challenge as the supply voltage and transistor channel length scale down with each generation of CMOS technology.

Operational amplifiers are the amplifiers that have sufficiently high forward gain so that when negative feedback is applied, the closed loop transfer function is practically independent of the gain of op-amp [9]. The primary requirement of an op-amp is to have an open loop gain that is sufficiently large to implement the negative feedback concept. Most of the CMOS op-amps that do not have a large enough gain require two or more gain stages.

The unbuffered operational amplifier (which is the main topic of discussion in this chapter) might be better described as operational transconductance amplifier since the output resistance typically will be very high (hence termed “as unbuffered”). The term “buffered” and “unbuffered” is used to distinguish between high output resistance (operational transconductance amplifiers or OTAs) and low output resistance amplifiers (voltage operational amplifiers).

5.3 Commonly used Topologies for Operational Amplifiers

There are several available op-amp architectures. A few popular topologies, which broadly cover all the CMOS op-amps, are discussed below:

5.3.1 Two Stage Op-amp

A two-stage op-amp consists of a cascade of $V \rightarrow I$ and $I \rightarrow V$ stages as shown in fig. 5.1. The first stage consists of a differential amplifier converting the differential input voltage to differential currents. These differential currents are applied to a current mirror load recovering the differential voltage. The second stage consists of a common-source MOSFET converting the second stage input voltage to current. This transistor is loaded by a current-sink load, which converts the current to voltage at the output. The second stage is nothing more than a current-sink inverter. The two-stage op-amp needs compensation to maintain the stability when negative feedback is applied around the op-amp [9].

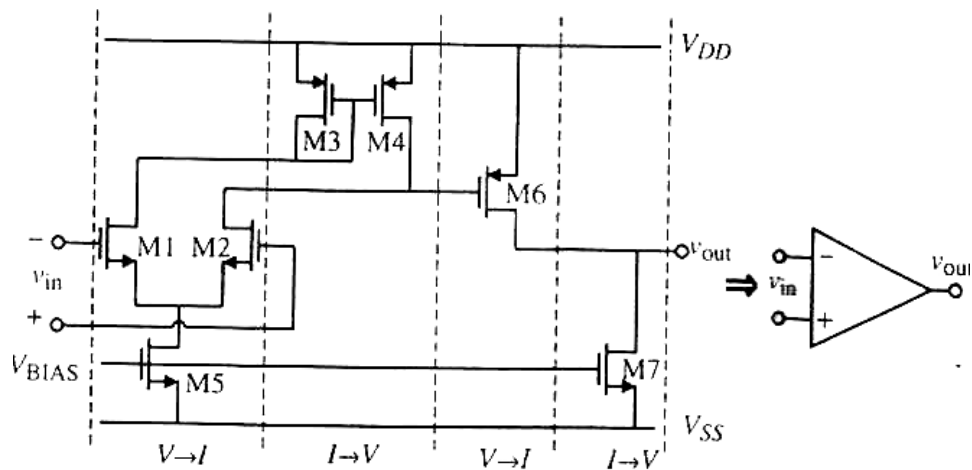


Figure 5.1 Two-stage op-amp broken into V-I and I-V stages

Advantage:

1. It has high output voltage swing.
2. It provides a high voltage gain to the user.
3. Noise associated with this op-amp is quite low.

Disadvantages:

1. It has a compromised frequency response.

2. This topology has high power consumption because of two stages in its design.
3. This has a poor negative Power-Supply Rejection at high frequencies.

This op-amp particularly has applications in telecommunication area. After initial success, it was noted that this suffers from a poor PSRR (Power-Supply rejection Ratio).

5.3.2 Folded Cascode Amplifier

A second architecture that results is shown in fig. 5.2. This is commonly called as Folded Cascode op-amp. The folded cascode amplifier was developed to improve the input common mode range and the power-supply rejection ratio performance of the two-stage op-amp. This amplifier is an example of a self-compensated op-amp. It is cascade of a differential transconductance stage with a current stage followed by a cascode current-mirror load. One of the advantages of folded cascode op-amp is that it has a push-pull output. That is, the op-amp can actively sink or source current from load. The output stage of previous two-stage op-amp is class A, which means that either it's sinking or sourcing capability is fixed [9].

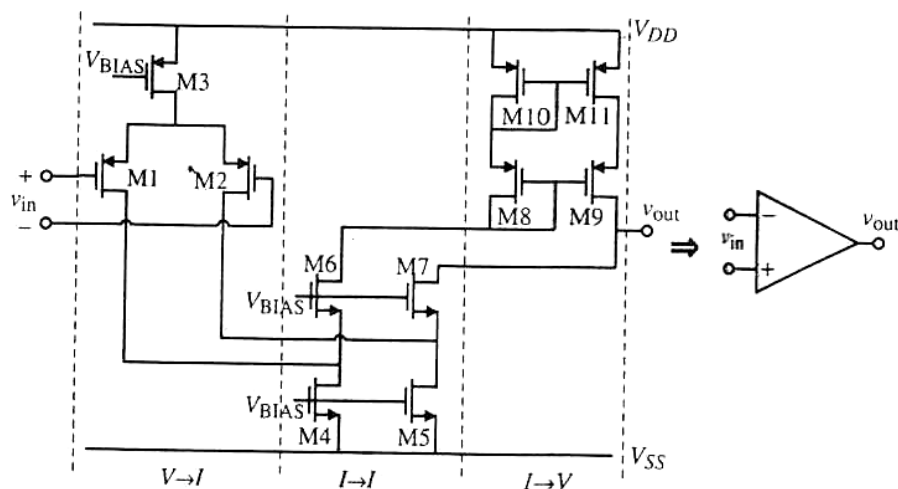


Figure 5.2 Folded cascode op-amp broken into stages

Advantages:

1. This design has corresponding superior frequency response than two-stage operational amplifiers.
2. It has better high frequency power Supply Rejection Ratio (PSRR).

Power consumption of this design is approximately same as that of the two-stage design. It provides moderate voltage gain.

Disadvantages:

1. Folded Cascode has two extra current legs, and thus for a given settling requirement, they will double the power dissipation.
2. The folded cascode stage also has more devices, which contribute significant input referred thermal noise to the signal.
3. Further it introduces a lower voltage gain and lower pole frequencies than that of Telescopic OTA.

5.3.3 Telescopic Cascode Amplifier

Telescopic architecture is the simplest version of the single stage OTA (Operational Transconductance Amplifier). The gain that can be achieved by a single stage is around 40 dB. Thus, in order to achieve 80 dB or so it is necessary to use a cascade of two stages. However, two stages bring about two poles one close to the other and this requires compensation network, besides increasing the global complexity, reduces the design flexibility. A cascade with cascode load permits us to achieve high gain without the disadvantage of having two poles one close to each other. Therefore the use of cascode based OTA is an interesting solution alternative to the two stages OTA

[9,5,11].

Although telescopic operational amplifier has smaller swing, which means reduced dynamic range, this is offset somewhat by the lower noise factor. The above reason implies that the Telescopic op-amp is a better candidate for low power, low noise single stage operational transconductance amplifier. The single stage architecture normally suggests low power consumption.

As shown in architecture (fig. 5.3), the transistors are placed one on the top of the other to create a sort of Telescopic composition (this led to the circuit name as telescopic op-amp). The input differential pair injects the signal currents into common gate stages. Then, the circuit achieves the differential to single ended conversion with a cascode current mirror. The small signal resistance at the

output node is quite high; it is the parallel connection of two cascode configurations. Such a high resistance benefits the small signal gain without limiting the circuit functionality when we require an OTA function.

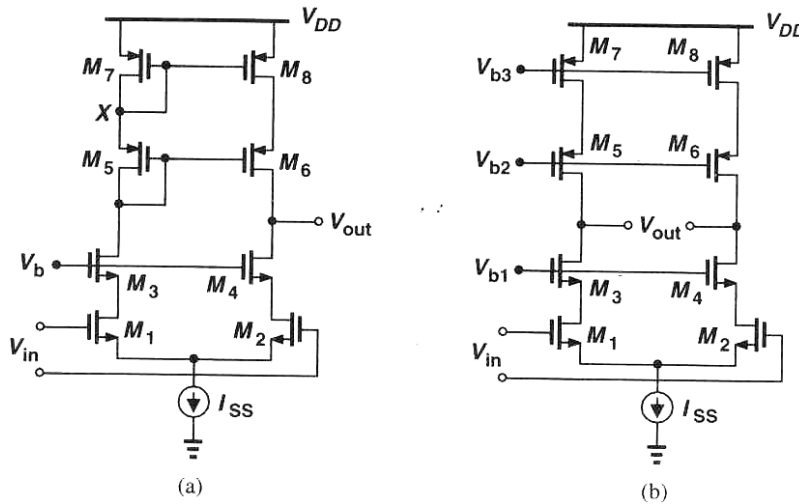


Figure 5.3 (a) Single ended (b) Double ended Telescopic OTA

Advantages:

1. The telescopic cascode achieves a gain similar to the one of the two stages architecture, without having two poles one close to each other.
2. All the nodes, excluding the output, show a pretty low small signal resistance.
3. Its lower noise factor makes it a better candidate for low power, low noise single stage operational transconductance amplifier.

Disadvantages:

1. Telescopic op-amp has severely limited output swing and hence the dynamic range. It is smaller than that of Folded Cascode because the tail transistor directly cuts into output swing from both side of op-amp.

5.4 OTA (Operational Transconductance Amplifier)

An OTA is a voltage controlled current source, more specifically the term “operational” comes from the fact that it takes the difference of two voltages as

the input for the current conversion. The ideal transfer characteristic is therefore
 (fig. 5.4)

$$I_{out} = g_m (V_{in+} - V_{in-}) \dots \dots \dots (5.1)$$

Or, by taking the pre-computed difference as the input,

$$I_{out} = g_m V_{in} \dots \dots \dots (5.2)$$

With the ideally constant transconductance g_m as the proportionality factor between the two. In reality the transconductance is also a function of the input differential voltage and dependent on temperature.

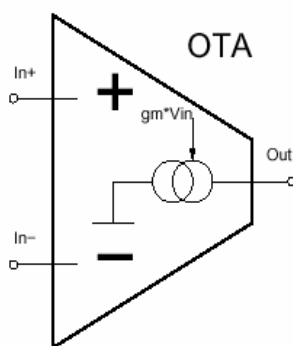


Figure 5.4 Symbol of OTA

The operational transconductance amplifier is basically an op-amp without output buffer. An OTA without buffer can only drive loads. It can be defined as an amplifier where all nodes are low impedance except the input and output nodes. The transconductance of the OTA is set by the transconductance of input differential amplifier. A useful feature of OTA is that its transconductance can be adjusted by bias current. Filters made using the OTA can be tuned by changing the bias current. OTA was developed to improve the input common mode range and Power Supply Rejection of two-stage op-amp. The symbol used for the OTA is shown in fig. 5.5, along with the ideal small signal equivalent circuit [28].

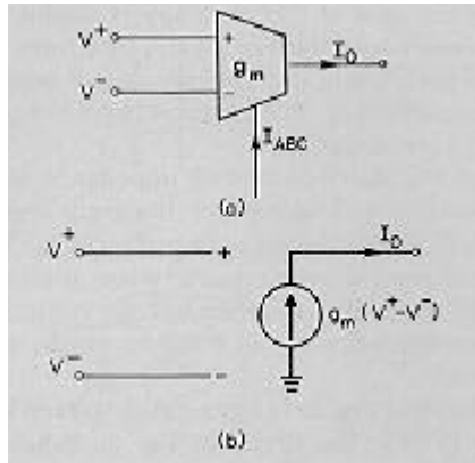


Figure 5.5 Symbol and small signal equivalent of OTA

The transconductance gain, g_m , can be varied over several decades by adjusting an external dc bias current, I_{ABC} . All the standard filter parameters of interest are directly proportional to g_m of the OTA. Thus, the g_m will be a design parameter much as are resistors and capacitors. Since the transconductance gain of the OTA is assumed proportional to an external dc bias current, external control of the filter parameters via the bias current can be obtained. The transconductance gain, g_m , is assumed proportional to I_{ABC} . The proportionality constant h is dependent upon temperature, device geometry, and the process [3].

$$G_m = h I_{ABC} \dots \dots \dots (5.3)$$

$$I_o = g_m (V^+ - V^-) \dots \dots \dots (5.4)$$

As shown in the model, the input and output impedances in the model assume ideal values of infinity. Current control of the transconductance gain can be directly obtained with control of I_{ABC} , since techniques abound for creating a current proportional to a given voltage, voltage control of the OTA gain can also be attained through the I_{ABC} input. When reference is made to either the current or voltage controllability of OTA based circuits' it is assumed to be attained via control of g_m by I_{ABC} .

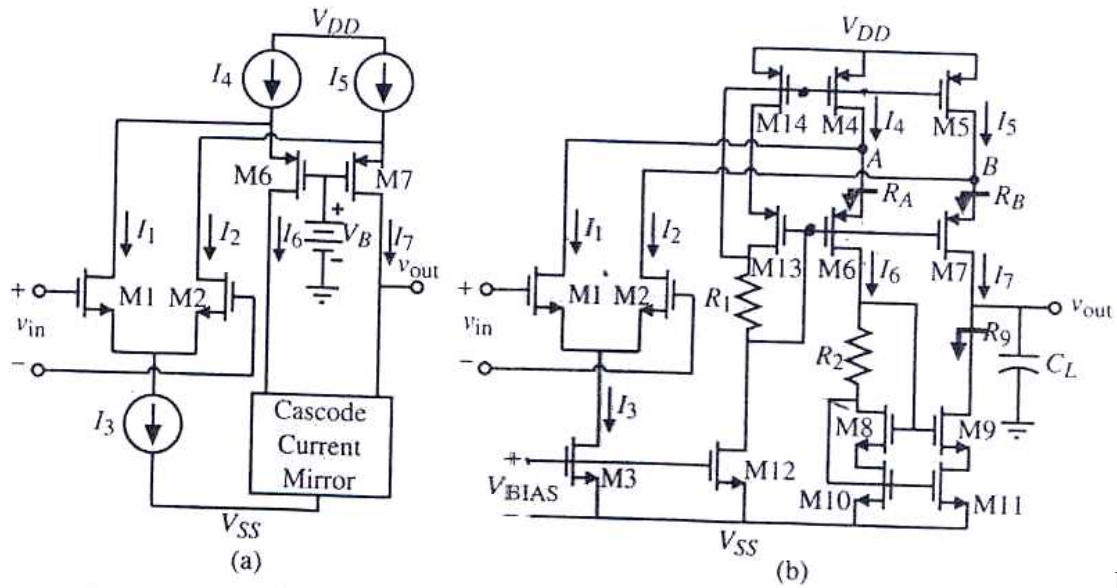
To summarize, an ideal OTA has two voltage inputs with infinite impedance (i.e. there is no input current). The common mode input range is also infinite, while the differential signal between these two inputs is used to control an ideal current source (i.e. the output current does not depend on the output voltage) that functions as an output. The proportionality factor between output current and input differential voltage is called

transconductance. Any real OTA will thus have circuitry to process the input voltages with low input current over a wide common mode input range, to produce an internal representation of the input differential voltage and to provide a current to the output that is relatively independent of the output voltage. Since an OTA can be used without feedback, the maximum output current and with it the transconductance can often be adjusted.

The OTA is popular for implementing voltage controlled oscillators (VCO) and filters (VCF) for analog music synthesizers, because it can act as a two-quadrant multiplier. Viewed from a slightly different angle an OTA can be used to implement an electrically tunable resistor that is referenced to ground, with extra circuitry floating resistors are possible as well. The primary application for an OTA is however to drive low-impedance sinks such as coaxial cable with low distortion at high bandwidth.

5.5 Folded Cascode CMOS OTA

Fig. 5.2 shows the architecture of Folded Cascode op-amp. It is cascade of a differential transconductance stage with a current stage followed by a cascade current-mirror load [9]. This op-amp uses cascading in output stage combined with an unusual implementation of the differential amplifier to achieve good input common mode range. Use of a cascade mirror leads to achieve the gain of two-stage and allows for self-compensation. The basic form of an n-channel input, folded cascode op-amp is shown in fig. 5.6.



Fig

Figure 5.6 (a) Simplified version of n-channel input, folded cascode OTA (b) practical version of (a)

The folded cascode does not require perfect balance of currents in differential amplifier because excess DC current can flow into or out of current mirror. Because the drains of M1 and M2 are connected to drains of M4 and M5, a positive input common mode voltage that can be achieved by using current source loads is achieved. The bias currents I_3 , I_4 and I_5 of folded cascode op-amp should be designed so that the DC current in the cascode mirror never goes to zero. If the current should go to zero, this requires a delay in tuning the mirror back on because of parasitic capacitances that must be charged. For example, suppose V_{in} is large enough so that M1 is on and M2 is off. Then, all of I_3 flows through M1 and none through M2, resulting in $I_1 = I_3$ and $I_2 = 0$. If I_4 and I_5 are not greater than I_3 , then the current I_6 will be zero. To avoid this, the values of I_4 and I_5 are normally between the values of I_3 and $2I_3$.

The small-signal differential-input voltage gain of folded-cascode op-amp is shown in fig. 5.7. The resistance designated as R_A & R_B are the resistances looking into the sources of M6 & M7, respectively.

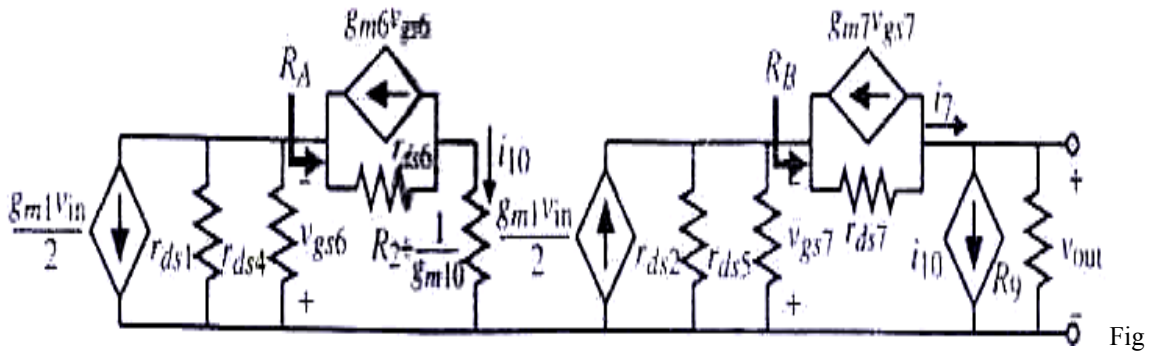


Figure 5.7 Small signal model of fig. 5.6(b)

Here R_A & R_B will be given by equations:

$$R_A = \frac{r_{DS6} + R_2 + \frac{1}{g_{m10}}}{1 + g_{m6} + r_{DS6}} \approx \frac{1}{g_{m6}} \dots\dots\dots(5.5)$$

and

$$R_B = \frac{r_{DS7} + R_9}{1 + g_{m7}r_{DS7}} \approx \frac{R_9}{g_{m7}r_{DS7}} \dots\dots\dots(5.6)$$

Where

$$R_9 = g_{m9}r_{DS9}r_{DS11} \dots\dots\dots(5.7)$$

The small signal voltage transfer function of fig. 5.7 can be found as follows. The current i_{10} is written as

$$i_{10} = \frac{-g_{m1}(r_{DS1} \parallel r_{DS4})V_{in}}{2(R_A + (r_{DS1} \parallel r_{DS4}))} \approx \frac{g_{m1}V_{in}}{2} \dots\dots\dots(5.8)$$

and the current i_7 can be expressed as

$$i_7 = \frac{g_{m2}V_{in}}{2\left(1 + \frac{R_9(g_{DS2} + g_{DS5})}{g_{m7}r_{DS7}}\right)} = \frac{-g_{m1}V_{in}}{2} \dots\dots\dots(5.9)$$

Where a low frequency balance factor, k , is defined as

$$k = \frac{R_9(g_{DS2} + g_{DS5})}{g_{m7}r_{DS7}} \dots\dots\dots(5.10)$$

Typical values of k are greater than one. The output voltage, V_{out} is equal to sum of i_7 and i_{10} flowing through R_{11} . Thus,

$$\frac{V_{out}}{V_{in}} = \left(\frac{g_{m1}}{2} + \frac{g_{m2}}{2(1+k)} \right) R_{11} = \left(\frac{2+k}{2+2k} \right) g_{m1} R_{11} \dots\dots\dots(5.11)$$

Where the output resistance R_{11} , is given as

$$R_{11} \approx g_{m9} r_{DS9} r_{DS11} \parallel \left(g_{m7} r_{DS7} (r_{DS2} \parallel r_{DS5}) \right) \dots\dots\dots(5.12)$$

5.5.1 Why I choose Folded Cascode configuration?

The gain that can be achieved by a single stage is around 40 dB. Thus, in order to achieve 80 dB or so it is necessary to use a cascade of two stages. However, two stages bring about two poles one close to the other and this requires compensation network, besides increasing the global complexity, reduces the design flexibility. A cascade with cascode load permits us to achieve high gain without the disadvantage of having two poles one close to each other. Therefore the use of cascode based OTA is an interesting solution alternative to the two stages OTA.

Thus two options have been left, one is Telescopic configuration and the other one is folded cascode configuration. The primary advantage of folded structure lies in the choice of voltage levels because it does not “stack” the cascode transistor on the top of the input device. Further Telescopic OTA suffers with limited output swing, and there is a difficulty in shorting the input and output (which is the foremost requirement of my filter).

The output swing of fully differential telescopic op-amp (fig. 5.3) is given by 2 [Vdd – (Vod1 + Vod3 + Vcss + /Vod5/ + /Vod7/)], which is higher than that of folded cascode op-amp by overdrive voltage of tail current source.

Another drawback of telescopic op-amp is difficulty in shorting input and outputs, e.g., to implement a unity gain buffer [5].

To understand the issue, the unity gain feedback topology shown in fig. 5.8 is considered. For M2 and M4 to be in saturation $V_{out} \leq V_x + V_{TH2}$ and $V_{out} \geq V_b - V_{TH4}$. Since $V_x = V_b - V_{GS4}$, $V_b - V_{TH4} \leq V_{out} \leq V_b - V_{GS4} + V_{TH2}$. As depicted in fig. 5.8, this voltage range

is simply equal to $V_{\max} - V_{\min} = V_{TH4} - (V_{GS4} - V_{TH2})$, maximized by minimizing the overdrive of M4 but always less than V_{TH2} .

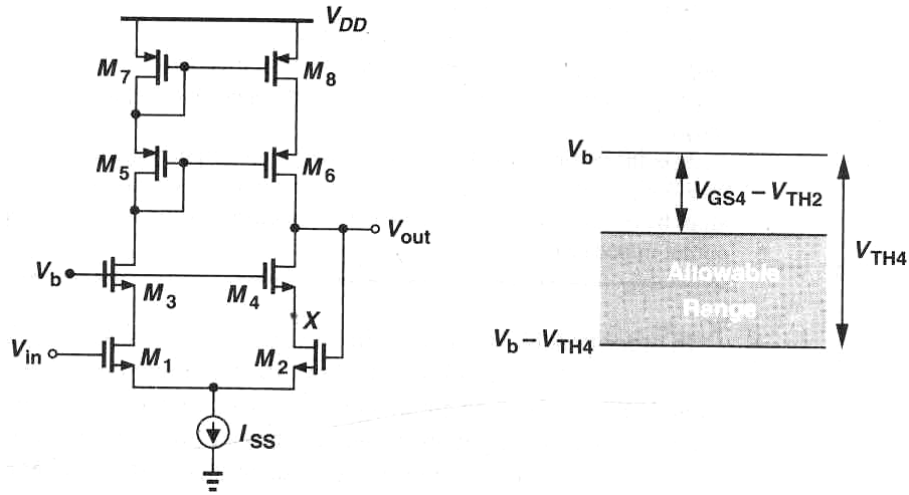


Figure 5.8 Telescopic OTA with input and output shorted

Since the op-amp attempts to force V_{out} to be equal to V_{in} , for $V_{in} < V_b - V_{TH4}$, we have $V_{out} + V_{in}$ and M4 is in triode region while other transistors are saturated. Under this condition, the open-loop gain of op-amp is reduced. As V_{in} and hence V_{out} exceed $V_b - V_{TH4}$, M4 enters saturation and the open-loop gain reaches a maximum. For $V_b - V_{TH4} < V_{in} < V_b - (V_{GS4} - V_{TH2})$, both M2 and M4 are saturated and for $V_{in} > V_b - (V_{GS4} - V_{TH2})$, M2, M1 enter the triode region, degrading the gain.

Further folded cascode op-amp has the capability of handling input common-mode levels close to one of the supply rails. The input CM level of telescopic op-amp (fig. 5.9(a)) cannot exceed $V_b - V_{GS3} + V_{TH1}$, whereas in fig. 5.9(b), it cannot be less than $V_b - V_{GS3} + |V_{THp}|$. It is therefore also possible to design the latter to allow shorting of input and output with negligible swing limitation.

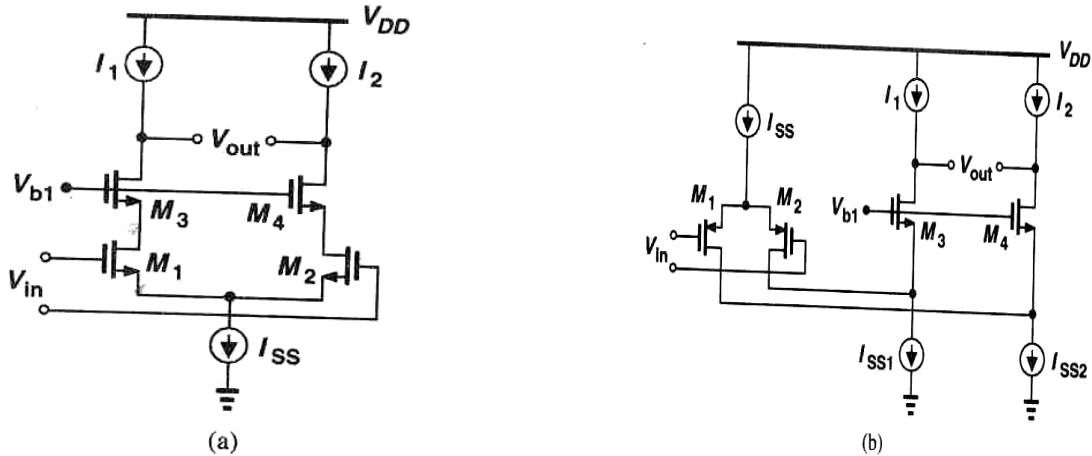


Figure 5.9 Folded cascode op-amp topology

5.5.2 Design Procedure of A Folded Cascode CMOS OTA

5.5.2.1 Necessary Parameters:

The following design procedure assumes that specifications for the following parameters are given:

- Gain at dc (A_V)
- Unity gain bandwidth (GB)
- Input common mode range (V_{in} (min) and V_{in} (max))
- Load capacitance (C_L)
- Slew rate (SR)
- Output voltage swing (V_{out} (max) and V_{out} (min))
- Power dissipation (P_{diss})

5.5.2.2 Design Procedure:

1. Choose the smallest design device length that will keep the channel length modulation parameter λ constant and give good matching for current mirrors.
2. Determine the value of tail current I_3 for the largest of two values.

$$I_3 = SR * C_L \dots \dots \dots (5.13)$$

3. Determine the value of bias current in output cascades. Avoid zero current in the cascades [9].

$$I_4 = I_5 = 1.2I_3 \text{ to } 1.5 I_3 \dots \dots \dots (5.14)$$

4. Design for S_5 and S_7 from the maximum output voltage, V_{out} (max).

Let $S_4 = S_{14} = S_5 = S_{13}$ and $S_6 = S_7$

$$S_5 = \left(\frac{W}{L}\right)_5 = \frac{2I_5}{K_p} / (V_{SD5})^2 \dots\dots\dots(5.15)$$

$$S_7 = \left(\frac{W}{L}\right)_7 = \frac{2I_7}{K_p} / (V_{SD7})^2 \dots\dots\dots(5.16)$$

Where,

$$V_{SD5} (sat) = V_{SD7} (sat) = (V_{DD} - V_{out} (max))/2 \dots\dots\dots(5.17)$$

5. Design for S_{11} and S_9 from the minimum output voltage, $V_{out} (min)$.

Let $S_{10} = S_{11}$ and $S_8 = S_9$

$$S_{11} = \left(\frac{W}{L}\right)_{11} = \frac{2I_{11}}{K_n} / (V_{DS11})^2 \dots\dots\dots(5.18)$$

$$S_9 = \left(\frac{W}{L}\right)_9 = \frac{2I_9}{K_n} / (V_{DS9})^2 \dots\dots\dots(5.19)$$

Where,

$$V_{DS9} (sat) = V_{DS11} (sat) = (V_{out} (min) - |V_{SS}|)/2 \dots\dots\dots(5.20)$$

6. Calculation of the resistances R_1 & R_2

$$R_1 = V_{SD13} (sat) / I_{12} \dots\dots\dots(5.21)$$

$$R_2 = V_{SD8} (sat) / I_6 \dots\dots\dots(5.22)$$

7. Design of S_1 & S_2 from unity-gain bandwidth, GB and load capacitor, C_L .

$$S_1 = S_2 = \frac{g_{m1}^2}{K_n I_3} = \frac{GB^2 * C_L^2}{K_n I_3} \dots\dots\dots(5.23)$$

Where

$$g_{m1} = GB * C_L \dots\dots\dots(5.24)$$

8. Design of S_3 from minimum input common mode voltage.

$$S_3 = \left(\frac{W}{L}\right)_3 = \frac{2I_3}{K_n \left[V_{in} (min) - V_{SS} - \sqrt{\frac{I_3}{K_n S_1}} - V_{t1} \right]^2} \dots\dots\dots(5.25)$$

9. Design of S_4 & S_5 from maximum input common mode voltage.

$$S_4 = S_5 = \frac{2I_4}{K_p [V_{DD} - V_{in} (max) + V_{t1}]^2} \dots\dots\dots(5.26)$$

It is needed to check that the values of are large enough to satisfy the maximum input common mode voltage.

10. Calculate the small signal, differential-input voltage gain.

$$A_v = \left(\frac{2+k}{2+2k} \right) g_{m1} R_{11} \dots \dots \dots (5.27)$$

11. Calculate the power dissipation.

$$P_{diss} = (V_{DD} - V_{SS})(I_3 + I_{12} + I_{10} + I_{11}) \dots \dots \dots (5.28)$$

5.5.3 Design of folded cascode op-amp with following specifications:

- The Slew rate (SR) is 10 V/μs
- The Load capacitance (C_L) is 10 pF
- The maximum and minimum output voltages are ±2 V for ±2.5 V power supplies.
- The unity gain bandwidth (GB) is 7 MHz
- The minimum input common-mode range is -1.5 V
- The maximum input common-mode range is 2.5 V
- The differential voltage gain should be greater than 5000 V/V
- The Power dissipation (P_{diss}) should be less than 5 mW

5.5.3.1 Design Flow:

1. $I_3 = SR * C_L$
 $= 10 * 10^6 * 10^{-11} = 100 \mu A$
2. $I_4 = I_5 = 1.25 * 100 * 10^{-6} = 125 \mu A$
3. Let $S_4 = S_{14} = S_5 = S_{13}$ and $S_6 = S_7$

$$S_4 = S_{14} = S_5 = S_{13} = \frac{2 * 125 * 10^{-6}}{2.63544 * 10^{-5} (0.25)^2} = 151.78$$

$$S_6 = S_7 = \frac{2 * 75 * 10^{-6}}{2.63544 * 10^{-5} (0.25)^2} = 91.066$$

Where, $V_{SD5} (sat) = V_{SD7} (sat) = (V_{DD} - V_{out} (max))/2 = (2.5 - 2)/2 = 0.25 V$

4. Let $S_{10} = S_{11}$ and $S_8 = S_9$

$$S_8 = S_9 = S_{10} = S_{11} = \frac{2 * 75 * 10^{-6}}{6.322664 * 10^{-5} (0.25)^2} = 37.9586$$

$$\text{Where, } V_{DS9}(sat) = V_{DS11}(sat) = \frac{V_{out}(\min) - |V_{SS}|}{2} = \frac{-2 + 2.5}{2} = 0.25 \text{ V}$$

5. $R_1 = V_{SD13}(sat) / I_{12} = 0.25 \text{ V} / 125 \mu\text{A} = 2000 \Omega$

$R_2 = V_{SD8}(sat) / I_6 = 0.25 \text{ V} / 125 \mu\text{A} = 2000 \Omega$

6. $S_1 = S_2 = \frac{GB^2 * C_L^2}{K_n I_3} = \frac{(14\pi * 10^6)^2 (10^{-11})^2}{6.322664 * 10^{-5} * 100 * 10^{-6}} = 30.5956$

7.

$$S_3 = \left(\frac{W}{L}\right)_3 = \frac{100 * 10^{-6} * 2}{6.322664 * 10^{-5} \left[-1.5 + 2.5 - \sqrt{\frac{100 * 10^{-6}}{6.322664 * 10^{-5} * 30.5956}} - 0.62249 \right]^2} = 140.092$$

8. $S_4 = S_5 = \frac{2 * 125 * 10^{-6}}{2.63544 * 10^{-5} [2.5 - 2.5 + 0.62249]^2} = 10.2$

It is needed to check that the values of are large enough to satisfy the maximum input common mode voltage.

9. $S_{12} = (125/100) * 140.092 = 175.115$

10. $P_{diss} = (2.5 - (-2.5))(100 + 125 + 75 + 75) = 1.875 \text{ mW}$

11. *The small signal voltage requires the following values to evaluate*

$$S_4, S_{14}, S_5, S_{13}; g_m = \sqrt{2 * 125 * 10^{-6} * 2.63544 * 10^{-5} * 151.78} = 1000 \mu\text{s}$$

$$g_{DS} = 125 * 10^{-6} * 0.01 = 1.25 \mu\text{s}$$

$$S_6, S_7; g_m = \sqrt{2 * 75 * 10^{-6} * 2.63544 * 10^{-5} * 91.066} = 600 \mu\text{s}$$

$$g_{DS} = 75 * 10^{-6} * 0.01 = 0.75 \mu\text{s}$$

$$S_8, S_9, S_{10}, S_{11}; g_m = \sqrt{2 * 75 * 10^{-6} * 6.322664 * 10^{-5} * 37.9586} = 600 \mu\text{s}$$

$$g_{DS} = 75 * 10^{-6} * 0.01 = 0.75 \mu\text{s}$$

$$S_1, S_2; g_{m1} = \sqrt{2 * 50 * 10^{-6} * 6.322664 * 10^{-5} * 62.44} = 628 \mu\text{s}$$

$$g_{DS} = 50 * 10^{-6} * 0.01 = 0.5 \mu s$$

Thus,

$$R_9 \approx g_{m9} * r_{DS9} * r_{DS11} = 600 \mu s * \frac{1}{0.75 \mu s} * \frac{1}{0.75 \mu s} = 1066.67 \text{ M}\Omega$$

$$R_{11} \approx (1066.67 \text{ M}\Omega) \parallel \left((600 \mu s) \left[\frac{1}{0.75 \mu s} \right] \parallel \left[\frac{1}{0.75 \mu s} \parallel \frac{1}{1.25 \mu s} \right] \right) = 290.71 \text{ M}\Omega$$

$$k = R_9 \left(\frac{g_{DS2} + g_{DS4}}{g_{m7} r_{DS7}} \right) = \frac{1066.67 \text{ M}\Omega (0.5 \mu s + 1.25 \mu s) (0.75 \mu s)}{600 \mu s} = 2.3333$$

The small signal, differential-input voltage gain is

$$A_V = \left(\frac{2+k}{2+2k} \right) g_{m1} R_{11} = \left(\frac{2+2.3333}{2+4.6666} \right) * 628 * 10^{-6} * 290.71 * 10^6 = 118668 \text{ V/V}$$

Table 5.1 Calculated aspect ratios for the folded cascode OTA

MOS	M1	M2	M3	M4	M5	M6	M7
W/L (in $\mu\text{m}/\mu\text{m}$)	61/2	61/2	281/2	303/2	303/2	182/2	182/2
MOS	M8	M9	M10	M11	M12	M13	M14
W/L (in $\mu\text{m}/\mu\text{m}$)	75/2	75/2	75/2	75/2	351/2	303/2	303/2

5.5.4 Simulation Results of Folded Cascode OTA

This section discusses the schematic of op-amp designed and the results obtained by the schematic level simulations. The schematic is drawn in S-Edit

module of Tanner EDA Tool and the simulations are done in T-Spice module of Tanner EDA Tool.

Following fig. 5.10 shows the schematic diagram of folded cascode op-amp with all the sources connected to their bulk reducing the body bias effect to zero. The input voltage is applied at one end and the other end is grounded.

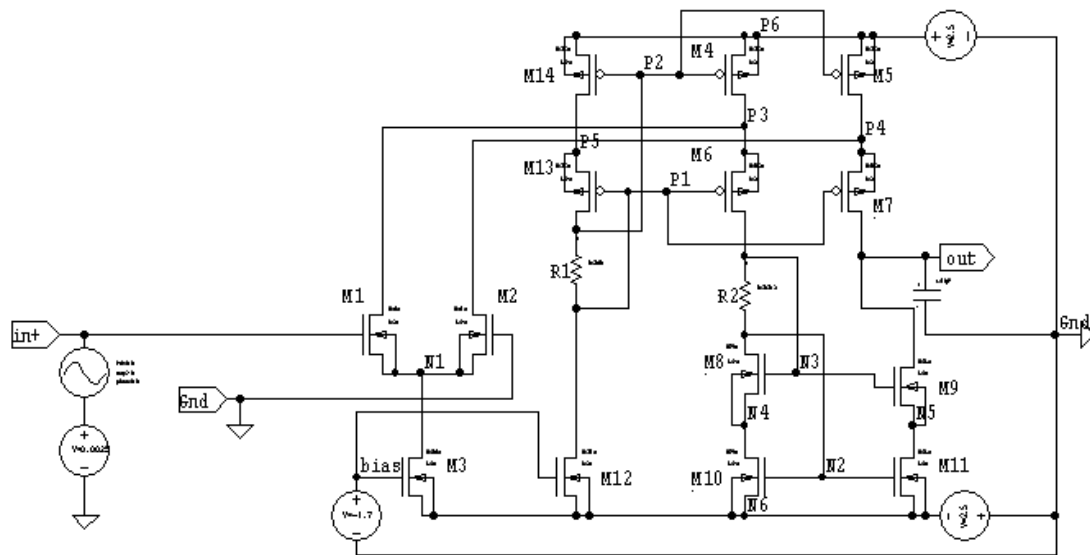


Figure 5.10 Schematic of folded cascode OTA

The T-Spice file is shown in Appendix A. As there is a trade-off between gain and unity gain bandwidth, the values of resistance, bias voltage and offset voltage are somewhat adjusted according the best possible combination of gain and unity gain bandwidth. For the maximum gain to achieve, all the transistors are made to work in saturation region.

Following fig. 5.11 shows the simulation results of frequency vs. gain plot. A gain of 62.7 dB and UGB of 15.6 MHz has been achieved.

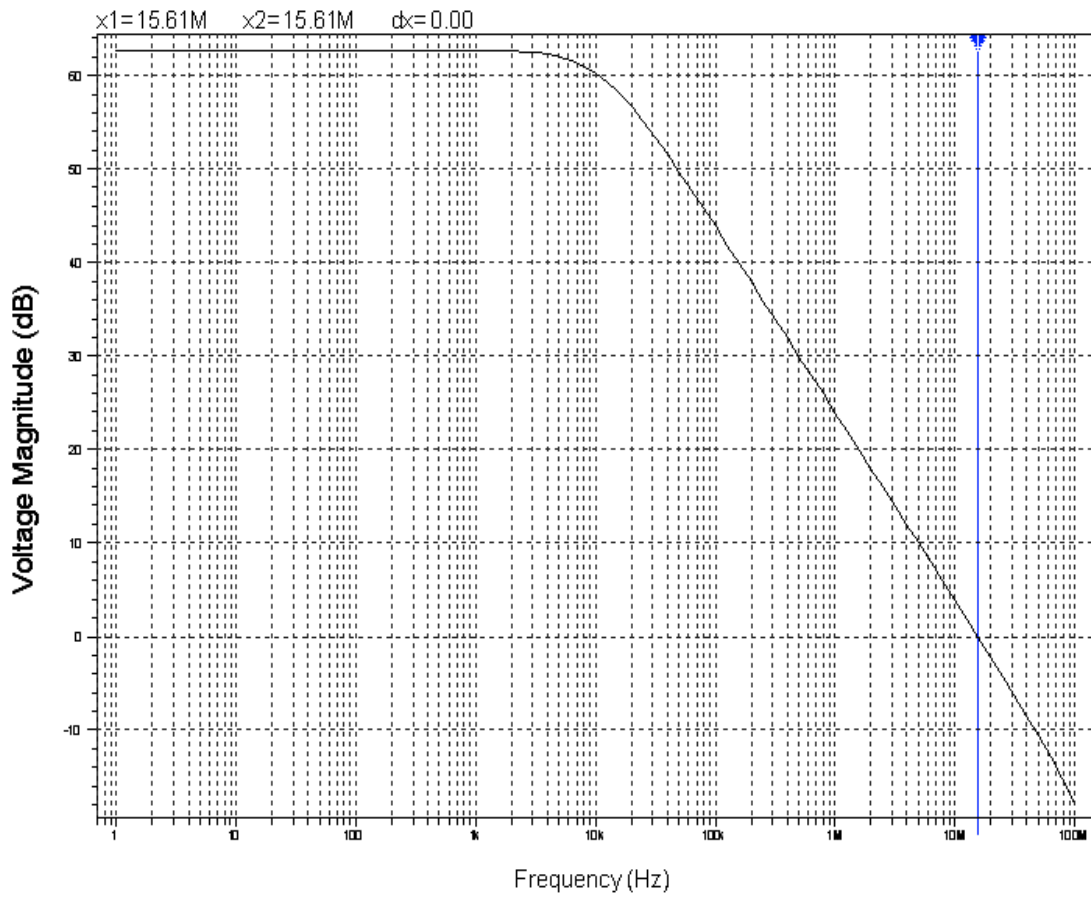


Figure 5.11 Frequency vs. gain response of schematic

Fig. 5.12 shows the phase plot of folded cascode op-amp. As shown a phase margin of -98.7 degree has been achieved which is quite good for the stability point of view.

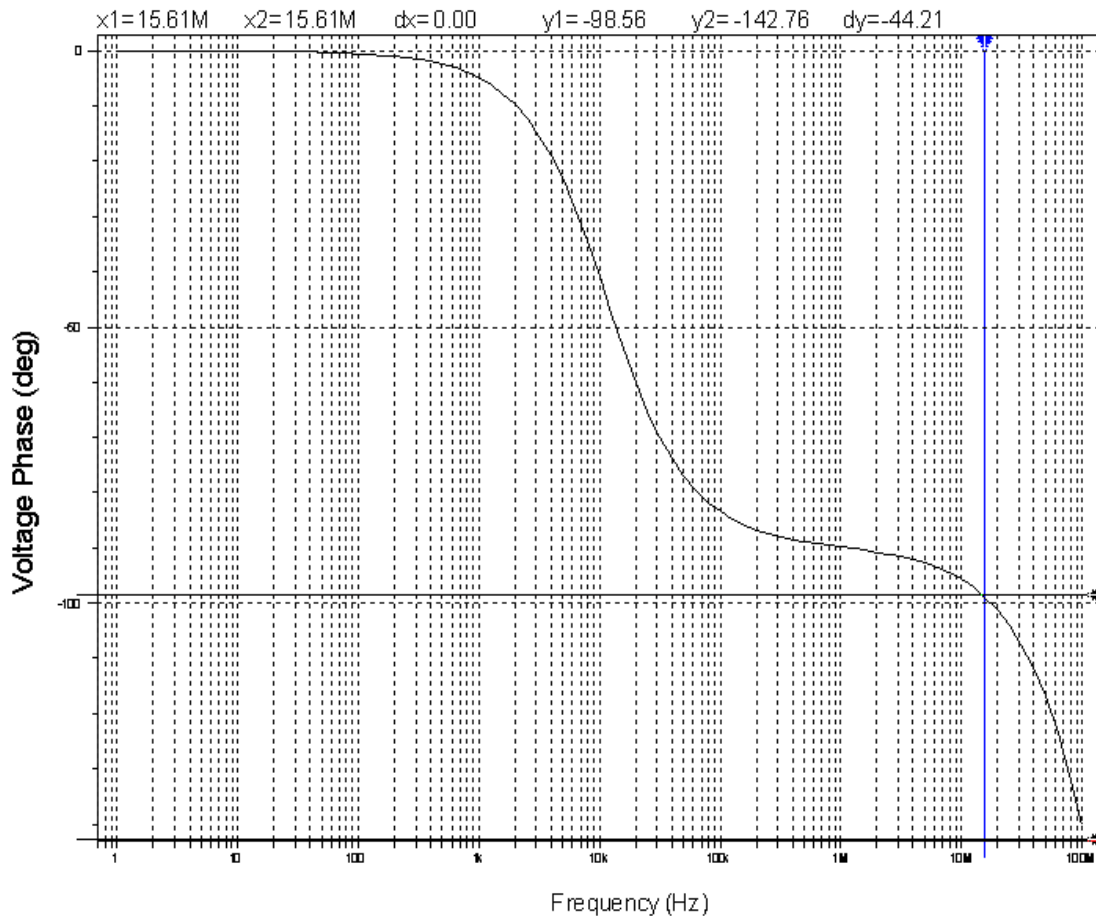


Figure 5.12 Frequency vs. phase response

5.5.5 Analysis of simulation results

1. It is observed that as the bias voltage is increased from -1.7 V, in positive direction the transistors start going in the linear region. The gain of op-amp starts decreasing with an increase in UGB. If bias voltage is increased from -1.7 V, in negative direction, the gain increases but UGB decreases and the transistor M3 goes into cut-off region.
2. Further it is observed that there is no significant change in UGB while altering the offset voltage. If the offset voltage is increased from 2.5 mV, the gain reduces significantly and if offset voltage is decreased, the insignificant change in gain occurs i.e. it decreases only by 1 dB to 2 dB.

5.5.6 Physical Design of Folded Cascode OTA

The physical design of folded cascode OTA is shown in fig. 5.13. The layout is drawn in L-Edit (Tanner Tool). For visibility reasons the resistors are not included in the layout shown.

While designing layout special analog layout methods like gate folding, common centriode geometries, interdigitization etc. have been used to take care of matching issues and other related problems. Interdigitization and common centriode techniques are used for matched transistors, gatefold are used for large devices so as to minimize the associated parasitic capacitances.

Fig. 5.14 shows the simulation results of layout of op-amp. A gain of 65.7 dB and a UGB of 15.02 MHz has been achieved from layout simulations. While a 62.7 dB of gain and a 15.6 MHz of UGB is achieved from schematic simulation. This minute change (due to parasitic capacitances) shows quite good matching of transistors.

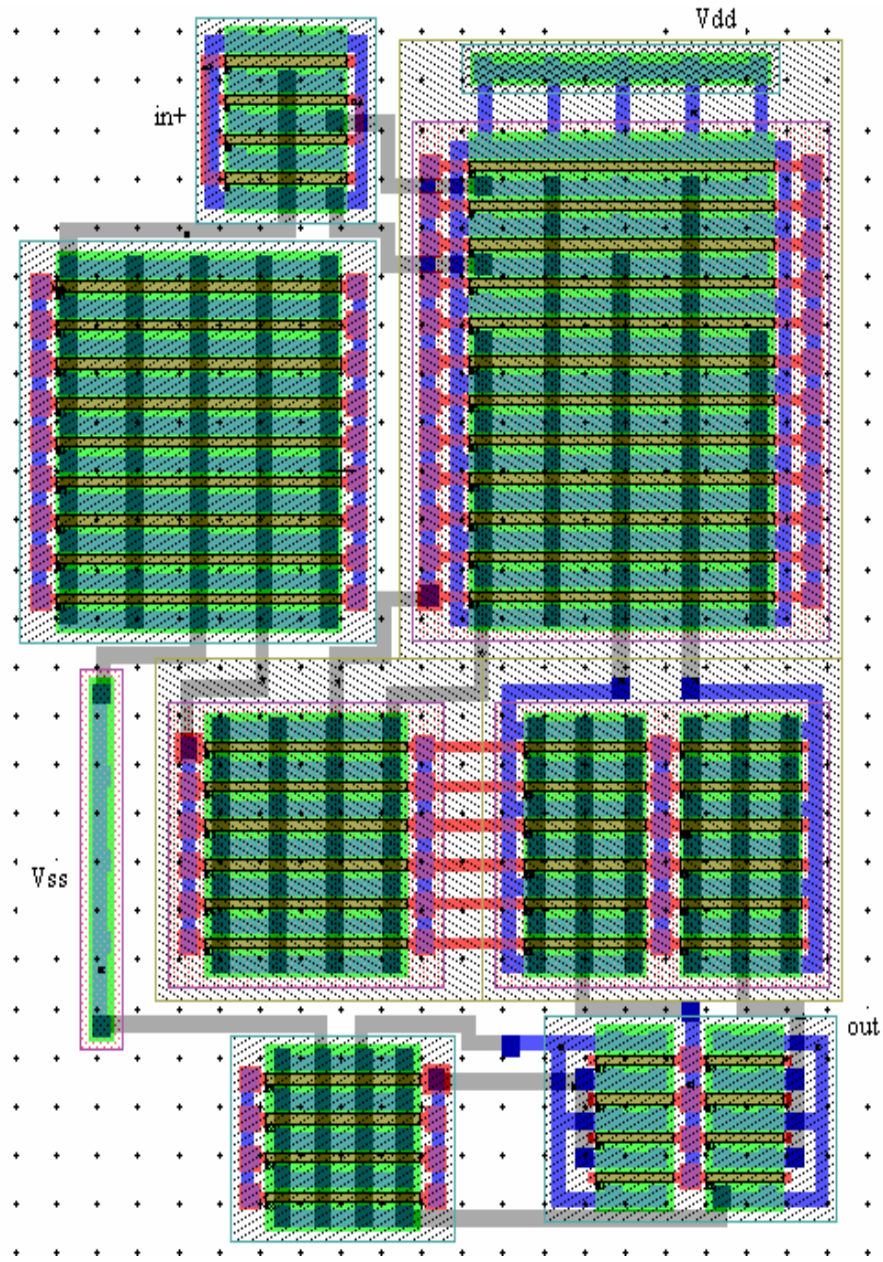


Figure 5.13 Layout of folded cascode OTA

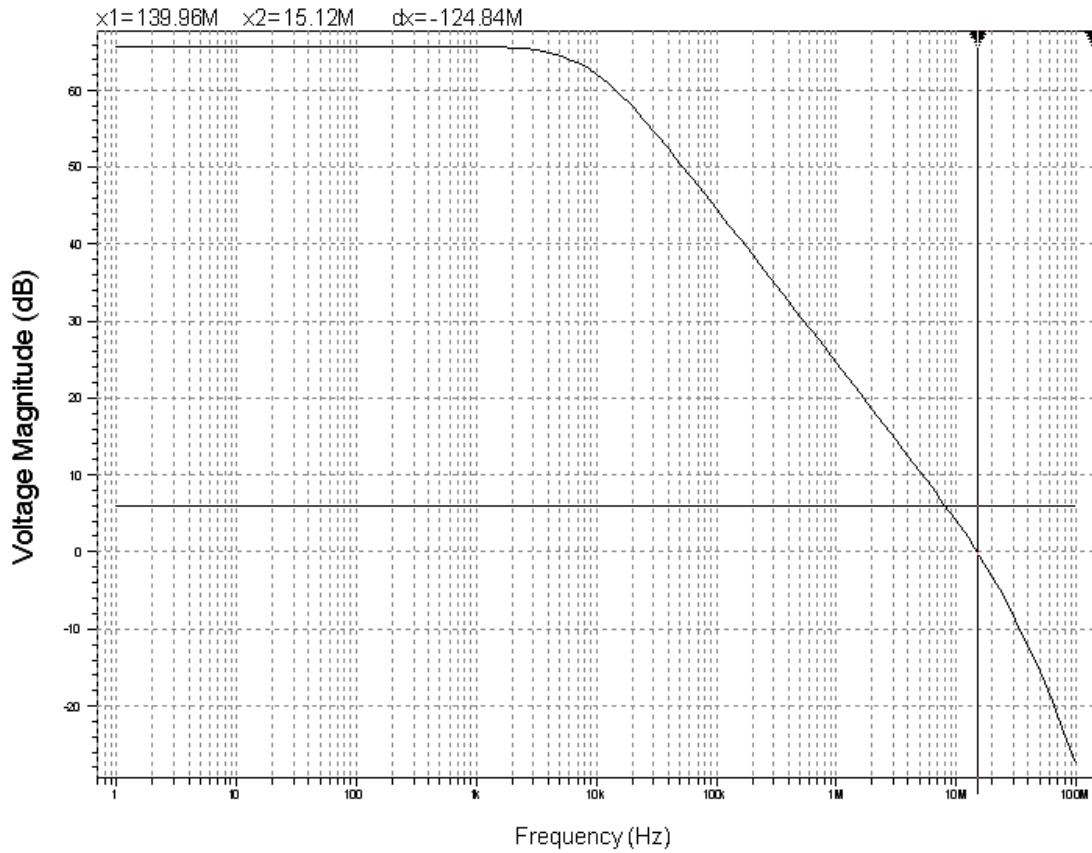


Figure 5.14 Frequency vs. gain response of layout

DC Gain 65.7 dB

UGB 15.02 MHz

Chapter 6

DESIGN & ANALYSIS OF 5TH ORDER CHEBYSHEV FILTER

6.1 Introduction

This section discusses the realization of a passive network of 5th order Chebyshev filter using the Operational Transconductance Amplifier (OTA) designed in the previous section. All the passive components resistors (floating and grounded) and inductors are implemented using folded cascode OTA and hence an active network of 5th order Chebyshev filter is obtained. Layout is drawn using L-Edit and results are compared to that with schematic simulations.

In analysis part, it is generalized that how to calculate the transconductance of folded cascode OTA. And then variation of transconductance with bias voltage and thus, that of 3dB-frequency with transconductance is analyzed. In the end an equation showing the relation 3dB-frequency and transconductance (g_m) is proposed.

6.2 Active vs. Passive Filters

6.2.1 Passive Filters

The filters used for the earlier examples were all made up of passive components: resistors, capacitors, and inductors, so they are referred to as passive filters. A passive filter is simply a filter that uses no amplifying elements (transistors, operational amplifiers, etc.). In this respect, it is the simplest (in terms of the number of necessary components) implementation of a given transfer function. Passive filters have other advantages as well. Because they have no active components, passive filters require no power supplies. Since they are not restricted by the bandwidth limitations of op amps, they can work well at very high frequencies. They can be used in applications involving larger current or voltage levels than can be handled by active devices. Passive filters also generate little noise when compared with circuits using active gain elements. The

noise that they produce is simply the thermal noise from the resistive components, and, with careful design, the amplitude of this noise can be very low. Despite all these, Passive filters have some important disadvantages in certain applications, however. Since they use no active elements, they cannot provide signal gain. Input impedances can be lower than desirable, and output impedances can be higher the optimum for some applications, so buffer amplifiers may be needed. Inductors are necessary for the synthesis of most useful passive filter characteristics, and these can be prohibitively expensive if high accuracy (1% or 2%, for example), small physical size, or large value is required. Standard values of inductors are not very closely spaced, and it is difficult to find an off-the-shelf unit within 10% of any arbitrary value, so adjustable inductors are often used. Tuning these to the required values is time-consuming and expensive when producing large quantities of filters. Furthermore, complex passive filters (higher than 2nd-order) can be difficult and time-consuming to design [20].

6.2.1 Active Filters

Active filters use amplifying elements, especially op amps, with resistors and capacitors (optional) in their feedback loops, to synthesize the desired filter characteristics. Active filters can have high input impedance, low output impedance, and virtually any arbitrary gain. They are also usually easier to design than passive filters. Possibly their most important attribute is that they lack inductors, thereby reducing the problems associated with those components. Performance at high frequencies is limited by the gain-bandwidth product of the amplifying elements, but within the amplifier's operating frequency range, the op amp-based active filter can achieve very good accuracy, provided that low-tolerance resistors and capacitors are used. Active filters will generate noise due to the amplifying circuitry, but this can be minimized by the use of low-noise amplifiers and careful circuit design [20].

Thus, Filter implementation can be either active or passive. In general, active filters are suitable for very low frequency applications (< 10 MHz), in which the

prototype element values are too large to be implemented using discrete components. At higher frequency the power consumption and noise contribution of active circuitry would be too large for practical purposes and IC implementation too challenging. The lumped passive filter is suitable for the medium frequency range (between 100 MHz and 1 GHz) whereas the distributed passive filter is typically used at very high frequencies (> 10 GHz) [34].

6.3 Passive Network of 5th Order Chebyshev Filter

Based on the synthesized prototype design, one can implement passive filters using either discrete lumped elements or distributed transmission lines. The particular selection depends on the frequency of interest. In general, the lumped design is suitable for application below 1 GHz, where parasitics associated with lumped elements are less of an issue. At very high frequency, the parasitics become significant and cause distortion in filter response. On the other hand, distributed (where each element in the prototype design is replaced by its equivalent transmission line implementation) filter design is more suitable at high frequency since the parasitics can be absorbed by being considered part of the transmission lines [34].

Fig. 6.1 shows the network for 5th order Chebyshev filter using *RLC* circuitry. The order of a passive filter is equal to the number of reactive components used in the network. Here two inductors and three capacitors form the 5th order network.

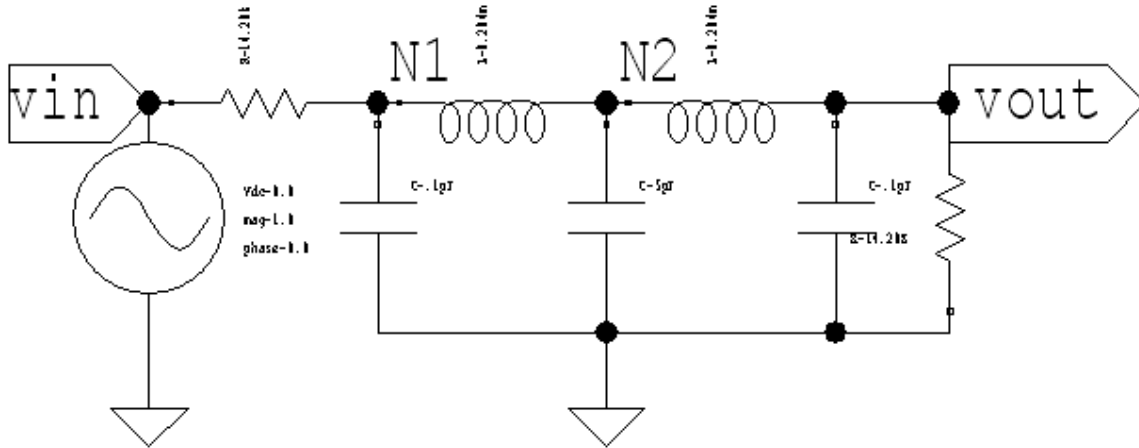


Figure 6.1 Passive network of 5th order Chebyshev filter

6.4 Equivalent Active Network of 5th Order Chebyshev Filter

Active filter implementations synthesize the desired filter transfer functions using active circuitry such as amplifiers. The approach begins with a synthesized prototype design and the necessary transformation to obtain the lumped-element prototype. Based on this prototype design, each passive element is replaced by its active equivalent [34].

6.4.1 Implementation of Grounded Resistor using OTA

Fig. 6.2 shows the implementation of grounded resistor using folded cascode OTA (discussed in previous chapter). Here the load resistance is replaced by a self-feedback transconductors [11, 18, 34]. V_1 and V_2 are the input and output voltages, respectively.

Where,

$$R = 1/g_m \dots \dots \dots (6.1)$$

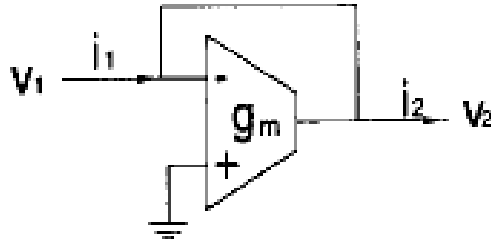


Figure 6.2 Implementation of grounded resistor using OTA

Fig. 6.3 shows the frequency response of grounded resistor with folded cascode CMOS OTA (discussed in previous chapter) implementation. It provides a gain of 6.02 dB.

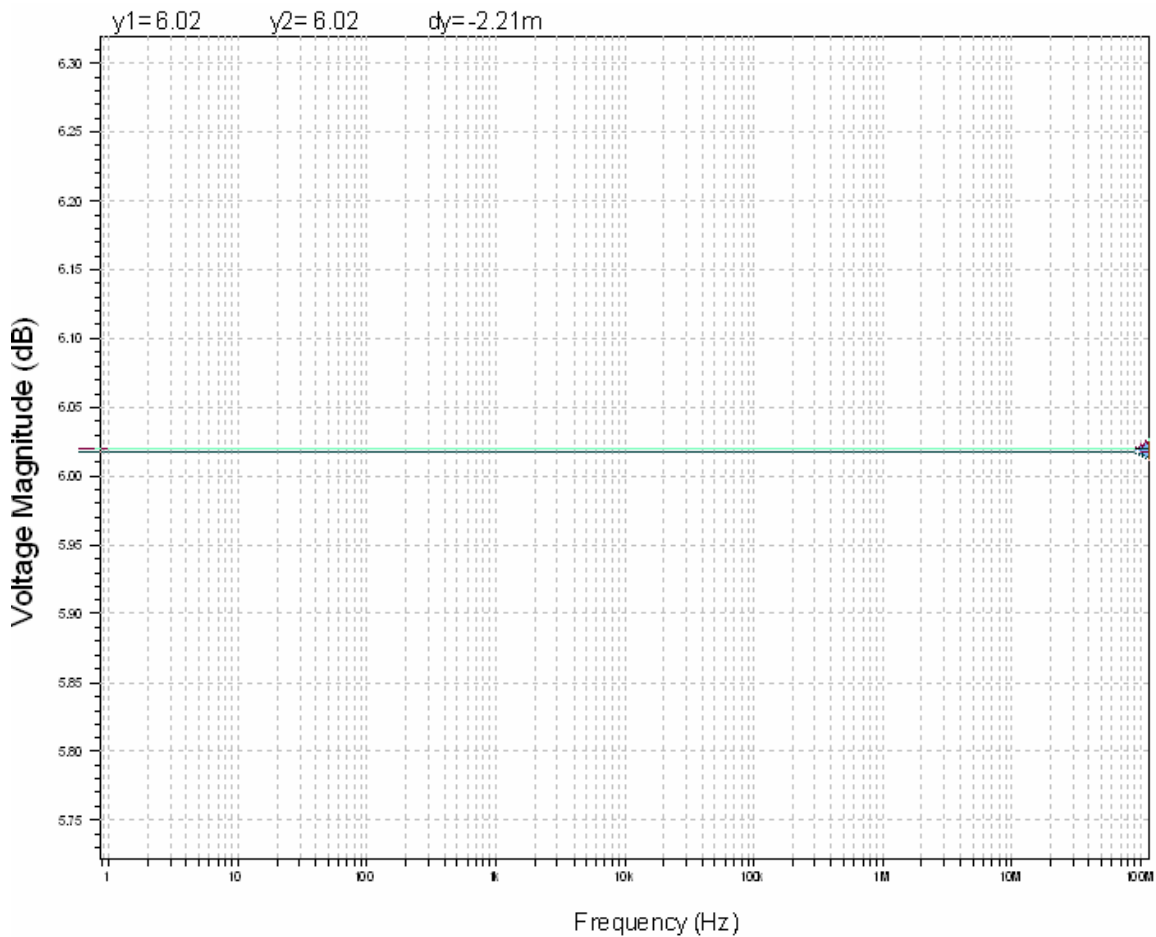


Figure 6.3 Frequency response of OTA implemented grounded resistor

6.4.2 Implementation of Floating Resistor using OTA

Like load resistances, source resistances are also replaced by self-feedback transconductors (fig. 6.4). The implementation includes a folded cascode OTA followed by a unity gain buffer [11,18,34]. V_1 and V_2 are again the input and output voltages, respectively.

Where,

$$R = 1/g_m \dots \dots \dots (6.2)$$

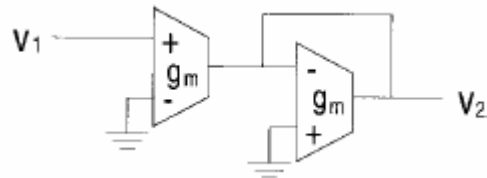


Figure 6.4 Implementation of floating resistor using OTA

Fig. 6.5 shows the frequency response of floating resistor with OTA implementation. It provides a gain of 0 dB.

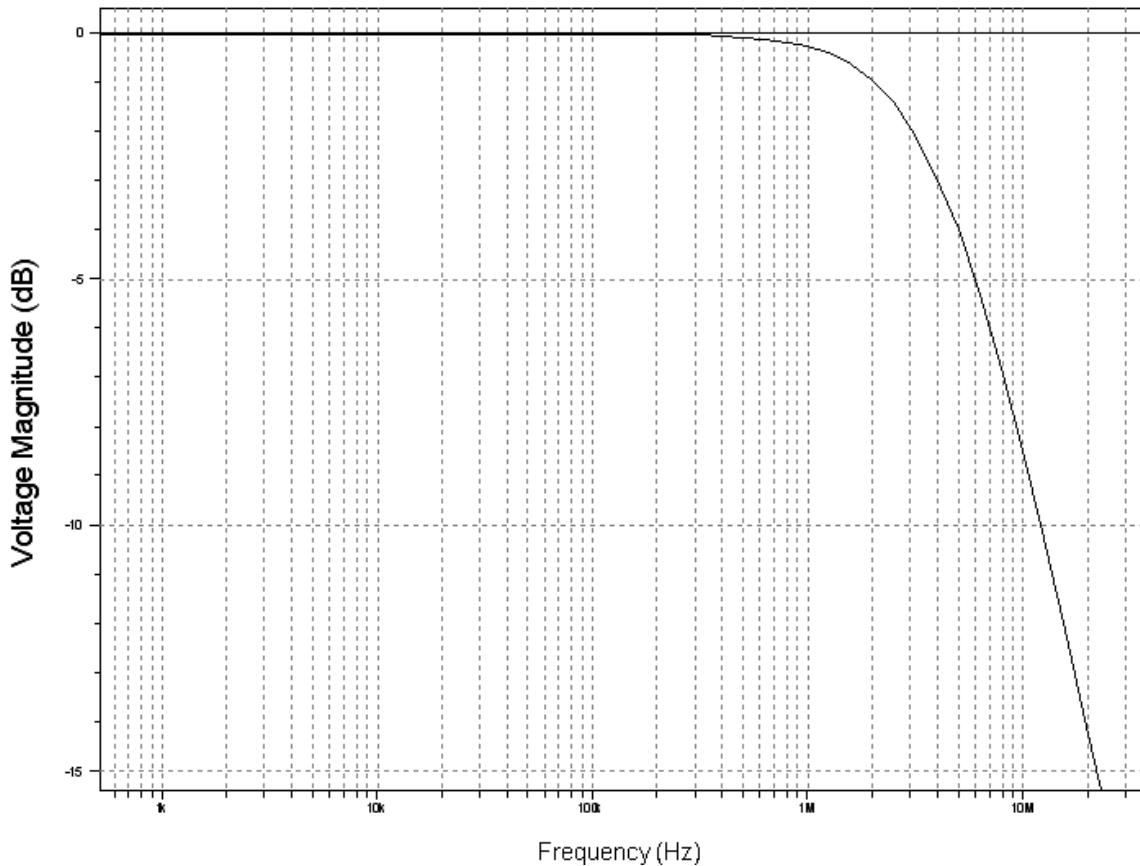


Figure 6.5 Frequency response of OTA implemented floating resistor

6.4.3 Implementation of Inductor using OTA

An inductor is implemented using four same transconductors and one capacitors connected [11,18,34] as shown in fig. 6.6 Here also, the designed folded cascode op-amp is used. The value of capacitor is fixed at 1 pF. Where,

$$L = C/g_m^2 \dots\dots\dots(6.3)$$

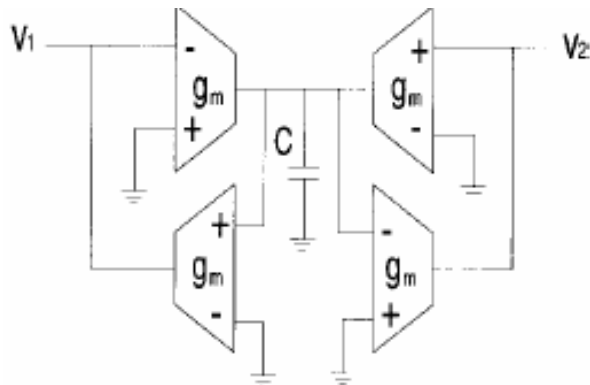


Figure 6.6 Implementation of inductor using OTA

Fig. 6.7 shows the frequency response of inductor with OTA implementation. It provides again a gain of 6.02 dB.

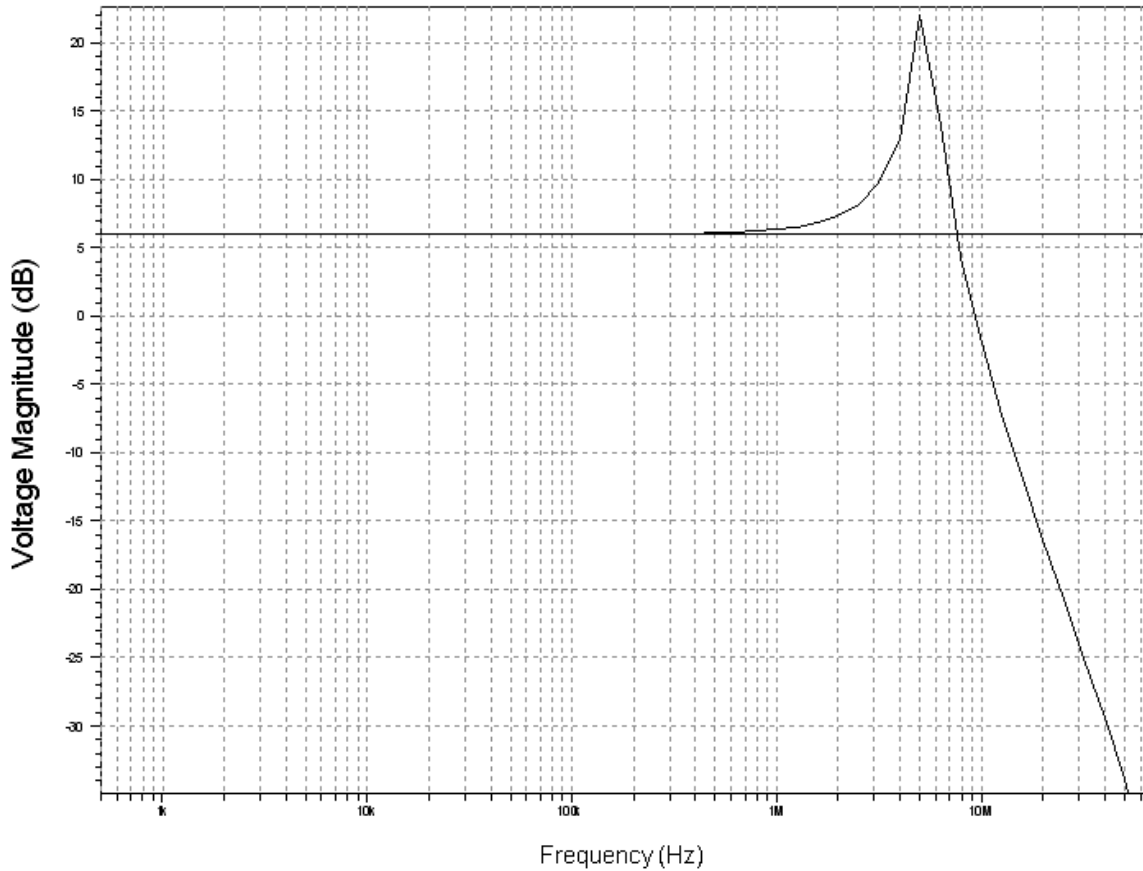


Figure 6.7 Frequency response of OTA implemented inductor

Capacitors in lumped design are normally not replaced since they can be readily implemented in integrated circuits.

6.4.4 5th order Active network

Replacing all the passive components by their active implementations results in the following fig. 6.8. The inductor and resistors are actively implemented using the folded cascode OTA (discussed in previous chapter). Thus, the figure represents the active equivalent of passive RLC network. It uses in total eleven

OTAs with five capacitances in between. A power supply of 2 V AC and an offset voltage of 2.5 mV are used.

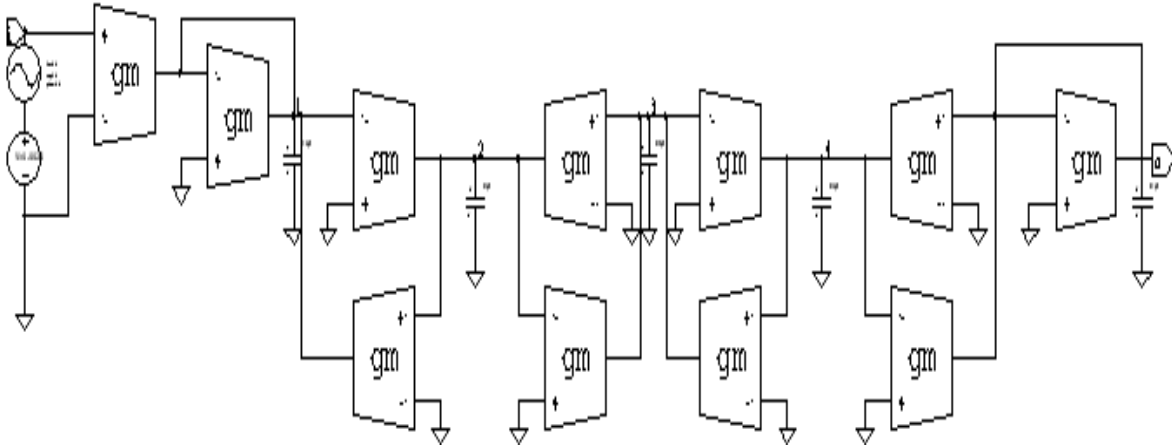


Figure 6.8 5th Order Chebyshev filter using folded cascode OTAs

The T-Spice net-list is shown in Appendix B. The fig. 6.9 shows the frequency response of 5th order Chebyshev filter. It shows a maximum gain of 0 dB and a 3dB-frequency of 5.77 MHz, when the OTA used is biased at a voltage of -1.7 V, with all the transistors in saturation. This much 3dB-frequency is pretty good for the video applications.

Further as discussed in the second chapter that the ripples in passband characterize the Chebyshev filter, ripples of 1.2 dB is achieved, as shown (fig. 6.10) by the enlarged view of the response. Also the response validates the statement that the total number of maxima and minima for an odd (5th order) ordered filter is odd (here total number of maxima and minima is three i.e. odd).

The roll-off rate is 111 dB/Dec.

Result summary:

3dB(passband) frequency	5.77 MHz
Ripples	1.2 dB
Roll-off rate	111 dB/Dec.
Gain	0 dB

Stopband Frequency

57 MHz

Attenuation Gain

120 dB

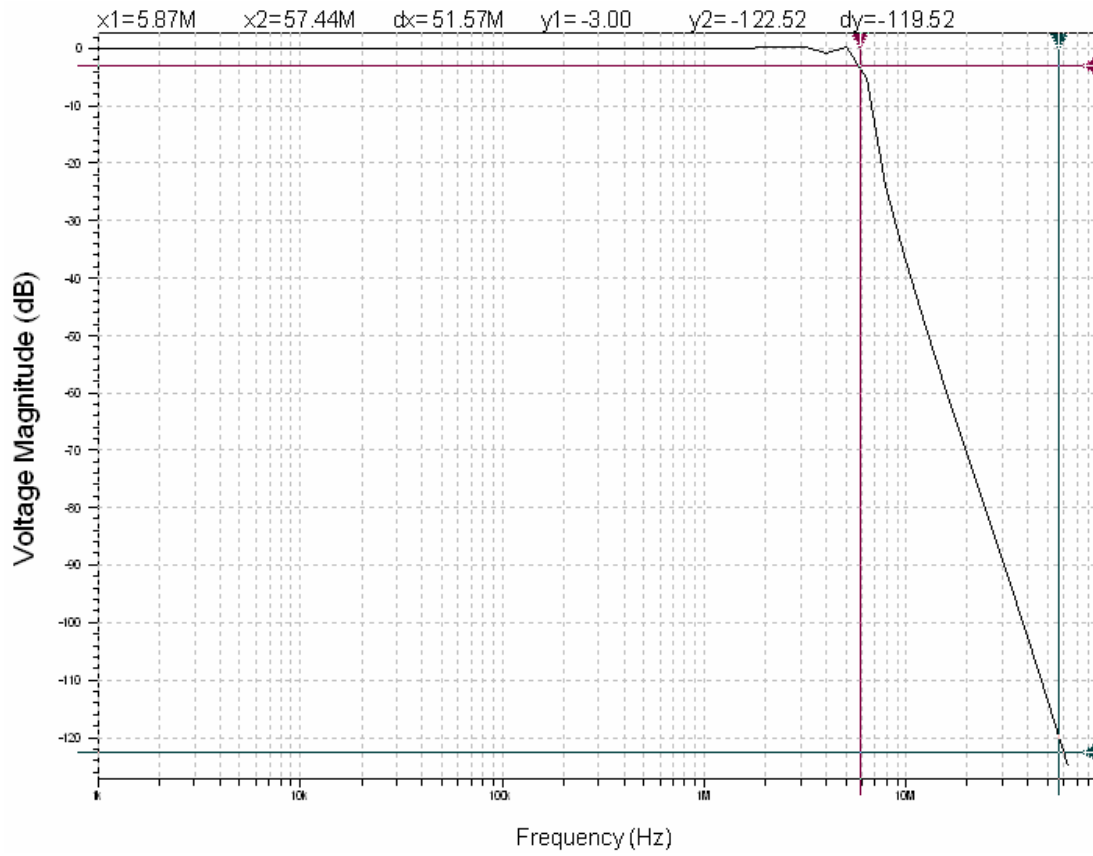
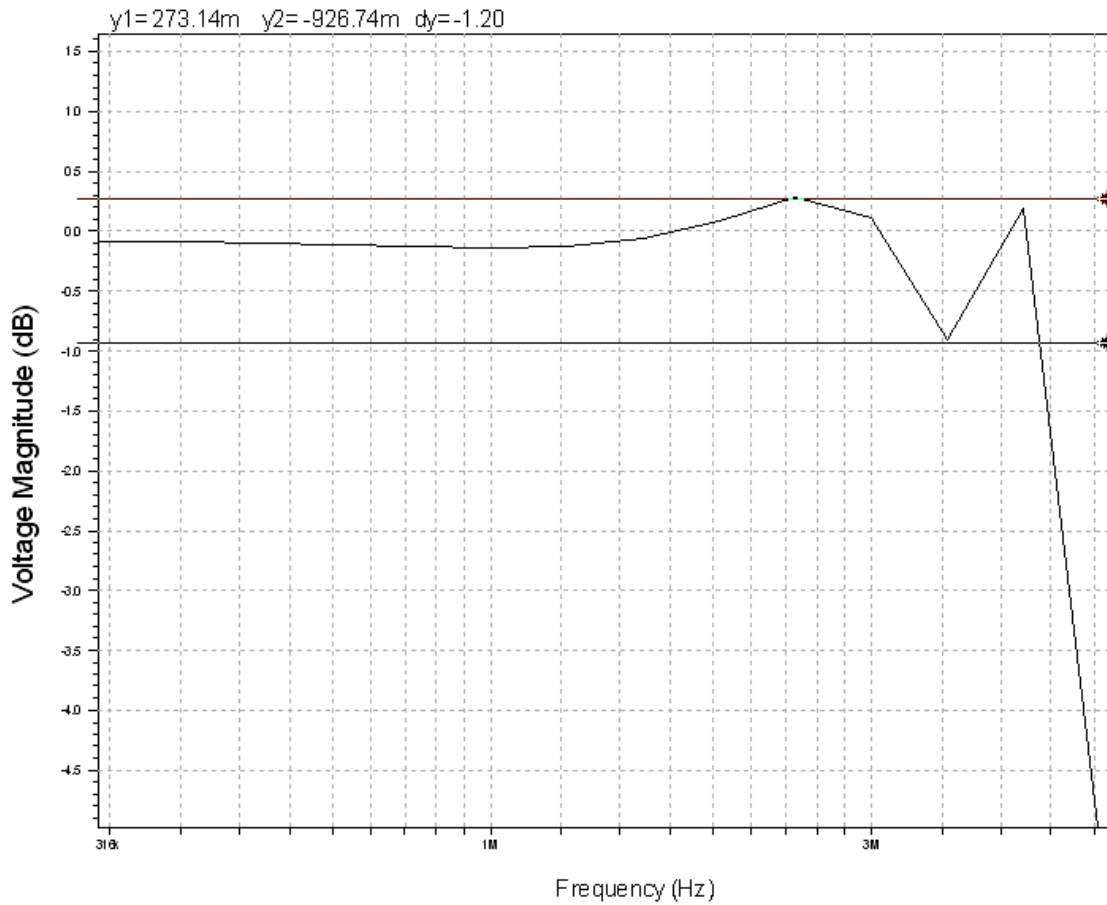


Figure 6.9 Frequency response of 5th order Chebyshev filter



Fig

Figure 6.10 Enlarged view to show ripples

6.4.5 Mathematical Proof of Accuracy of Results

n , Order of filter

δ_2 , Stopband attenuation = -120 dB

δ_1 , Passband ripple in dB = $10\log(1+\epsilon^2) = 1.2$ dB

ϵ , Parameter related to passband ripple = 0.56 dB

After putting values from results summary in equation 3.21,

$$n = 5.05 \sim 5$$

6.5 Analysis of Experimental Calculation of Transconductance (g_m) of OTA

Transconductance (g_m) is a major parameter in Operational Transconductance Amplifiers and so in OTA-C filters. The bias voltage in an OTA controls the bias current flowing through the current mirror circuit, which in turns affects the g_m .

Now as discussed in previous chapter that bias voltage affects the gain and frequency, it is this transconductance (g_m) that results a change in frequency. So calculating g_m is of great importance, so that one can observe the relation between g_m and frequency. Theoretically g_m can be calculated by using the small signal model of the circuit. But it's very tedious job. In this section a graphical method of calculating g_m is analyzed. The accuracy of the method is proved by doing the same for a number of times on a number of values.

This analysis is done in following steps:

- 1. To start with the g_m of the designed folded cascode OTA has been calculated. For this a typical value of $90 \mu\text{A/V}$ is assumed. Using this value, the values of R and L are calculated using equations $R = 1/g_m$ and $L = C/g_m^2$, which comes out to be $R = 11.11 \text{ K}\Omega$ and $L = 0.123 \text{ mH}$.*
- 2. Putting these values in the passive network of fig. 6.1 results in a 3dB-frequency of 6.85 MHz, which is found to be greater than that obtained in the previous section (= 5.77 MHz) for active implemented network (fig. 6.8). This shows that the g_m assumed is greater than the actual value. The g_m is then reduced and the steps 1 and 2 are repeated until both of networks provide similar 3dB-frequencies.*
- 3. Finally, at $g_m = 70 \mu\text{A/V}$ their frequencies are found to be very close. At this value of g_m the values of R and L are, $14.28 \text{ K}\Omega$ and 0.204 mH , respectively, resulting a 3dB-frequency of 5.36 MHz shown in fig. 6.11, which is very close to 5.77 MHz. Also, the gain is -6 dB , which is 6 dB more than the gain obtained in previous section (= 0 dB) by its active implementation. This rise in gain is due to the fact that active implementations of resistors and inductor*

provide a maximum gain of 6 dB. This proves that the g_m of OTA designed in previous chapter is $70 \mu A/V$.

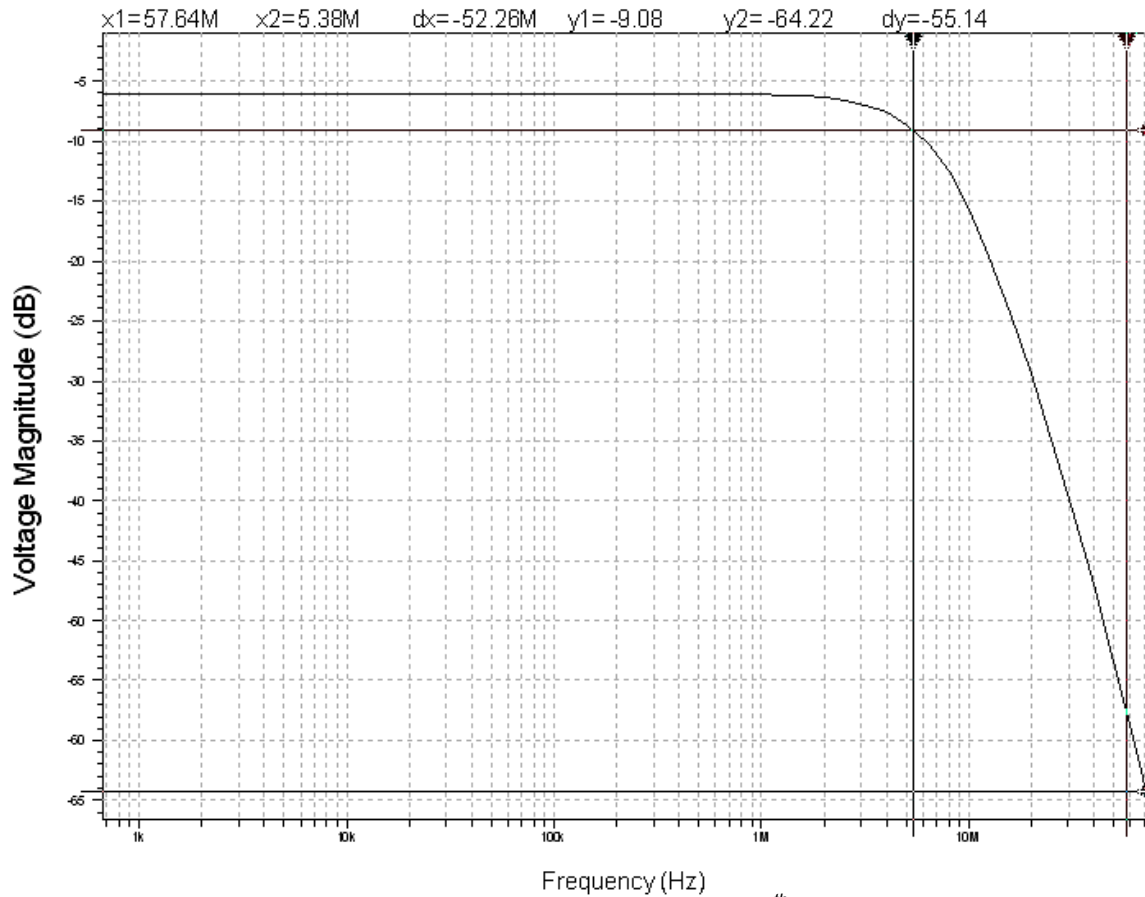
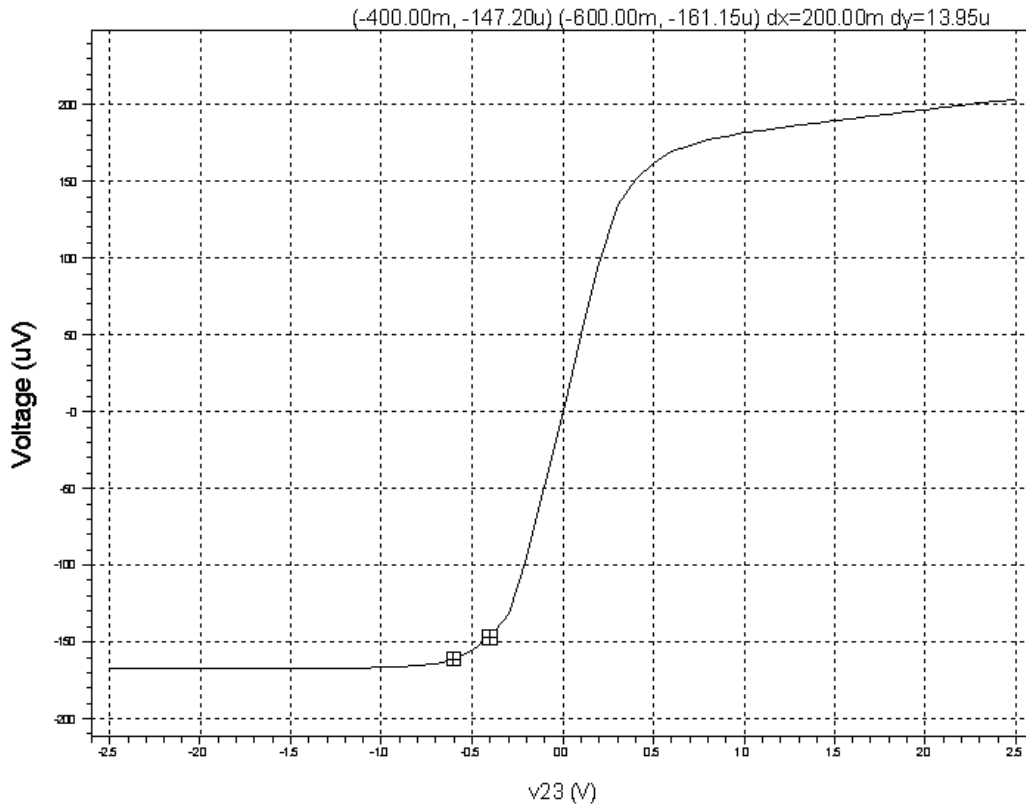


Figure 6.11 Frequency response of passive network of 5th order Chebyshev filter with $R = 14.28 K\Omega$ and $L = 0.203 mH$

4. Next a 1Ω resistor is placed at the output of folded cascode OTA (fig. 6.12) so that the output voltage axis (Y-axis) in Voltage Transfer Characteristics (VTC) curve acts as output current axis and graph of VTC would act as input voltage vs. output current graph. Now, g_m can be calculated from this VTC curve, as g_m is the change in output current with respect to change in input voltage. It is observed from the fig. 6.13, that the value of g_m for folded cascode designed ($= 70\mu A/V$) is found to lie in the region, where op-amp just enters the linear region and this is shown in the graph (fig. 6.13) with the help of the markers.



Fig

ure 6.13 VTC curve (with Y-axis voltage equivalent to output current) of folded cascode

5. This analysis is then verified by changing the bias voltage, calculating the value of g_m from the graph (fig. 6.13), calculating the values of R & L , and putting these values in the passive network (fig. 6.1). The value of 3dB-frequency obtained from passive network is found to be similar to the value obtained, when the active network has been biased with that particular value of bias voltage at which g_m has been calculated. An error of only $\pm 5\%$ in 3dB-frequencies of both networks (active and passive) proves the accuracy of analysis.

6.6 Analysis of variation of 3dB-Frequency with g_m and V_b

This section discusses how 3dB-frequency varies with g_m and hence with bias voltage (V_b). Table 6.1 shows different parameters like ripples, roll-off rate, and gain etc. measured at different bias voltages. Error between the Passive and Active network cut-off frequency is within $\pm 5\%$ showing that there is not much difference between the two.

Table 6.1 Different parameters of Chebyshev filter with change in bias voltage

$-V_b$ (volts)	g_m ($\mu A/V$)	Active n/w 3dB- frequency (MHz)	Passive n/w 3dB- frequency (MHz)	Error (%age)	Gain (dB)	Ripple (dB)	Roll-off rate (dB/Dec.)
0.01	213	16.36	16.4	0.2	-16.7	1.81	113
0.1	215	16.53	16.5	0.28	-16.1	1.18	114
0.5	224	16.6	17.04	2.6	-9.65	0.515	114
0.7	232	17	17.66	3.8	-4.27	1.96	115
0.9	241	17.26	18.37	6.4	-3.19	3.14	119
1	243	17.39	18.4	5.8	-3.17	3.43	122
1.1	217	17.02	16.65	2.17	-3.42	2.82	124
1.2	178	13.32	13.58	1.9	-5.22	1.3	123
1.5	142	11.26	10.88	3.3	0.0	8.05	118
1.6	108	8.79	8.3	5.5	-0.134	5.66	117
1.7	70	5.77	5.36	7.1	-0.0584	1.16	111
1.8	42.15	3.6	3.23	10.2	-0.06	1.22	120
1.9	18.2	1.35	1.39	2.9	-2.58	4.16	122
2	4.2	0.311	0.321	3.2	-0.354	0	106
2.1	0.209	0.014	0.016	14	-28.63	0	126

Following Table 6.2 shows the different values of resistances and inductances required for a particular 3dB-frequency.

Table 6.2 Values of resistances and inductances required for particular 3dB-frequency

-V _b (volts)	g _m (μA/V)	Resistance (K ohm)	Inductance (μH)	Passive n/w cut-off frequency (MHz)
0.01	213	4.69	22.0	16.4
0.1	215	4.64	21.57	16.5
0.5	224	4.45	19.8	17.04
0.7	232	4.3	18.57	17.66
0.9	241	4.15	17.2	18.37
1	243	4.12	16.96	18.4
1.1	217	4.6	21.2	16.65
1.2	178	5.6	31.25	13.58
1.5	142	7	49.45	10.88
1.6	108	9.21	84.89	8.3
1.7	70	14.28	203.9	5.36
1.8	42.15	23.72	562.87	3.23
1.9	18.2	54.95	3018.95	1.39
2	4.2	237.3	56.3*10 ⁻³	0.321
2.1	0.209	4780	22.89*10 ⁻⁶	0.016

6.6.1 Analysis of Various Graphs

Various graphs have been drawn to analyze the relation between bias-voltage (V_b), Transconductance (g_m) and 3dB-frequency.

1. From the graphs (V_b vs. g_m and V_b vs. 3dB frequency) (fig. 6.14), it is analyzed that as V_b increases in negative direction, g_m & hence the 3dB-frequency increases upto V_b = -1.0 V. After that both start decreasing. Further the shapes of graphs (fig. 6.14 and fig. 6.15) for V_b vs. g_m and V_b vs. active network 3dB-frequency are same. This shows that there is a linear relation between g_m and 3dB-frequency.

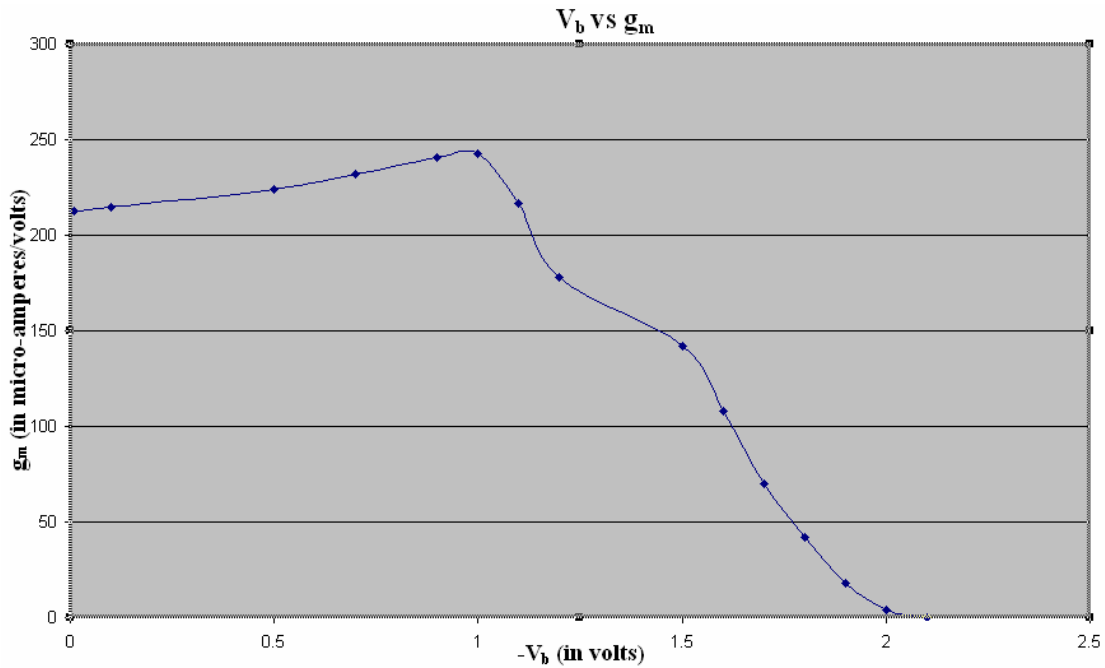


Figure 6.14 V_b vs. g_m graph

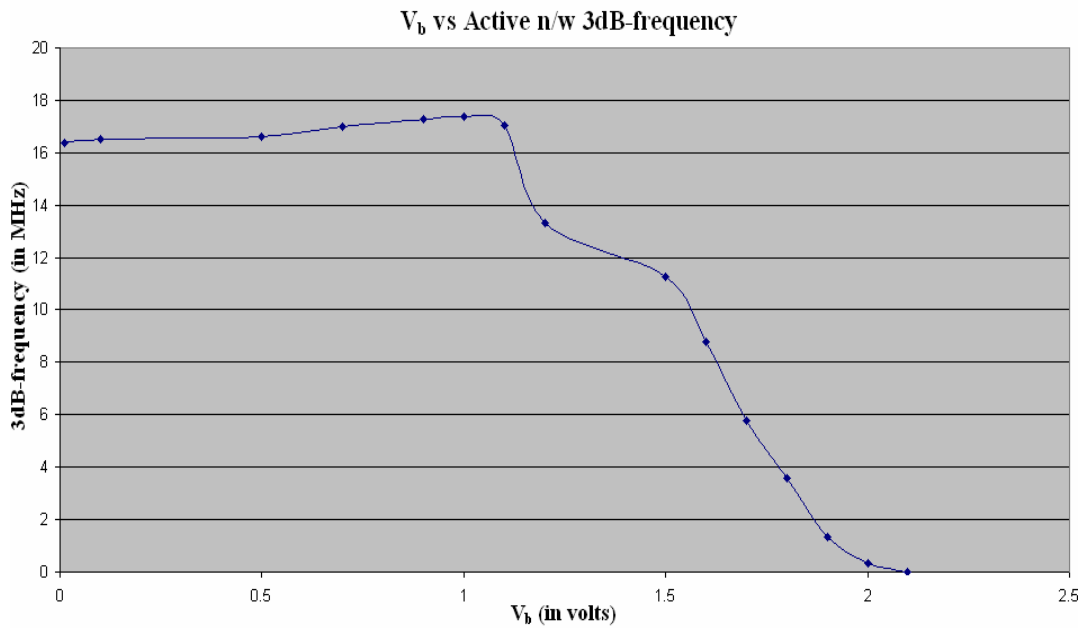


Figure 6.15 V_b vs. 3dB-frequency of active network

- From the following graph (fig. 6.16) it is clear that there is a linear relation between the 3dB-frequencies and g_m . Also, g_m is varied over a wide range of $0.2 \mu\text{A/V}$ to $243 \mu\text{A/V}$. So, from this graph, one can estimate the value of g_m required for a particular 3dB-frequency.

3. Fig. 6.17 shows the variation between the passive network frequency and active network frequency, which is very less and proves the accuracy of active implementation of passive network.

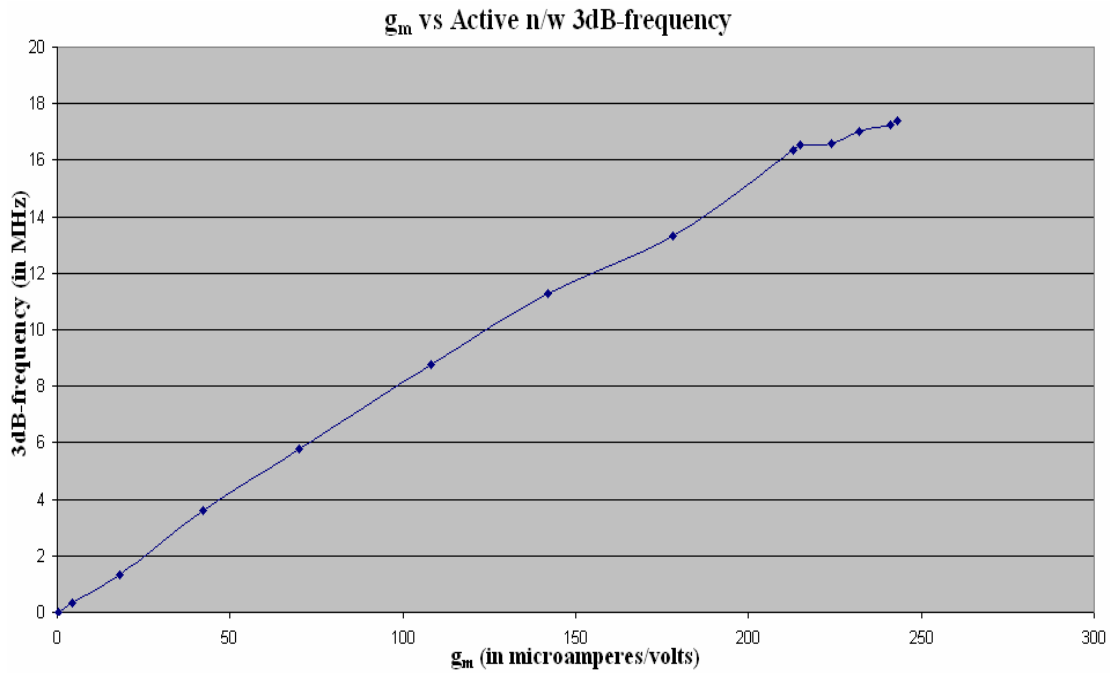


Figure 6.16 gm vs. 3dB-frequency of active network

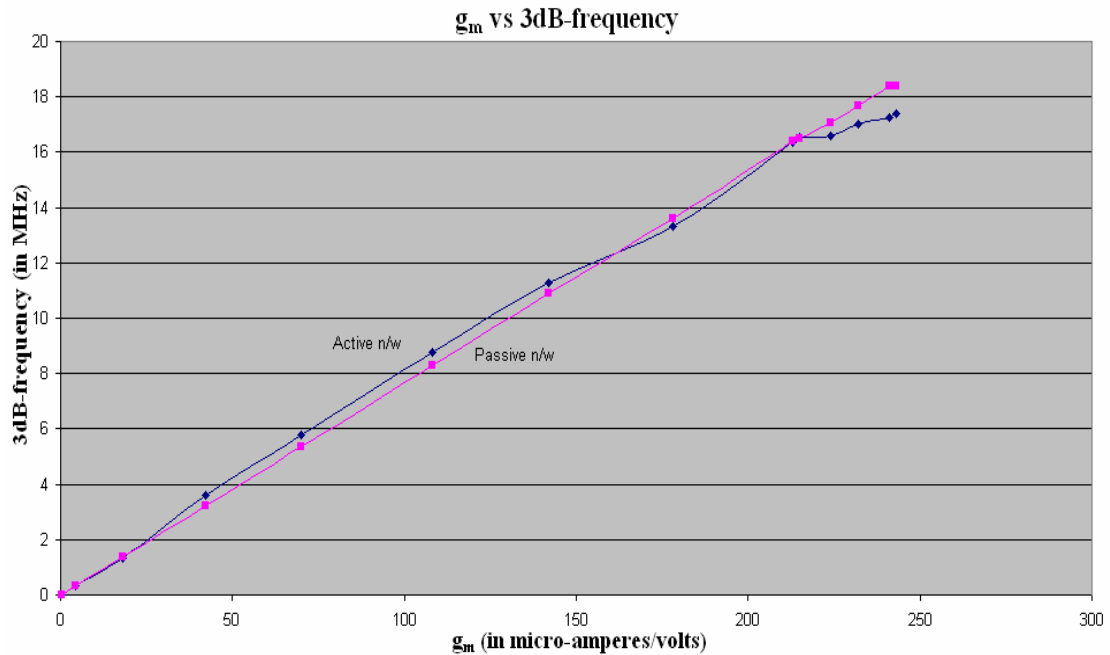


Figure 6.17 gm vs. 3dB-frequency of both networks

6.7 Proposed Equation

Fig. 6.16 shows a straight-line graph between g_m and 3dB-frequency. An equation (equ. 6.5) has been proposed for this graph, which is as follows:

Using, straight-line equation,

$$(Y-Y_1) = (X-X_1)((Y_2-Y_1)/(X_2-X_1)) + C \dots\dots\dots(6.4)$$

Where, X is g_m & Y is 3dB-frequency (f_{3dB}), and

Putting values of X_1, X_2, Y_1, Y_2 from graph,

$$g_m = 12.987 f_{3dB} - 0.39 \dots\dots\dots(6.5)$$

This equation is valid for all values of g_m , outside the range of graph also.

It can be proved by an example: let required $f_{3dB} = 20$ MHz

From equation $g_m = 264 \mu A/V$

Experimentally, $R = 1/g_m = 3.8 K\Omega$, and $L = 14.4 \mu H$

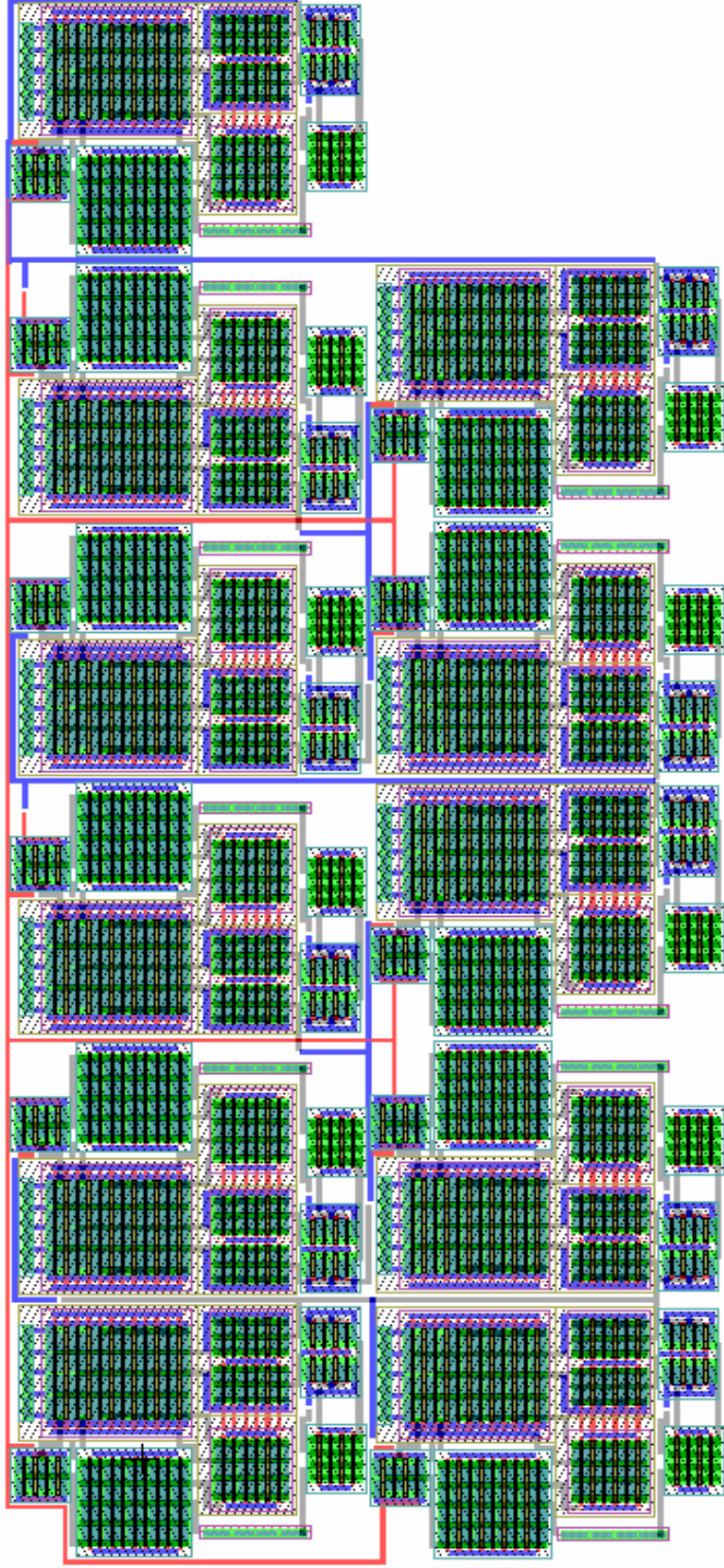
Putting these values in passive n/w, $f_{3dB} = 20.07$ MHz ≈ 20 MHz

Therefore, it is analyzed that for a particular value of 3dB-frequency, one can get to know the value of g_m required and by designing an OTA of that much value can get the desired response.

6.8 Physical Design of 5th Order Chebyshev Filter

The physical design of 5th order Chebyshev filter is shown in fig. The layout is drawn in L-Edit (Tanner Tool). For visibility reasons the resistors are not included in the layout shown. While designing layout special analog layout methods like gate folding, common centriode geometries, fingering etc. have been used to take care of matching issues and other related problems. Interdigitization and common centriode techniques are used for matched transistors, gatefold are used for large devices so as to minimize the associated parasitic capacitances.

Simulation results are shown in fig. 6.18. The 3dB-frequency of 5.67 MHz has been obtained. Simulation results are very much close to schematic simulation results (3dB-frequency, 5.77 MHz), which shows perfect matching of transistors.



Layout of 5th order Chebyshev Filter

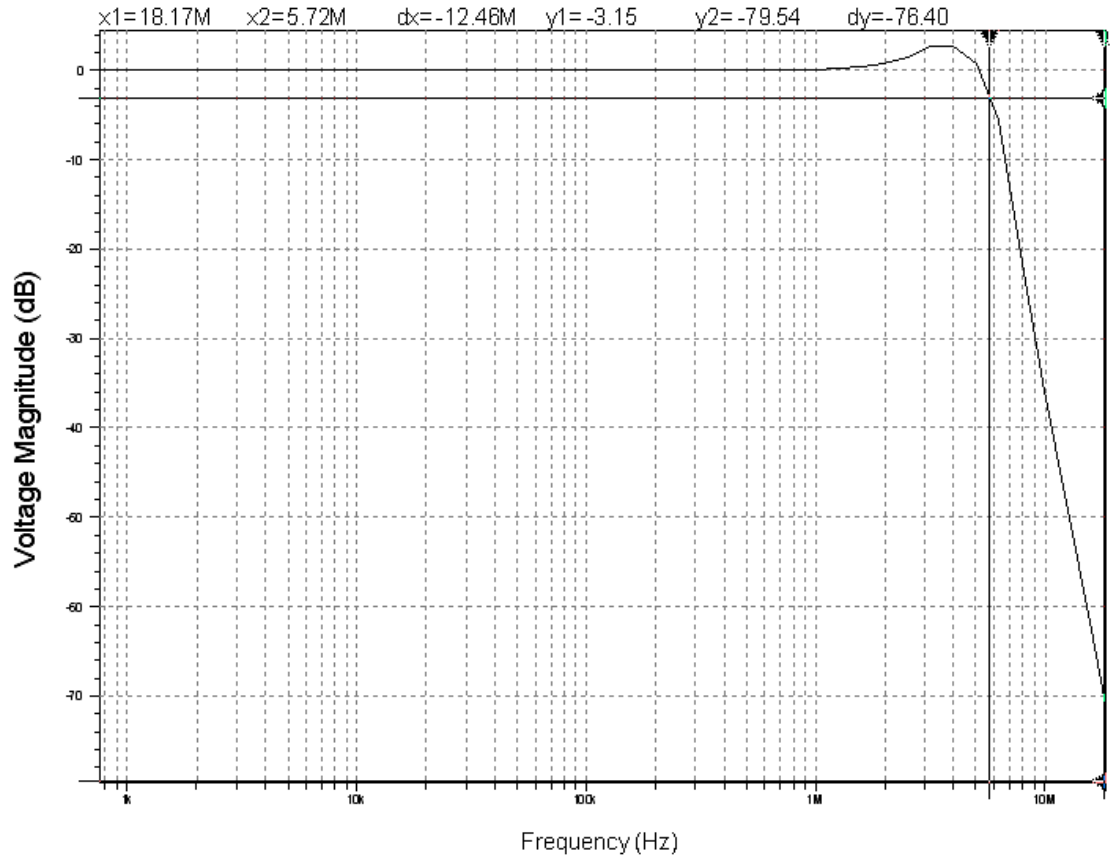


Figure 6.18 Simulation results of layout of 5th order Chebyshev filter

Result summary:

3dB-frequency	5.67 MHz
Ripples	2.7 dB
Roll-off rate	150 dB/Dec.
Gain	0 dB

Chapter 7

CONCLUSION AND FUTURE SCOPE

7.1 Conclusion

Filters are the indispensable parts of any communication systems. There are various methods to design a filter depending upon the specifications and the application in which the filter has to be employed like for low frequency applications, active implementation is best suited. Out of all mathematical approaches, Chebyshev filter is well known for voice synthesizer, antialiasing purpose and for video applications.

Keeping in view these applications, the filter has been designed by replacing all the passive components in a passive network with an active device. For this first a selection is made for the active device used. Folded cascode OTA is selected as it suits best for the purpose and a design procedure to design the folded cascode OTA is described. The development of a design procedure provides a quick, well-integrated and effective mechanism for estimating the filter parameters. The steps highlighted make it easy to redesign the circuit for different sets of specifications. The frequency response is simulated using the T-Spice environment of Tanner EDA tool. The simulated results of the OTA are in compliance with the theoretical values.

The 5th order Chebyshev filter designed, has passband frequency of 5.77 MHz, ripples of 1.2 dB, DC gain of 0 dB and roll-off rate of -120 dB/Dec. So, these filter specifications are quite favorable with that of the video-frequency CMOS IC-filters reported to date and are suitable for video processing applications like HDTV.

The physical mask layout of any circuit to be manufactured using a particular process must conform to a set of geometric constraints or rules, which are generally called layout design rules. Using the analog layout techniques of matching transistors, fingered structures and centroid geometry, the layouts are drawn. The results of the simulation of layout are nearly same as that shown by the schematic of the filter.

Further, analysis for the graphical calculation of transconductance of OTA has been done and a procedure for the same has been proposed. Also, the analysis is done to show the change in filter parameters like 3dB-frequency, ripples etc. with change in bias voltage and hence transconductance of OTA. The analysis shows that with increase in bias voltage in negative direction the transconductance and hence 3dB-frequency increases up to -1.0 V after that both starts decreasing. An equation, that relates g_m and 3dB-

frequency has been proposed, which can help in deciding the g_m of OTA used for required 3dB-frequency.

Future Scope-OTA is one of the methods to design an active Chebyshev filter. Other active devices like DDA can also be used. The design can be developed keeping in view low power and low voltages constraints as the filters are now being used in many portable applications that have requirement of low power and low voltages. Active devices can be designed in such a way that they may not restrict the passband frequency from expected passband frequency.

REFERENCES

- [1] A. A. Hussain, O. Elwan Hassan, and Ismail Mohammed, "A CMOS Highly Linear Channel-Select Filter for 3G Multistandard Integrated Wireless Receivers", *IEEE journal of Solid-State Circuits*, vol. 37, no. 1, January 2002.
- [2] A. B. Jayyousi, M. J. Lancaster, and F. Huang, "Filtering Functions With Reduced Fabrication Sensitivity", *IEEE Microwave and Wireless Components letters*, vol. 15, no. 5, May 2005.
- [3] A. Budak and P. Aronhime, "Maximally flat low-pass filters with steeper slopes at cutoff", *IEEE Tram Audio Electroacoust.*, vol. AU-18, pp. 63-66, March. 1970.
- [4] An Introduction to Analog Filters.htm, Sensors Magazine Online, July 2001.
- [5] Behzad Razavi, "Design of Analog CMOS Integrated Circuits", Edition 2002.
- [6] C. William Brown and Y. J. Szeto Andrew, "reconciling Spice results and Hand Calculations: Unexpected problems", *IEEE Transaction on Education*, vol. 43, no.1, February 2000.
- [7] Darwin Cheung, Klaas Bultj and Aaron Buchwaldy, "10-MHz 60-dB Dynamic-Range 4th-Order Butterworth Lowpass Filter", *IEEE press*.
- [8] Deyasini Majumdar and Brent J. Maundy, "Low voltage Gm-C filters and OTAs for HDSL2", *IEEE*, Montreal, Mayima 2003.
- [9] E. P. Allen, R. D. Holberg, "CMOS analog circuit design", Oxford University Press London, Second Edition, 2003.
- [10] Edward Sackinger and Walter Guggenbuhl, "A Versatile Building Block: The CMOS Differential Difference Amplifier", *IEEE J. Solid-state Circuits*, vol. sc-22, pp. 287- 294, April 1987.

- [11] Franco Maloberti, "Analog Design for CMOS VLSI Systems", Kluwer.
- [12] H. Watanabe et al., "Group delay characteristics of Chebyshev filters", presented at *the 1960 Nat'l Conv. of IECE*, no. 7.
- [13] <http://www.filter-solutions.com/chevy1.html>
- [14] <http://www.filter-solutions.com/chevy2.html>
- [15] <http://en.wikipedia.org/wiki/chebyshevfilter>
- [16] <http://www.k.ext.ti.com/SRVs/Data/ti/KnowledgeBases/analog/document/faqs/ch.htm>
- [17] J. D. Allstot., "A family of High-Swing CMOS Operational Amplifiers", *IEEE Journal of Solid State Circuits*, vol. 24, no. 6, December 1989.
- [18] J. E. Kardontchik, "Introduction to the Design of Trans. Conductor-Capacitor Filters", Norwell, Kluwer, 1992.
- [19] John G. Prokis, Dimtris G. Manolakis, "Digital Signal Processing: Principles Algorithm and Application", Third Edition, 2001.
- [20] Kerry Lacanette, "A Basic Introduction To Filter Devices-Active, Passive And Switched-Capacitor", National Semiconductor Application Note 779, April 1991.
- [21] Kuen-Jong Lee, Wei-Chiang Wang, and Kou-Shung Huang, "A Current-Mode Testable Design of Operational Transconductance Amplifier-Capacitor Filters", *IEEE Transactions on Circuits and Systems—II: Analog And Digital Signal Processing*, vol. 46, no. 4, April 1999.
- [22] L. Weinberg, *Network Analysis and Synthesis*, New York, McGraw-Hill, 1962.
- [23] M.C. Agarwal, Adel S. Sedra, "On Designing Sharp Cutoff Low-Pass Filters", *IEEE Transactions on Audio and Electro-acoustics*, vol. Au-20, no. 2; June 1972.

- [24] M. Guglielmi and G. Connor, "Chained function filters," *IEEE Microw. Guided Wave Lett.*, vol. 7, no. 12, pp. 390–392, December 1997.
- [25] Masao Hibino, Yasutoshi Ishizaki, and Hitoshi Watanabe, "Design of Chebyshev Filters with Flat Group-Delay Characteristics", *IEEE Transactions on circuit theory*, vol. CT-15, no. 4; December 1968.
- [26] Pan Wu and Rolf Schaumann, "Design Considerations for CMOS and GaAs OTAs: Frequency Response, Linearity, Tuning, And Common-mode Feedback", *Analog Integrated Circuits and Signal Processing*, November 1991.
- [27] R. Cameron, "General coupling matrix synthesis methods for Chebyshev filtering functions," *IEEE Transaction on Microw. Theory Tech*, vol. MTT-47, no. 4, pp. 433–442, April 1999.
- [28] R. L. Geiger and E. Sánchez-Sinencio, "Active Filter Design Using Operational Transconductance Amplifiers: A Tutorial", *IEEE Circuits and Devices Magazine*, vol. 1, pp.20-32, March 1985.
- [29] S. C. Dutta Roy, "On Maximally Flat Sharp Cutoff Low-Pass Filters," *IEEE Trans. Audio Electroacoust.*, vol. AU-19, pp. 58-63, March 1971.
- [30] S. V. Ginde and Joseph A. N. Noronha, "Design of IIR Filters", DSP and filter design (ECE 4624).
- [31] Sedra S. Adel and Smith C. Kenneth, "Microelectronics Circuits", Oxford University Press, 1998.
- [32] Sergio Solís-Bustos, José Silva-Martínez, Franco Maloberti and Edgar Sánchez-Sinencio, "A 60-dB Dynamic-Range CMOS Sixth-Order 2.4-Hz Low-Pass Filter

for Medical Applications”, *IEEE transactions on Circuits And Systems - II: Analog And Digital Signal Processing*, vol. 47, no. 12, December 2000.

[33] Tanner EDA User Guide.

[34] Theerachet Soorapanth, “CMOS RF Filtering at GHz Frequency”, A Dissertation, Department of Electrical Engineering and The Committee on Graduate Studies, Stanford University, August 2002.

[35] Y.P. Tsvividis and J.O. Voorman. “Integrated Continuous-Time Filters”, *IEEE press*, New York, 1992.

APPENDIX - A

The **T-Spice file** for the folded cascode OTA designed is given below.

* SPICE netlist written by S-Edit Win32 8.10

* Written on Sep 9, 2006 at 10:18:29

* Waveform probing commands

```
.probe
.options probefilename="jj folded cascode wd single end input_trs name as in design
procedure.dat"
+ probesdbfile="C:\Documents and Settings\student\Desktop\filter\simulations\final
simulations\jj folded cascode wd single end input_trs name as in design procedure.sdb"
+ probetopmodule="Module0"
```

* Main circuit: Module0

C1 out Gnd 10pF

M2 P3 in+ N1 N1 NMOS L=2u W=61u AD=66p PD=24u AS=66p PS=24u

M3 P4 Gnd N1 N1 NMOS L=2u W=61u AD=66p PD=24u AS=66p PS=24u

M4 N1 bias N6 N6 NMOS L=2u W=281u AD=66p PD=24u AS=66p PS=24u

M5 P3 P2 P6 P6 PMOS L=2u W=303u AD=66p PD=24u AS=66p PS=24u

M6 P4 P2 P6 P6 PMOS L=2u W=303u AD=66p PD=24u AS=66p PS=24u

M7 N3 P1 P3 P3 PMOS L=2u W=182u AD=66p PD=24u AS=66p PS=24u

M8 out P1 P4 P4 PMOS L=2u W=182u AD=66p PD=24u AS=66p PS=24u

M9 N2 N3 N4 N4 NMOS L=2u W=75u AD=66p PD=24u AS=66p PS=24u

M10 out N3 N5 N5 NMOS L=2u W=75u AD=66p PD=24u AS=66p PS=24u

M11 N4 N2 N6 N6 NMOS L=2u W=75u AD=66p PD=24u AS=66p PS=24u

M12 N5 N2 N6 N6 NMOS L=2u W=75u AD=66p PD=24u AS=66p PS=24u

M13 P1 bias N6 N6 NMOS L=2u W=351u AD=66p PD=24u AS=66p PS=24u

M14 P2 P1 P5 P5 PMOS L=2u W=303u AD=66p PD=24u AS=66p PS=24u

M15 P5 P2 P6 P6 PMOS L=2u W=303u AD=66p PD=24u AS=66p PS=24u

R16 P2 P1 2000 TC=0.0, 0.0

R17 N3 N2 3333.3 TC=0.0, 0.0

v18 in+ N7 0.0 AC 2.0 0.0

v19 P6 Gnd 2.5

v20 Gnd N6 2.5

v21 bias Gnd -1.7

v22 N7 Gnd 0.0025

.ac dec 10 1 100meg

.include "C:\Tanner\TSpice91\models\ml2_125.md"

.print ac vdb(in+) vdb(out) vp(out)

.op

* End of main circuit: Module0

APPENDIX – B

The **T-Spice file** for the designed 5th order Chebyshev filter is given below.

* SPICE netlist written by S-Edit Win32 8.10

* Written on Sep 14, 2006 at 09:46:34

* Waveform probing commands

```
.probe  
.options probefilename="jj 5th order cheb using folded cascode _trs name acc to design  
procrdure.dat"
```

```
+ probesdbfile="C:\Documents and Settings\student\Desktop\filter\simulations\final  
simulations\jj 5th order cheb using folded cascode _trs name acc to design procrdure.sdb"
```

```
+ probetopmodule="Module0"
```

```
.SUBCKT module_for_folded_cascode__trs_name_acc_to__design_procedure in+ in-  
+ out Gnd
```

```
C1 out Gnd 10pF
```

```
M2 P3 in+ N1 N1 NMOS L=2u W=61u AD=66p PD=24u AS=66p PS=24u
```

```
M3 P4 in- N1 N1 NMOS L=2u W=61u AD=66p PD=24u AS=66p PS=24u
```

```
M4 N1 bias N6 N6 NMOS L=2u W=281u AD=66p PD=24u AS=66p PS=24u
```

```
M5 P3 P2 P6 P6 PMOS L=2u W=303u AD=66p PD=24u AS=66p PS=24u
```

```
M6 P4 P2 P6 P6 PMOS L=2u W=303u AD=66p PD=24u AS=66p PS=24u
```

```
M7 N3 P1 P3 P3 PMOS L=2u W=182u AD=66p PD=24u AS=66p PS=24u
```

```
M8 out P1 P4 P4 PMOS L=2u W=182u AD=66p PD=24u AS=66p PS=24u
```

```
M9 N2 N3 N4 N4 NMOS L=2u W=75u AD=66p PD=24u AS=66p PS=24u
```

```
M10 out N3 N5 N5 NMOS L=2u W=75u AD=66p PD=24u AS=66p PS=24u
```

```
M11 N4 N2 N6 N6 NMOS L=2u W=75u AD=66p PD=24u AS=66p PS=24u
```

```
M12 N5 N2 N6 N6 NMOS L=2u W=75u AD=66p PD=24u AS=66p PS=24u
```

```
M13 P1 bias N6 N6 NMOS L=2u W=351u AD=66p PD=24u AS=66p PS=24u
```

```
M14 P2 P1 P5 P5 PMOS L=2u W=303u AD=66p PD=24u AS=66p PS=24u
```

```
M15 P5 P2 P6 P6 PMOS L=2u W=303u AD=66p PD=24u AS=66p PS=24u
```

```
R16 P2 P1 2000 TC=0.0, 0.0
```

```
R17 N3 N2 3333.3 TC=0.0, 0.0
```

```
v18 P6 Gnd 2.5
```

```
v19 Gnd N6 2.5
```

```
v20 bias Gnd -1.7
```

```
.ENDS
```

* Main circuit: Module0

```
C1 1 Gnd .1pF
```

```
C2 2 Gnd 1pF
```

```
C3 3 Gnd 5pF
```

```
C4 4 Gnd 1pF
```

```
C5 o Gnd .1pF
```

```
Xmodule_for_folded_cascode__trs_name_acc_to__design_procedure_1 Gnd 3 4 Gnd
```

```
+ module_for_folded_cascode__trs_name_acc_to__design_procedure
```

```
Xmodule_for_folded_cascode__trs_name_acc_to__design_procedure_2 i Gnd 1 Gnd
```

```

+ module_for_folded_cascode_trs_name_acc_to__design_procedure
Xmodule_for_folded_cascode_trs_name_acc_to__design_procedure_3 Gnd 1 1 Gnd
+ module_for_folded_cascode_trs_name_acc_to__design_procedure
Xmodule_for_folded_cascode_trs_name_acc_to__design_procedure_4 Gnd 1 2 Gnd
+ module_for_folded_cascode_trs_name_acc_to__design_procedure
Xmodule_for_folded_cascode_trs_name_acc_to__design_procedure_5 Gnd 2 3 Gnd
+ module_for_folded_cascode_trs_name_acc_to__design_procedure
Xmodule_for_folded_cascode_trs_name_acc_to__design_procedure_6 Gnd 4 o Gnd
+ module_for_folded_cascode_trs_name_acc_to__design_procedure
Xmodule_for_folded_cascode_trs_name_acc_to__design_procedure_7 Gnd o o Gnd
+ module_for_folded_cascode_trs_name_acc_to__design_procedure
Xmodule_for_folded_cascode_trs_name_acc_to__design_procedure_8 2 Gnd 1 Gnd
+ module_for_folded_cascode_trs_name_acc_to__design_procedure
Xmodule_for_folded_cascode_trs_name_acc_to__design_procedure_9 3 Gnd 2 Gnd
+ module_for_folded_cascode_trs_name_acc_to__design_procedure
Xmodule_for_folded_cascode_trs_name_acc_to__design_procedure_10 o Gnd 4 Gnd
+ module_for_folded_cascode_trs_name_acc_to__design_procedure
Xmodule_for_folded_cascode_trs_name_acc_to__design_procedure_11 4 Gnd 3 Gnd
+ module_for_folded_cascode_trs_name_acc_to__design_procedure
v6 i N1 0.0 AC 2.0 0.0
v7 N1 Gnd 0.0025
.ac dec 10 1 70meg
.include "C:\Tanner\TSpice91\models\ml2_125.md"
.print ac vdb(i) vdb(o)
.op
* End of main circuit: Module0

```

The folded cascode and the filter designed, works wells at a bias voltage of -1.7 V and an offset of 0.0025 V, these specifications provide a 3dB-frequency of 5.77 MHz. Analysis has been done by varying the bias voltage.

APPENDIX – C

Papers Published:

During this work the following two review papers were accepted in the National Conference on Emerging Trends in Electronics and Communication (sponsored by IEEE)

to be held on 14th - 15th September 2006 at Pardre Conceicao College of Engineering, Verna, Goa.

1. Jyoti Jain, Nimisha Saini and Alpana Agarwal, "Methods of Designing Elliptic Filter: A Review" *National Conference on Emerging Trends in Electronics and Communication*, September 2006.

2. Nimisha Saini, Jyoti Jain and Alpana Agarwal, "Different Methods to Design Analog CMOS Filters: A Review" *National Conference on Emerging Trends in Electronics and Communication*, September 2006.